UNIVERSITY OF TRENTO

## PhD Program in Biomolecular Sciences

## Department of Cellular, Computational and Integrative Biology – CIBIO

## 36th Cycle

# Investigating the roles of lncRNA TERRA in telomerase-to-ALT transition using cancer cell lines and multicellular organisms


**Tutor**

Prof. Emilio CUSANELLI

*Department of CIBIO*

**Advisor**

Prof. Maria Caterina MIONE

*Department of CIBIO*

**Ph.D. Thesis of**

Claudio OSS PEGORAR

*Department of CIBIO*



Academic Year 2023-2024

Declaration

I, Claudio Oss Pegorar, confirm that this is my own work and the use of all material from other sources has been properly and fully acknowledged.

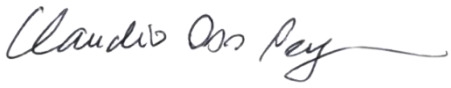

# Index

# List of abbreviations

| | |
|---|---|
| ALT | Alternative Lengthening of Telomeres |
| APB | ALT-associated PML Bodies |
| ASO | Antisense Oligonucleotide |
| ATM | Ataxia Telangiectasia Mutated |
| ATR | Ataxia telangiectasia and Rad3-related |
| BIR | Break-induced Replication |
| BLM | Bloom Syndrome Protein |
| CTCF | CCCTC-binding Factor |
| DDR | DNA Damage Response |
| DNMT | DNA Methyl Transferase |
| dpf | days post fertilization |
| DSB | Double Strand Break |
| ECTR | Extra Chromosomal Telomeric Region |
| FISH | Fluorescence in situ Hybridization |
| GBM | Glioblastoma Multiforme |
| HDR | Homology-directed Repair |
| hnRNP | Heterogenous Nuclear Ribonucleoprotein |
| hpf | hours post fertilization |
| ITR | Internal Telomeric Repeats |
| lncRNA | Long Non-coding RNA |
| m7G | N7-methylguanosine |
| MO | Morpholino |

| | |
|---|---|
| mpf | months post fertilization |
| NMD | Non-sense Mediated Decay |
| ORC | Origin Replication Complex |
| PML | Promyelocytic Leukemia Protein |
| RT | Reverse Transcription |
| RTEL | Regulator of Telomere Elongation Helicase |
| SCRB-ASO | ASO targeting nothing (control) |
| *t;p;p* | *trt-1; pot-2; pot-1::mCherry* |
| TERRA | Telomeric-repeat containing RNA |
| TERRA-ASO | ASO targeting TERRA |
| TMM | Telomere Maintenance Mechanism |
| TPE | Telomere Position Effect |
| TRF | Telomere Restriction Fragment |
| T-SCE | Telomeric Sister Chromatid Exchange |
| TSS | Transcription Start Site |

# Abstract

Telomeres protect eukaryotic chromosomes from fusions and degradations and progressively shorten over generations due to the “end replication problem” in human somatic cells, leading to cell cycle arrest, senescence and ultimately cell death. To achieve replicative immortality, tumors elongate their telomeres in two possible ways: by reactivating telomerase, in about 85-90% of cancers, or through homologous recombination (HR) by the mechanism of alternative lengthening of telomeres (ALT), in about 10-15% of cancers. Even though anti-telomerase treatments are currently being developed, there is a number of tumors that can change from one mechanism to the other with a switch named telomerase-to-ALT, about which almost nothing is known to date. One of the ALT hallmarks is the presence of high levels of telomeric lncRNA TERRA, which is thought to play a role in HR during ALT. However, little is known about the involvement of TERRA in the onset of ALT. In this PhD project, we aim at investigating the roles of TERRA in ALT and during telomerase-to-ALT transition. In particular, we employed an ALT-positive human cancer cell line in which we downregulated TERRA through antisense oligonucleotide (ASO) and measured changes in the ALT phenotype. In addition, we employed *C. elegans* mutant strains to study the dynamics of TERRA in worms lacking telomerase and elongating their telomeres using an ALT-like mechanism. We also took advantage of a zebrafish brain cancer model that was characterized to be ALT-positive and expressing high TERRA levels. With this model, we performed micro-injections of ASO targeting TERRA with the aim of downregulating TERRA and studying its effects on the development of the tumor and ALT. The results obtained helped us to shed light on the involvement of TERRA in the ALT mechanisms both in a non-cancerous context using *C. elegans* and in cancer using human cells and the zebrafish model.

# Introduction

## Telomeres

Telomeres, present at the terminal regions of eukaryotic chromosomes, are ribonucleoprotein structures which primary function is to safeguard chromosome ends against potential genome instability occurrences, including chromosome degradation, fusion, and improper recombination[1,2]. Telomeres consist of repetitive DNA sequences that are organized in tandem arrays, and the specific sequence varies depending on the organism. For instance, vertebrate telomeres consist of $(TTAGGG)_n$ sequences, while in nematodes telomeres are made of $(TTAGGC)_n$ sequences. Additionally, the length of telomeres varies across species: in *Mus musculus*, they range from 20 to 50 kb, in *Homo sapiens* from 5 to 15 kb, in *Danio rerio* from 15 to 20 kb, in *Caenorhabditis elegans* from 2 to 9 kb, and in *Saccharomyces cerevisiae* and *Saccharomyces pombe*, they are about 300 base pairs long[3–5]. While genomic DNA typically exists in the double-helix form, it is worth noting that telomeres have a distinctive structure. At the 3' end of telomeres, there is a G-rich single-stranded overhang of approximately 150 to 200 nt in length. This overhang can invade and pair with a double-stranded telomeric region on the same chromosome end, creating a structure referred to as a telomeric loop (t-loop) (Figure 1)[6].

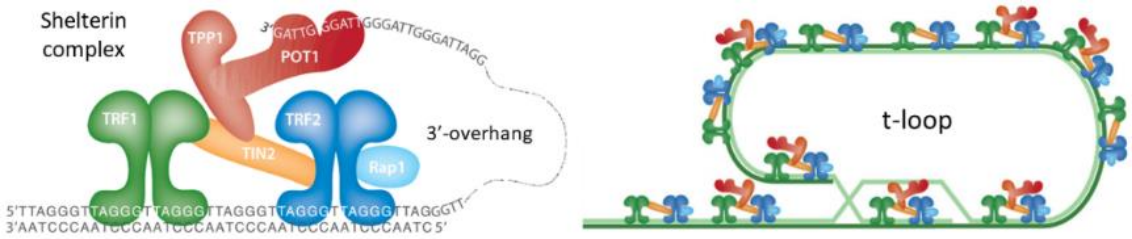


***Figure 1 |*** *The shelterin complex and the formation of t-loop. Representative images showing how the six subunits form the shelterin complex on chromosome ends (**left**) and the formation of the t-loop through the invasion of the 3'-overhang into the double-stranded telomeric DNA (**right**). Adapted from De Lange 2018 [7].*

The t-loop formation is orchestrated by the activity of the shelterin protein complex, which is composed of six distinct subunits: TRF1, TRF2, TIN2, Rap1, TPP2, and POT1[8]. TRF1 and TRF2 create homodimers, which have the capability to strongly attach to double-stranded telomeric DNA. In contrast, POT1 and TPP1 operate as a heterodimer and attach to the single-stranded telomeric DNA located at the 3'-overhang. TIN2 serves to link POT1/TPP1 with TRF1 and TRF2, thereby reinforcing their connection to the ends of chromosomes.

Rap1 interacts with TRF2, enhancing its selectivity for binding to telomeric DNA and controlling its positioning within telomeres[7].

As mentioned at the very beginning, telomere main role is to discriminate between the natural occurrence of linear chromosome ends and potentially harmful double strand breaks (DSBs). For this reason, the concealment of the 3'-overhang through the formation of the t-loops impedes the activation of DNA damage response (DDR) pathways. For instance, TRF2 was shown to impede the activation of the ataxia telangiectasia mutated (ATM) pathway[9], while POT1 independently represses the ataxia telangiectasia and Rad3-related (ATR) kinase[10].

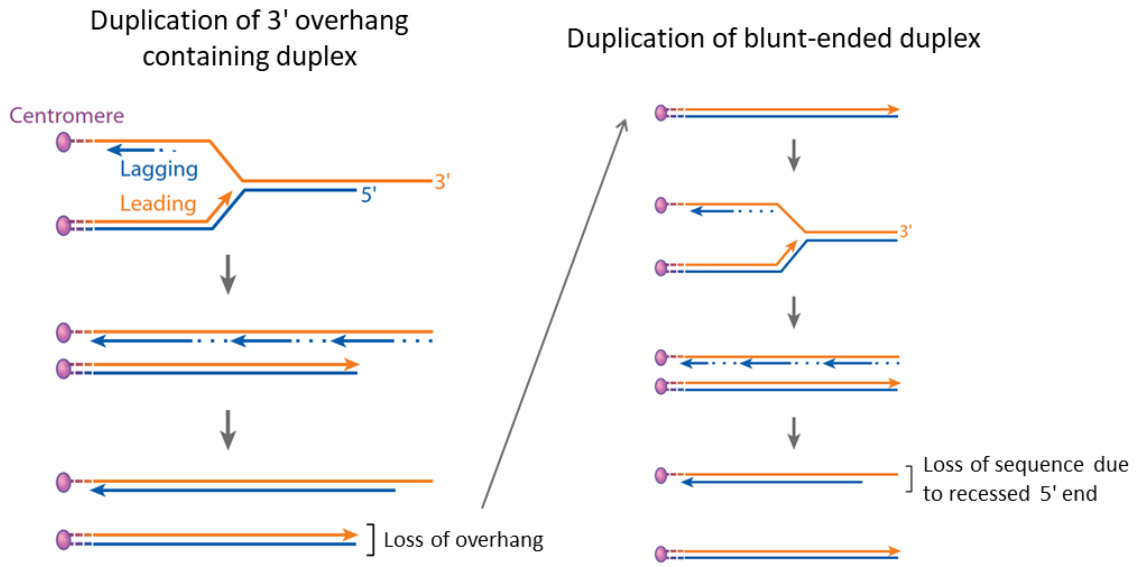


***Figure 2 |*** *Schematic representation of the end-replication problem. The dashed lines illustrate the RNA primers employed to commence the process of DNA synthesis. The leading-strand synthesis encounters challenges when attempting to completely replicate a linear molecule concluding with a 3'-overhang (**left**), while the lagging-strand synthesis faces obstacles in fully copying molecules that have blunt ends (**right**). Adapted from Jain & Cooper 2010 [5].*

Moreover, TRF1 and TRF2 play essential roles in facilitating the replication of telomeric sequences during the S-phase. They achieve this function by physically interacting with the Bloom syndrome helicase (BLM)[11] and the regulator of telomere elongation helicase 1 (RTEL1)[12], respectively, and guiding their localization at the telomeres. BLM and RTEL1 unravel t-loops and resolve the G-quadruplex structures that naturally form within the G-rich chromosome ends. This activity facilitates the advancement of the replication fork, preventing fork stalling and the subsequent activation of DDR mechanisms. The "end replication problem" occurs as a result of the semiconservative replication of DNA, where

chromosome ends progressively shorten after each cell division (Figure 2). This shortening happens because DNA polymerase is unable to fully replicate the extremities of a double stranded DNA molecule [13,14]. In the absence of telomere elongation, telomeres will shorten to a point where less and less shelterin proteins will be bound to telomeres, thus becoming dysfunctional and recognized as DSB sites by the DDR machinery. The persistent activation of the DDR system eventually results in cellular senescence, largely influenced by the Rb and p53 signaling pathways[15]. This process serves as a robust tumor suppressive mechanism.

## Telomerase

Eukaryotic cells that require to overcome the issue posed by telomere shortening and replicative inhibition rely on the activity of an enzyme named telomerase. Telomerase is a ribonucleoprotein that catalyzes the addition of the TTAGGG repeats to chromosome ends[16]. The telomerase holoenzyme is highly conserved in evolution and is composed of TERT, the protein part which acts as the reverse transcriptase (RT), and TERC, the built-in RNA moiety which serves as template to drive the reverse transcription of telomeric repeats (Figure 3)[17,18].

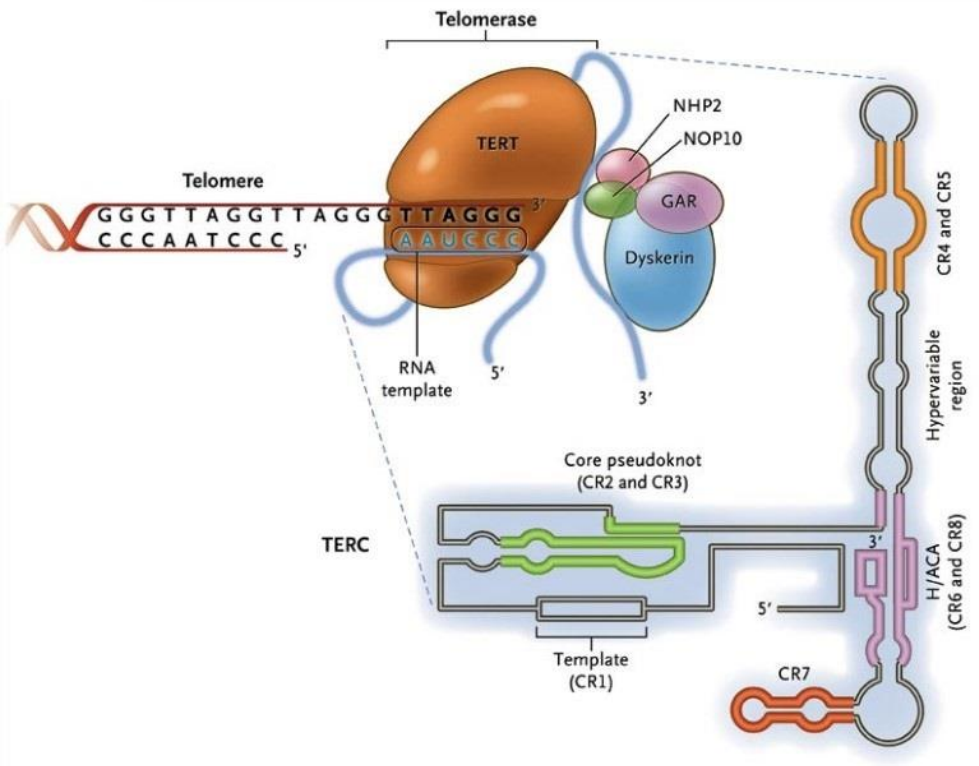


***Figure 3 |*** *The structure of telomerase. The activity of telomerase is achieved through TERT, the catalytic component of the holoenzyme, with additional accessory proteins, and TERC, the RNA template, here schematized with its secondary structures highlighted. Adapted from Calado 2009 [19].*

Telomerase is not active in all cells, with germ cells and stem cells being exceptions due to their need for continual replication. In contrast, somatic cells typically do not express telomerase under normal physiological conditions, leading to telomere shortening, aging, and eventual cell death[20]. A notable exception is represented by cancer cells, as their quest for replicative immortality necessitates the maintenance of sufficiently long telomeres to evade cell cycle arrest and growth inhibition. For this reason, mutations and epigenetic

modifications within the TERT promoter that re-activate the expression of the enzyme are frequently present in cancer cells[21]. While the activation of telomerase stands out as the prevailing mechanism for telomere elongation in cancer, accounting for about 85-90% of cases[22], an alternative mechanism known as alternative lengthening of telomeres (ALT), is observed in the remaining 10-15% of cancer types. In ALT, telomere elongation is facilitated through break-induced replication (BIR) and homology-directed replication (HDR) processes occurring among telomeres of different lengths[23]. Telomeres exhibit heterochromatic marks, including trimethylated lysine 20 of histone H4 (H4K20me3), lysine 9 of histone H3 (H3K9me3), heterochromatin protein 1 (HP1) proteins, and methylated cytosines[24]. The epigenetic profile of telomeres is hypothesized to act on both telomerase activity and ALT mechanisms[25]. Specifically, the absence of histone methyltransferases leads to the over-elongation of telomeres in mice[26]. Moreover, compromised formation of telomeric heterochromatin may create an environment suitable for recombination, thereby promoting ALT development[27].

## Telomeric-repeat containing RNA (TERRA)

Due to the telomere position effect (TPE) found in *S. cerevisiae* and in humans, telomeres were thought to be transcriptionally silent, mainly because of their heterochromatin nature[28]. Nonetheless, in the mid 2000's telomeres were discovered to be actually transcribed into a class of long non-coding RNA which is called TERRA, for Telomeric Repeat containing RNA[29,30]. TERRA transcription initiates from the subtelomeres and is carried out by RNA polymerase II. The polymerase utilizes the C-rich strand of the telomeric tract as a template for its activity[31]. Consequently, the 5' end of TERRA transcripts consists of distinctive sequences resembling subtelomeric regions, which can vary from one telomere to another and thus, from molecule to molecule. In contrast, the 3' end of these transcripts consists of repetitive sequences of UUAGGG repeats, which are shared among all TERRA molecules. TERRA transcripts exhibit considerable heterogeneity, as it has been shown through Northern blot analysis, with transcript sizes ranging from 0.1 to 9 kb in mammalian cells[29,30]. In human cells, the majority of TERRA molecules are 7-methylguanosine ($m^7G$) capped at their 5' end, and only about 7% of the bulk TERRA population is polyadenylated at the 3' end[32] (Figure 4). Poly(A) TERRA transcripts have a longer half-life (8 hours) compared to the non poly(A) TERRA (3 hours)[33].

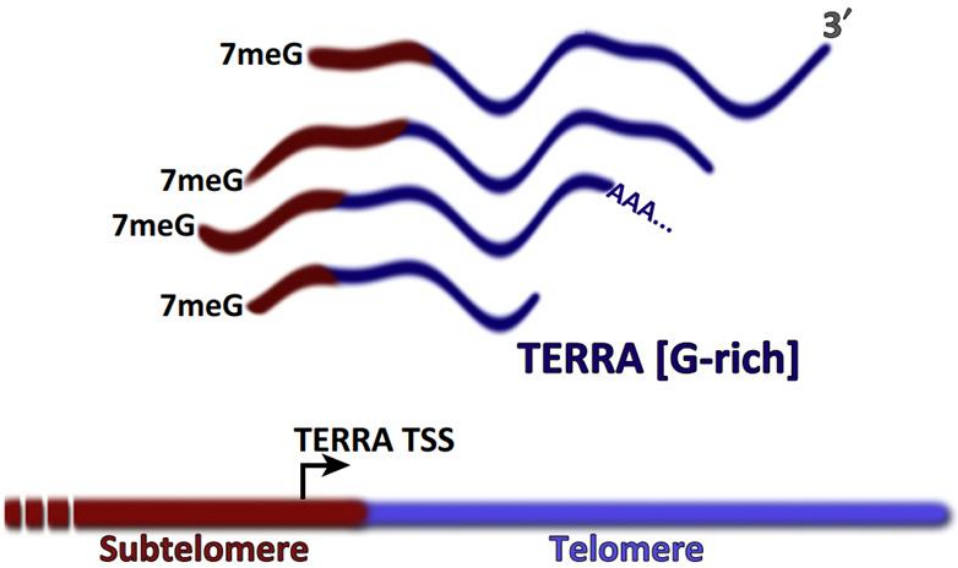


***Figure 4 |*** *TERRA biogenesis. The transcription of TERRA starts from subtelomeric regions and proceeds toward chromosome ends. For this reason, TERRA molecules contain unique sequences originating from the subtelomere of origin at their 5' ends, while at their 3' end they are composed of UUAGGG repeats originating from common telomeric tracts. Adapted from Azzalin & Lingner 2015 [31].*

The mechanism of TERRA polyadenylation is yet to be elucidated, given the absence of a canonical polyadenylation signal at telomeres. In human cells, TERRA transcription occurs from CpG islands situated within specific subtelomeric regions, close to the telomeric tract[34]. A second class of TERRA promoters has been identified in HeLa cells and are located approximately 5 to 10 kb from the telomeric tract of 10 distinct chromosome ends[35]. Intriguingly, both classes of TERRA promoter regions contain binding motifs for the chromatin organizing factor CTCF (CCCTC-binding factor), a pivotal regulator of TERRA expression[36]. Numerous studies, in which telomeric repeat-specific RT primers were employed, along with subtelomeric repeat-specific PCR and qPCR primers, have demonstrated the expression of TERRA from various chromosome ends in human cells[34,35,37–39]. Accordingly, TERRA transcription is influenced by the heterochromatic conditions found in telomeres and subtelomeric regions. Specifically, the methylation of telomeric DNA, along with trimethylation of H3K9 and H4K20, serves to suppress TERRA expression[30,40]. Conversely, histone acetylation is positively correlating with TERRA transcription[41]. TERRA expression is demonstrated to depend on the cell cycle in human, with TERRA levels peaking in the G1 phase and gradually decreasing during the S phase[33].

TERRA molecules are predominantly nuclear and RNA fluorescence *in situ* hybridization (FISH) analyses as well as cellular fractionation studies revealed the enrichment of TERRA at human telomeres[29], with roughly 50% of TERRA molecules not being tightly associated with chromatin. Interestingly, the localization of TERRA appears to be influenced by polyadenylation. TERRA molecules featuring a poly(A) tail are identified in the nucleoplasm and exhibit minimal association with chromatin. In contrast, non-poly(A) TERRA molecules are more uniformly distributed, with 60% of the subpopulation found in the nucleoplasm and 40% in a chromatin-bound state[36]. As previously mentioned, RNA-FISH experiments have shown that TERRA transcripts form distinct foci, with a subset of these foci localizing at telomeres. The localization of TERRA at telomeres is, at least partially, facilitated by its interaction with the shelterin protein TRF2. Indeed, the expression of a dominant-negative form of TRF2 results in a more diffuse nuclear localization of TERRA molecules and a reduced number of TERRA foci in the nucleus[42]. The interaction between TERRA and shelterin components is not the sole mechanism through which TERRA molecules can bind to telomeres. Evidence has demonstrated that

endogenous TERRA transcripts can form RNA-DNA hybrid structures called R-loops with their template DNA strand, occurring in both yeast and human cells[43–45]. However, numerous indications suggest that TERRA transcripts are not stable components of telomere structures, and their positioning at telomeres is meticulously regulated by multiple mechanisms. Depletion of components related to the non-sense mediated mRNA (NMD) pathway or heterogeneous nuclear ribonucleoproteins (hnRNPs), which bind to TERRA, leads to an increased association of TERRA at chromosome ends without influencing its overall expression levels[29]. Conversely, inducing TERRA expression in human cancer cells lacking DNA methyltransferases DNMT1 and DNMT3b does not correspond to an elevated localization of TERRA transcripts at chromosome ends[38]. Collectively, these findings suggest that TERRA transcripts are actively displaced from telomeres. Consistent with this evidence, RNA-FISH analyses clearly indicate that only a specific subset of TERRA transcripts localizes at telomeres at any given time. Additionally, in two separate studies employing the MS2-GFP system to tag and visualize endogenous TERRA molecules expressed from a single telomere in living yeast cells and cancer cells, TERRA molecules were observed to accumulate in foci that transiently localized at chromosome ends[46,47]. Notably, in yeast, TERRA transcripts were found to be selectively recruited to their telomere of origin, positively regulating telomerase activity at the TERRA-transcribing telomere[48]. Taken together, these findings suggest that, both in yeast and mammalian cells, the localization of TERRA transcripts is meticulously regulated at each chromosome end.

The presence of a fine-tuned regulation of the expression and localization of TERRA underscores its potential crucial functions at telomeres[49]. TERRA expression has been identified in diverse organisms, such as yeast, zebrafish, mouse, and human. The considerable conservation observed across evolution implies that TERRA likely performs crucial functions in cell biology. Several lines of evidence suggest that TERRA plays a role in the establishment of telomeric heterochromatin. RNA pull-down experiments have revealed associations between TERRA and heterochromatic proteins, including histone H3K9me3, HP1α, HP1β, and the origin replication complex (ORC), which participates in transcriptional silencing and heterochromatin formation[42]. Additionally, chromatin remodeling factors such as MORF4L2, a component of the NuA4 histone acetyltransferase

complex, and ARID1A, a component of the BAF-type SWI/SNF nucleosome remodeling complex, have been found to interact with TERRA-mimicking oligonucleotides containing the sequence UUAGGG[50]. Consequently, TERRA molecules are proposed to function as scaffold molecules, facilitating the recruitment of proteins and enzymatic activities at telomeres, ultimately promoting heterochromatin formation at chromosome ends and influencing telomere structure and stability. TERRA molecules also interact with numerous extratelomeric DNA loci in the genome to regulate gene expression, particularly in mouse ES cells[51]. Moreover, depletion of TERRA using antisense oligonucleotides results in telomere dysfunction, as evidenced by the accumulation of the DNA damage marker γ-H2AX at telomeres, as well as the dysregulation of various TERRA target genes. These results suggest that TERRA transcripts not only exert their effects locally (in *cis*) at chromosome ends but also globally (in *trans*), influencing widespread gene expression[51].

## Alternative lengthening of telomeres (ALT)

As previously mentioned, it has long been thought that there are two mutually exclusive telomere maintenance mechanisms (TMMs) by which tumor cells can assure telomere homeostasis, with one being the re-expression of telomerase (85-90% among all tumors) and the other being ALT, found in the remaining 10-15% of tumors. Nonetheless, recent studies have highlighted how this distinction is imprecise, for such a simplistic subdivision of TMMs does not reflect the reality found in cancer. In this regard, Barthel and colleagues analyzed 18'430 samples of 31 different cancer types, showing the 73% of samples presented an overexpression of hTERT (indicating a telomerase-positive background), 5% of samples presented alterations in ALT-associated genes (namely ATRX and DAXX) and augmented expression of TERRA (indicating an ALT-positive background), while the remaining 22% of samples did not present any feature related to either telomerase-positive or ALT-positive, suggesting the existence of tumors lacking a TMM[52]. In addition to that, it was also demonstrated that there could be the coexistence of the two TMMs both intra-and inter-tumors. Studies done *in vitro*, working with the known ALT-positive cancer cell lines VA13, GM847 and HOSE demonstrated the presence of both TMMs upon transfection of hTERT and/or hTERC[53–55]. Similar results were obtained working with cell hybrids between the ALT-positive GM847 and several telomerase-positive cell lines which showed telomerase as the only TMM present, suggesting that there is the possibility that telomerase-positive cells harbor factors that inhibit ALT activation[54]. Correlating with a constantly increasing knowledge over the ALT mechanism and the development of ALT-detecting assays (which will be further discussed later on in this thesis work), a coexistence of telomerase and ALT was also found in *ex vivo* human cancers such as soft tissue sarcomas, peritoneal mesothelioma, adrenocortical carcinoma, gastric carcinoma and Wilms tumors[56], as well as in murine TERC-positive keratocytes and squamous cell carcinoma (SCC)[57]. Research has indicated that the activation of the ALT pathway is commonly linked with a distinct phenotype. This phenotype comprises cells heterogeneity, heterogenous telomere lengths, occurrences of telomeric sister chromatid exchanges (T-SCEs), the presence of abundant extrachromosomal telomeric repeats (ECTRs), such as C-circles, nuclei containing ALT-associated promyelocytic leukemia (PML) bodies (APBs) and an increased expression of TERRA[58].

About 90% of ALT-related human tumor cells present mutations in the chromatin remodelers alpha-thalassemia/mental retardation X-linked (ATRX) and death domain-associated protein (DAXX), and a similar mutation rate is found also in cancer cell lines[59]. ATRX collaborates with DAXX to produce the histone variant H3.3 and is predominantly concentrated within repeat sequences found in telomeres, subtelomeres, and pericentromeres. This collaborative effort aims to enhance the cohesion of sister telomeres, thereby elevating the rate of break-induced replication (BIR) in telomeres associated with ALT[59]. In ALT-positive cells lacking ATRX, heterochromatin protein 1 (HP1α) is mobilized to telomeres, resulting in their heterochromatinization and promoting the transcription of TERRA. In the proposed model, TERRA then binds to telomeres, facilitating the formation of R-loops and thereby promoting the activation of the ALT pathway[60].

APBs are observed in about 90% of ALT-positive cells and are a prominent marker for the ALT mechanism. These structures are created by a shell composed of the proteins PML and Sp100, held together by SUMO-interacting motif (SIM) interactions, and involve various proteins related to DNA repair, recombination, replication, telomeric DNA, and shelterin proteins[61,62]. While the exact function of APBs remains unclear, it is hypothesized that they play a role in maintaining telomeres through the ALT pathway. Some studies suggest that APBs function as active centers in the ALT pathway, facilitating telomere clustering and acting as platforms for the concentration of proteins like RPA, Rad51, BLM, and BRCA1, which are essential for ALT-mediated telomere maintenance[63,64]. Notably, disrupting APB formation through PML depletion has been shown to result in the loss of key ALT characteristics and progressive telomere shortening in ALT-positive cells[65].

The ALT pathway exhibits a distinctive feature characterized by a substantial number of extrachromosomal telomeric repeats, consisting of a single-stranded C-rich circles and a double-stranded telomere circles (T-circles). The abundance of C-circles is directly correlated with telomere DNA synthesis in ALT-positive cells, with higher C-circles levels indicating increased activity in the ALT pathway[66,67]. Despite such correlation, the exact mechanism behind C-circles generation in ALT-positive cells remains unknown, as studies shows that telomere DNA damage, in particular DSBs could promote the production of C-circles in ALT-positive cells. Deletion of proteins associated with telomere replication like SMARCAL1 or CTC1-STN1-TEN1 (CST) has been shown to enhance C-circles abundance in

ALT-positive cells, suggesting a connection between C-circles formation and repair of telomeric DNA damage or replication defects in ALT-positive cells[68,69]. T-circles are proposed to be generated through either intramolecular recombination between repeat sequences within telomeres or excision of a sequence from the T-loops[70]. In ALT+ cells, the T-circles can act as a template for telomere elongation through rolling-circle replication. Aberrant HR of telomere sequences triggers the recruitment of DNA repair proteins such as XRCC3, NBS1, and SLX4, leading to T-loop excision in the context of the ALT pathway[71,72]. Furthermore, depletion of FANCD2[73] and overexpression of the helicase BLM[74] result in an increase in ECTRs in ALT-positive cells, indicating that ECTR DNA is linked to the intramolecular resolution of stalled replication forks in telomeric DNA. Additionally, recent reports suggest that damaged single-strand telomeres tend to form internal loops (I-loops), comprising the majority of extrachromosomal telomeric circle structures detected in ALT cells. These I-loops function as substrates for the generation of extrachromosomal telomeric circles, including C-circles[75].

## *C. elegans* as model to study telomere maintenance and ALT

The maintenance of telomeres is an intriguing topic due to its association with aging and cancer. Although telomeres have been extensively studied in numerous organisms, there is insufficient knowledge on telomere biology in *C. elegans*. *Caenorhabditis elegans* serves as a widely utilized animal model for exploring genetics, behavior, development, neurobiology, and meiosis[76]. Therefore, it is particularly important to gain a deeper understanding of the molecular processes occurring at the ends of chromosomes in this nematode. Notably, while telomere transcription has been observed in various organisms, ranging from yeast to humans, where TERRA transcripts are recognized for playing crucial roles in telomere biology, the question of whether *C. elegans* telomeres undergo transcription remains unanswered. The adult nematode of *C. elegans* measures 1 mm in length, with a lifecycle lasting 3 days when cultivated at 25°C from egg to adult. Predominantly existing as a self-fertilizing hermaphrodite, only 0.2% of the *C. elegans* population comprises males. The hermaphrodite is capable of reproduction through self-fertilization or by mating with a male[77].

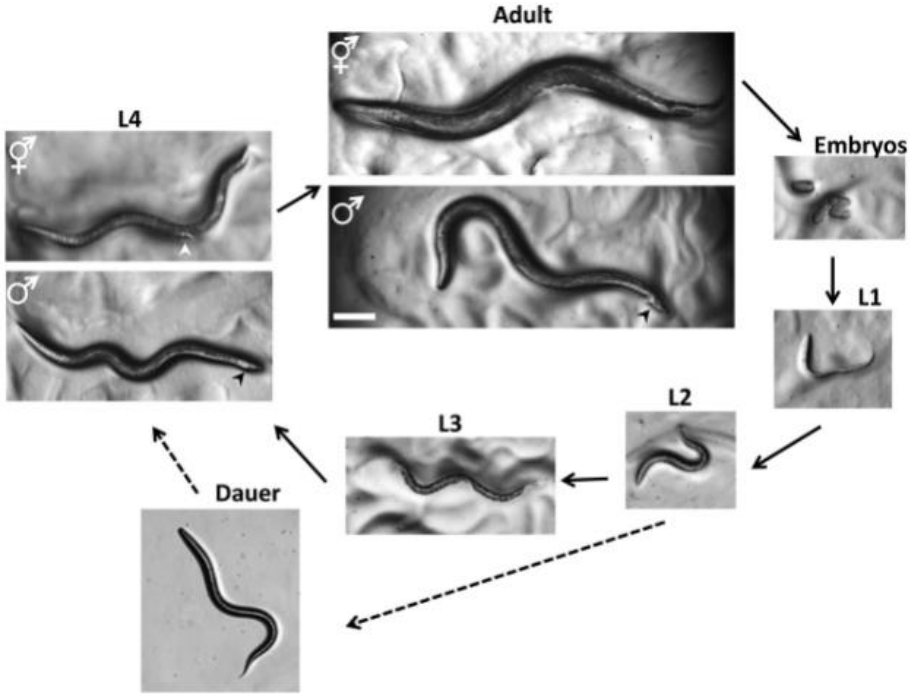


***Figure 5 |*** *The life cycle of C. elegans. Representative images of C. elegans during different developmental stages, showing the differences between hermaphrodite and male. Adapted from Corsi 2015 [77].*

Worms are diploid, possessing a genome consisting of five autosomal chromosomes and one sex chromosome. Hermaphrodites have a genome with two X chromosomes (XX), while males possess only one (XO), a result of a non-disjunction event that may occur during meiosis[78]. *C. elegans* made history as the first animal genome to be sequenced, with a size of approximately 100 million base pairs[79]. Intriguingly, it has been estimated that 30 to 60% of *C. elegans* genes have orthologues in the human genome, emphasizing its potential as a valuable model for studying human pathologies[77]. *C. elegans* undergoes a simple life cycle, where adult hermaphrodites lay embryos that progress through four distinct larval stages (L1, L2, L3, and L4) before reaching sexual maturity (Figure 5). In the absence of food, the worms experience developmental arrest between the L2 and L3 stages, entering an alternative larval stage known as dauer. Upon the resumption of food availability, the nematodes skip directly to the L4 stage to complete their development[76,77].

*C. elegans* quickly became a practical and widely used animal model because of its small size, facilitating easy maintenance and manipulation; its ability to propagate in large numbers, aiding genetic analysis; its transparency, making it suitable for microscopy imaging of cells; and the ability to induce and maintain mutations in homozygosity through self-fertilization. Additionally, by occasionally mating hermaphrodites with males, new mutants and genotypes can be created[80,81]. The anatomy of *C. elegans* is characterized by its simplicity, consisting of a specified number of post-mitotic cells (959 in hermaphrodites and 1031 in males) along with about 1000 germ cells in hermaphrodites and 2000 germ cells in males. The body is organized into tissues, forming concentric tubes, with the outer layer comprising the epidermis, while the interior being a cavity filled with fluid that envelops all the organs. Within the epidermis, there are bands of muscles and ventral and dorsal nerve cords that provide innervation to the muscles. Within the neuromuscular region can be found the digestive, excretory, and reproductive systems[77]. Telomeres in *C. elegans* consist of TTAGGC hexameric repeats, spanning a region from approximately 2 to 9 kb in length. In a study, Raices and colleagues revealed that *C. elegans* telomeres can possess both a C-rich and a G-rich overhangs, along with t-loops, suggesting the involvement of both C-rich and G-rich overhangs in their formation[4]. Notably, telomere length in *C. elegans* is under the regulation of telomerase, with the gene *trt-1* identified as

the catalytic subunit of the enzyme[82]. Intriguingly, mutations such as *trt-1* (*ok410*) do not impact the lifespan of the organisms, as adult nematode somatic cells are post-mitotic and unaffected by telomere shortening; however, in the absence of telomerase activity, germ cells experience progressive telomere shortening over generations, triggering DDR and genome instability, ultimately leading to sterility. The study of telomeres in the *C. elegans* germline is primarily focused on generational aging rather than organismal aging. Conversely, in post-mitotic cells, *C. elegans* offers insights into the non-ageing-related functions of telomeres. Surprisingly, a number of studies indicate that *C. elegans* strains can survive without telomerase by activating Alternative Lengthening of Telomeres (ALT) mechanisms[83,84]. ALT strains, resulting from mutations like *trt-1* and the single-strand DNA telomere binding proteins *pot-1* (*tm1620*) or *pot-2* (*tm1400*), present an intriguing model for investigating ALT mechanisms (Figure 6).

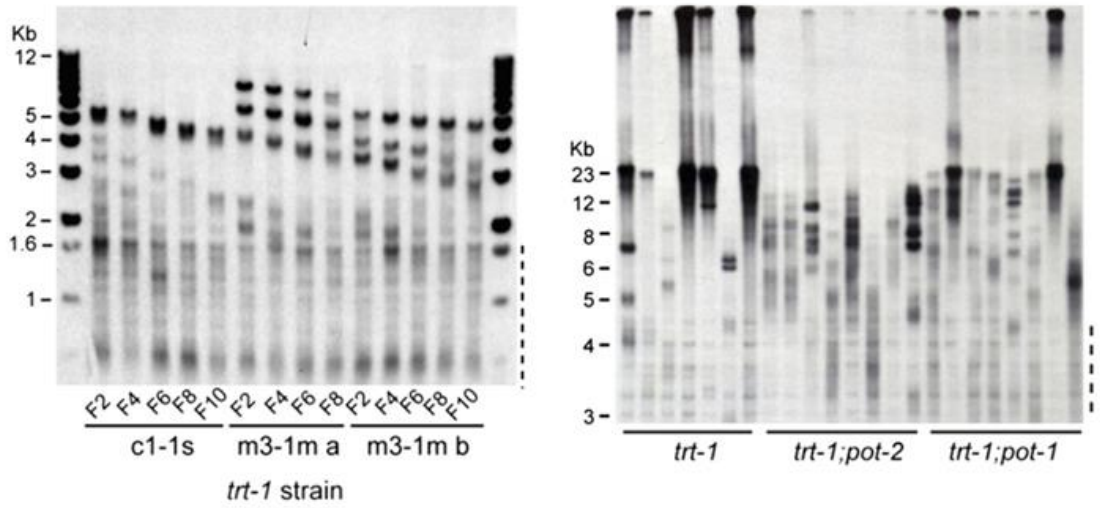


***Figure 6 |*** *Telomere homeostasis in C. elegans. The trt-1 mutant strain displays a progressive telomere shortening over generations (**left**); the lack of trt-1, in combination also with the absence of pot-1 or pot-2, can trigger telomere elongation (**right**). Dotted lines corresponds to internal telomeric repeats (ITRs). Adapted from Cheng 2012 [83].*

Collectively, the mentioned characteristics of *C. elegans* make it a valuable model for investigating molecular mechanisms relevant to human biology. The nematode provides a simplified platform for visualizing these mechanisms, offering new insights into their study in human cells and in particular telomere biology.

## Zebrafish as model to study cancer and TMMs

The zebrafish (*Danio rerio*) is a freshwater fish belonging to the minnow family (*Cyprinidae*) within the Cypriniformes order. In scientific research, the zebrafish has emerged as a prominent choice among animal models for the investigation of developmental processes and gene functionalities[85]. Significantly, its external development and embryonic optical transparency enable visual analyses of developmental processes and the examination of organ alterations across distinct developmental phases. The complete sequencing of its genome has revealed remarkable genetic similarities between zebrafish and human genomes, allowing the study of human genetic diseases in zebrafish. Other advantages include a high reproductive rate and swift generation turnover, facilitating genetic analyses. Embryos and eggs display transparency and resilience, aiding manipulation methods like microinjections[86]. Compared to other animal models the zebrafish offers advantages with notably diminished spatial demands and lower costs associated with maintenance and breeding[87]. Another advantage of the zebrafish lies in its externally occurring early developmental processes, in contrast to mice, making observation and investigation more accessible. While established models like *C. elegans* and *D. melanogaster* are valuable for studying biological processes and large-scale screenings, they fall short in addressing vertebrate developmental processes and other features that are unique to vertebrates. Zebrafish mutant traits, identified through genetic screenings, often resemble stages of human diseases, providing a potent approach to understanding corresponding pathophysiology and discovering novel therapeutic treatments.

An evident example of such diseases is cancer, as zebrafish manifests a broad spectrum of cancers similar to human malignancies. This similarity arises from the conservation of pathways governing vertebrate development, including signaling, proliferation, cell mobility, differentiation, and apoptosis. Shared pathways frequently undergo dysregulation during tumorigenesis. Zebrafish, with its high fertility rate, real-time visualization of tumor progression in vivo, and the possibility of chemical screenings in a large population of genetically identical individuals, represents a robust model for investigating cancer. In cancer research, the unique ability to observe tumor expansion through *in vivo* observation is exclusive to zebrafish, allowing monitoring of tumor

development from larval stages to adulthood[88]. Furthermore, the creation of established zebrafish transgenic strains, incorporating fluorescently labeled cells (such as GFP and mCherry), proves invaluable for tracking cancer cell growth, localized dissemination, and real-time observation of the tumor microenvironment within specific fish body regions. These transgenic strains also serve as functional tools for investigating the expression of human oncogenes within zebrafish-specific tissues, such as the brain, through tissue-specific promoters[89].

Additionally, the successful development of transplanting human cancer cells into zebrafish expands the scope of cancer investigation, including treatments targeting carcinogenesis, genetic screening for proliferation and genomic stability, and situ-specific mutagenesis. Transgenic lines can be generated by expressing human oncogenes under a tissue-specific promoter using the Tol2-mediated Gal4-UAS system[90]. This binary system was subsequently refined to produce stable transgenic lines[91]. The zic4 enhancer mediates the transcription of the human oncogene in brain tissue, specifically expressed in the dorsal midline of the neural tube. This expression is crucial for 4$^{th}$ ventricle morphogenesis and cell proliferation in the dorsal hindbrain[92]. The Tol2-mediated Gal4-UAS system enables the creation of both germline and somatic oncogene-expressing animals. Germline expression is achieved by crossing a fish line carrying the Gal4 sequence under the zic4 promoter with a fish line containing the oncogene under UAS. Consequently, all cells expressing zic4 also express the human oncogene. Conversely, somatic expression involves injecting a plasmid containing the human oncogene under the UAS promoter into one-cell stage embryos that already express Gal4 under the zic4 promoter. In this scenario, only cells that have integrated the plasmid express the oncogene[3].

For the sake of this study, the zebrafish model for brain tumors utilized was established by Mayrhofer and colleagues, in which the binary Gal4-UAS system was employed to trigger the expression of the GFP-HRAS$^{G12V}$ human oncogene[93], fused with the green fluorescent protein (GFP), under the influence of the zic4 enhancer active in neural cells during development[94]. Such induction leads to tumor formation in the adult zebrafish (Figure 7). The expression of zic4 can be confirmed through the incorporation of the enhancer with the red fluorescent protein mCherry. The generation of GFP-HRAS$^{G12V}$ expressing animals, and the analysis of global RNA expression in this model revealed molecular similarities

between this zebrafish brain tumor and human glioblastoma (GBM) of the mesenchymal subtype[95].

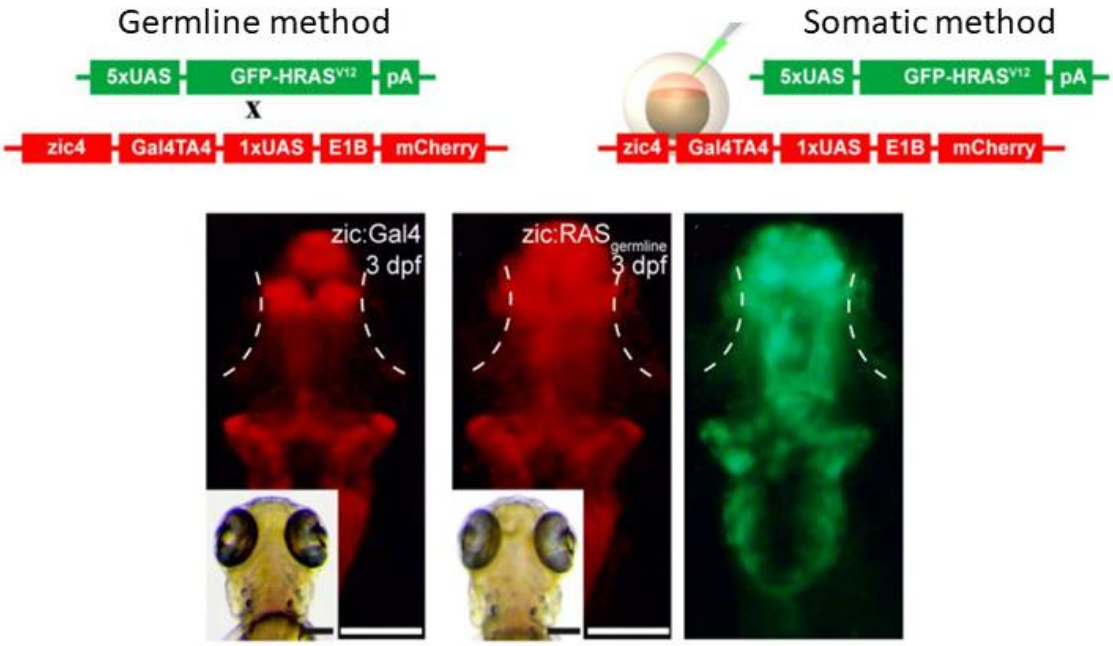


***Figure 7 |*** *The Gal4-UAS system to drive the expression of human oncogene HRAS$^{G12V}$ in the nervous system of the zebrafish. Schematic representation of the generation of the brain cancer model through the germline method (**top, left**) and through the somatic method (**top, right**). The visualization of Gal4-mCherry and GFP-HRAS$^{G12V}$ enables the live monitoring of the formation and progression of the brain tumor (**bottom**). Scale bar: 0.5 mm. Adapted from Mayrhofer 2016 [94].*

The study of the ALT mechanism in cancer has primarily utilized ALT-positive sarcoma cell lines along with their telomerase-positive counterparts[96]. Only more recently TMMs begun to be assessed in primary cancers[97]. Mouse models have played a crucial role in investigating telomere biology and leading to significant advancements in the field[98]; however, mouse telomeres are considerably longer than human telomeres (50 kb versus 15 kb)[99]. Moreover, telomerase remains active in most adult mouse tissues and organs, preventing telomere shortening from being a limiting factor for cellular lifespan in mice. In contrast, zebrafish telomeres range from 15 to 20 kb, and show a closer resemblance to human telomeres (5 - 15 kb).

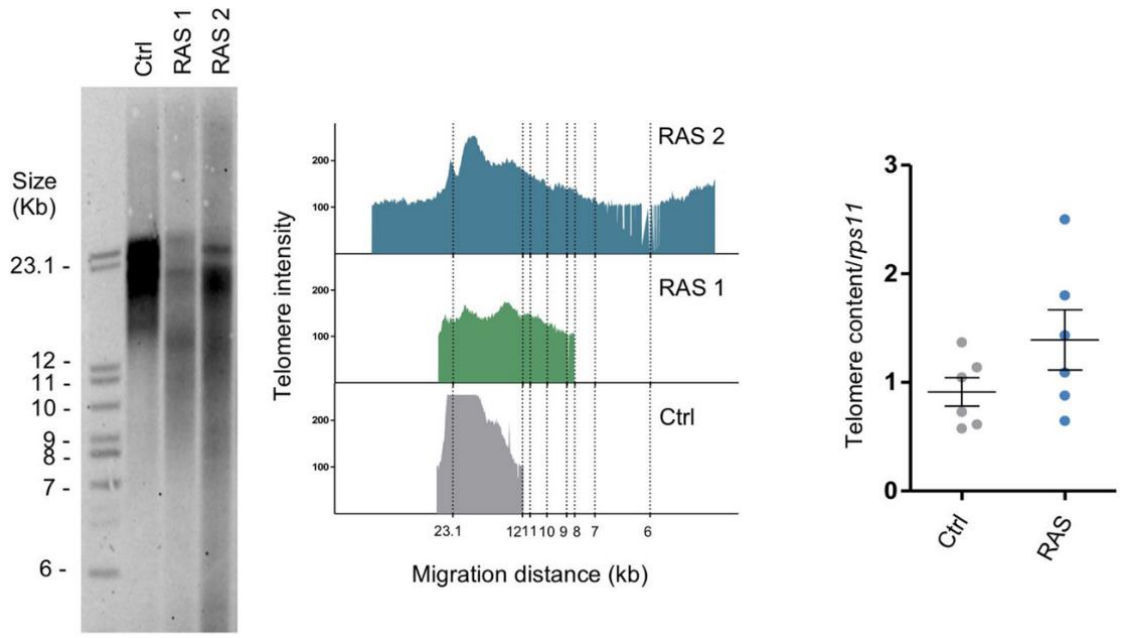


***Figure 8 |*** *TRF coupled with Southern blotting analysis shows long and heterogeneous telomeres in brain cancers (**left**), with a quantification of the intensity of the signal to better emphasize the heterogeneity of telomeres (**middle**). qPCR analysis shows the telomere content, which is higher in RAS brain tumors (**right**). Adapted from Idilli 2020 [3].*

While telomerase is constitutively active in some zebrafish organs, the expression of *tert* mRNA, telomerase activity, and telomere length all undergo significant decreases with age, mirroring patterns observed in human cells. Additionally, levels of *tert* in the zebrafish brain are notably low[100–102]. Finally, this zebrafish brain cancer model is of particular interest and was chosen for this project as it was deeply characterized by Mione lab at CIBIO to be an ALT-positive tumor[3]. Indeed, this model showed ALT-related features that are commonly found in other human cancers, including the presence of long and heterogeneous telomeres in the brain tumor when analyzed with Telomere Restriction Fragment (TRF) coupled with Southern blotting, as well as a higher telomere content through a qPCR analysis (Figure 8).

Furthermore, an increased amount of chromosomal aberrations, namely Telomeric-Sister Chromatid Exchange (T-SCE) was found as a result of the recombinogenic nature of ALT telomeres in tumor (Figure 9).

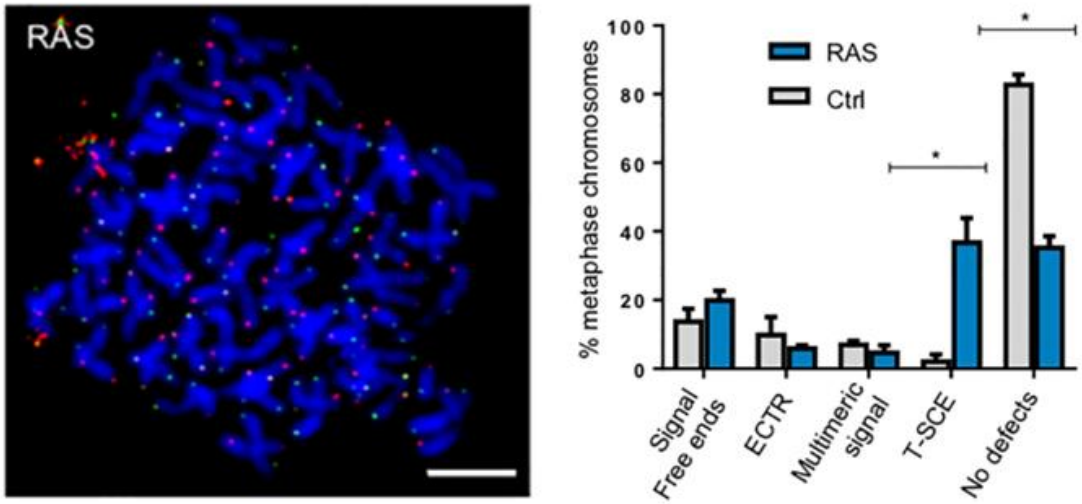


***Figure 9 |*** *Chromosomal rearrangements are found to be enriched in RAS tumors, in particular T-SCE. A representative imagine of chromosome spreads* ***(left)*** *and the quantification of chromosome aberrations identified between tumors and controls (****right****). Scale bar: 5 µm. Adapted from Idilli 2020* [3].

In addition, low levels of telomerase were detected in the RAS tumor, which is a common feature of tumors that rely on ALT to elongate their telomeres. This evidence correlates with a reduction of telomerase activity detected in the tumors through quantitative Telomerase Repeated Amplification Protocol (q-TRAP), as well as a reduction in both TERT mRNA and TERC RNA levels, as assessed through RT-qPCR analysis (Figure 10).

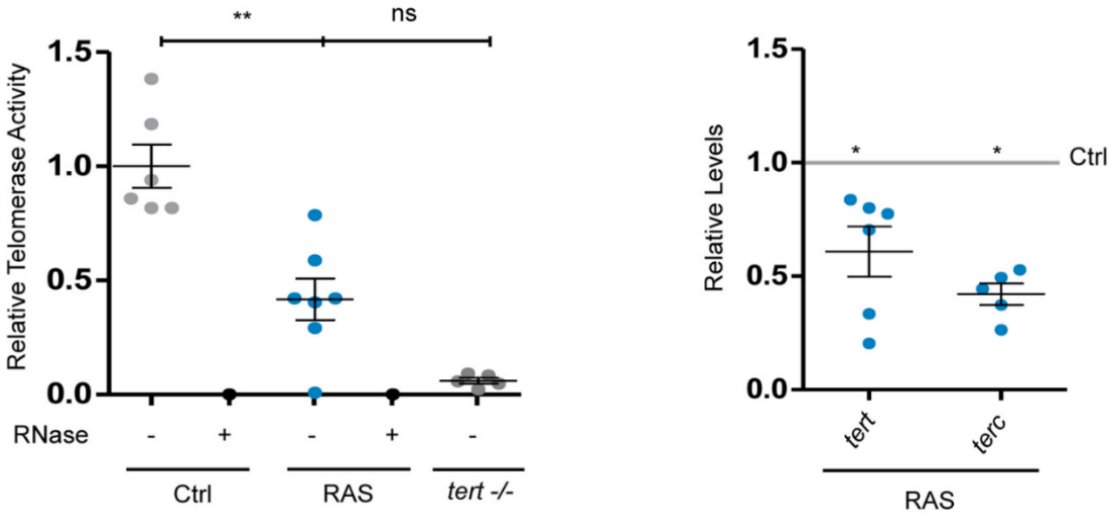


***Figure 10 |*** *Telomerase is not involved in the maintenance of telomeres in the RAS tumor. Q-TRAP analysis shows a reduced activity of telomerase in the tumor as in comparison to the control and to the telomerase-deficient line (tert -/-). RNase was used as a control (****left****). Reduced mRNA levels of both TERT and TERC were found in tumors as in comparison to controls (****right****). Adapted from Idilli 2020* [3].

Importantly, increased TERRA levels were also found in RAS-expressing cultured primary tumor cells, as measured through RNA-FISH using a probe for the detection of the repetitive repeats present at the 3' end of all TERRA molecules (Figure 11). In particular, both the number of foci and relative intensity (meaning the brightness) of the foci were found to be upregulated in the brain tumor cells, consistent with the expected increase of TERRA in ALT-positive tumors.

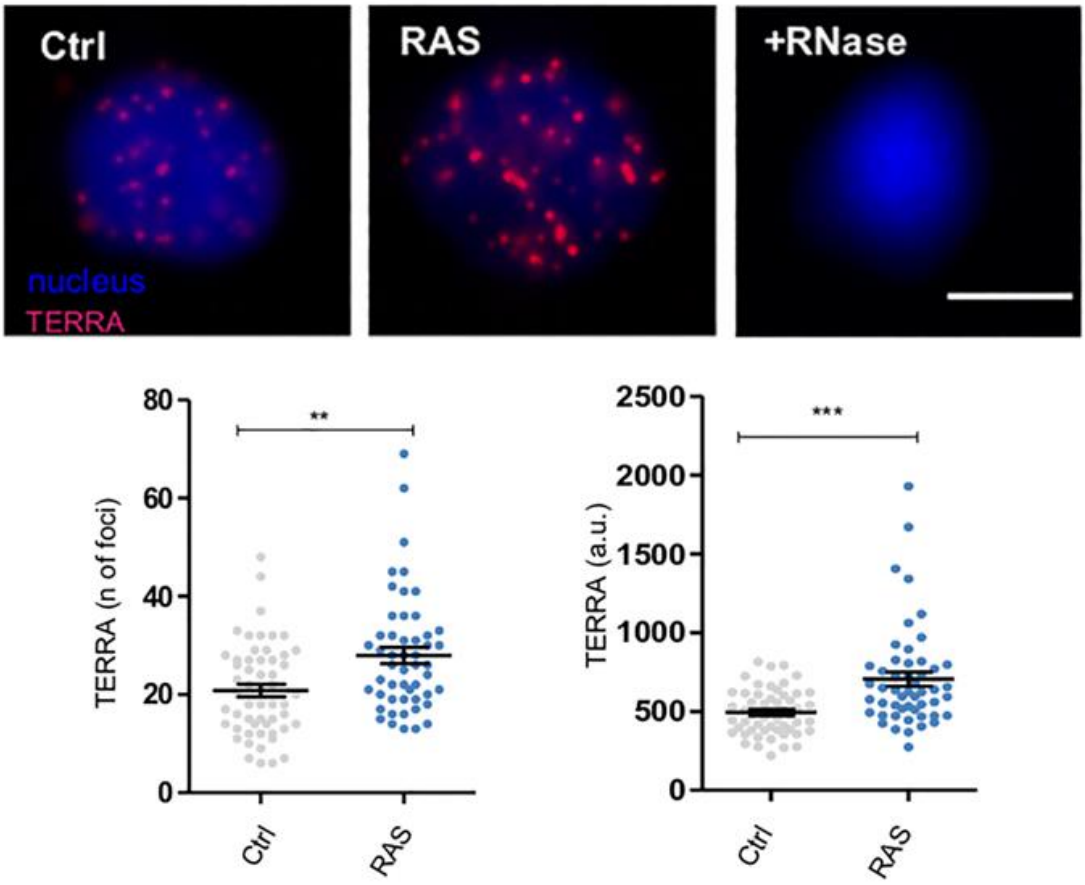


***Figure 11 |*** *High TERRA levels are detected in the nucleus of RAS cells through RNA-FISH (**top**). Scale bar: 5 µm. The number of TERRA foci (**bottom, left**) and the intensity of the foci (**bottom, right**) were significantly higher in RAS tumors. Adapted from Idilli 2020 [3].*

An increase of the bulk population of TERRA was also observed through RNA dot blot, in RAS brain tumors as in comparison to control brains (Figure 12).

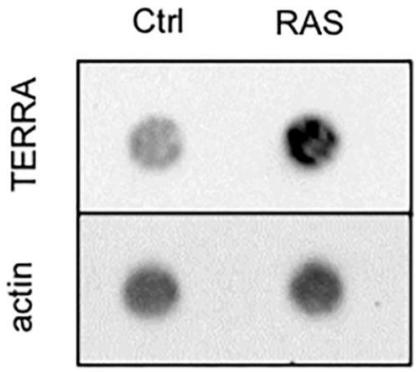


***Figure 12 |*** *RNA dot blot analysis on RAS tumor shows an increased amount of TERRA signal as in comparison to control animals. Normalization of the signals was done on the housekeeping gene actin. Adapted from Idilli 2020* [3].

Lastly, an increase in C-circles was detected in RAS brains compared to controls, a condition that is found exclusively in ALT tumors that elongate their telomeres through HDR (Figure 13).

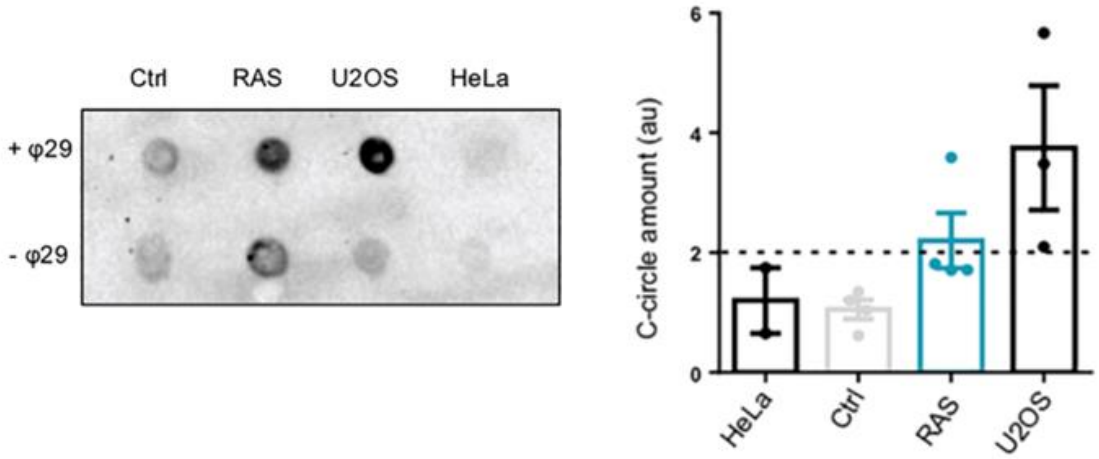


***Figure 13 |*** *C-circles were measured upon rolling circle amplification (RCA) of gDNA and hybridization using a CCCAAT-specific probe for their detection (**left**) and the relative quantification (**right**). HeLa and U2OS human cell lines were used as negative and positive controls, respectively. Adapted from Idilli 2020* [3].

# Aims

In this PhD thesis we want to gain insight on the involvement of TERRA in the ALT mechanism for telomere elongation and maintenance. In particular, we are interested in deregulating TERRA levels and studying the effect on the capacity of cells to maintain and/or switch the ALT mechanism.

To address this point, we decided to employ multiple models to gain a more comprehensive role of TERRA in different organisms with different backgrounds, in particular:

- We aim to study TERRA levels and localization in a non-tumoral telomerase-deficient *C. elegans* model. Nothing is known about TERRA expression and function in this model, which is of particular interest for this project as it was shown to be able to survive and grow in the absence of a functional telomerase through the activity of an ALT-like mechanism.
- We aim to perform a downregulation of TERRA through the use of ASO in an ALT-positive human cancer cell line and check whether TERRA depletion impacts ALT; in addition, we are willing to induce the telomerase-to-ALT transition in an ALT-negative human cancer cell line and analyze the effects of TERRA downregulation during the transition.
- We aim to perform a downregulation of TERRA through the use of ASO in an ALT-positive model of brain tumor in zebrafish, which has been characterized to have high TERRA levels. The zebrafish model is particularly suitable for this task as it is possible to micro-inject the ASO in 1-cell stage embryos, enabling the ASO to diffuse through all tissues, prior the formation of the tumor and the activation of ALT.

# Materials and Methods

## *C. elegans*

### *C. elegans* strains and experimental model

Worms were grown at 20°C on nematode growth media (NGM) plates seeded with OP50 *E. coli*.

The strains used in this study are listed in the following table:

| Strain | Genetic background | Source |
|---|---|---|
| N2 | Wild type, Bristol | Acquired from Caenorhabditis Genetics Center (CGC) |
| *pot-1* | Allele: *tm1620 III* | Acquired from Caenorhabditis Genetics Center (CGC) |
| *pot-2* | Allele: *tm1400 II* | Acquired from Caenorhabditis Genetics Center (CGC) |
| *trt-1* | Allele: *ok410 I* | Acquired from Caenorhabditis Genetics Center (CGC) |
| *pot-1::mCherry* | Allele: *ypSi2 [Pdaz-1::pot-1::mCherry::tbb-2 3'UTR+Cbr-unc-119(+)] II* | Acquired from Caenorhabditis Genetics Center (CGC) |
| *pot-2; pot-1::mCherry* | Alleles: *tm1400 II; ypSi2 [Pdaz-1::pot-1::mCherry::tbb-2 3'UTR+Cbr-unc-119(+)] II* | Generated in this study |
| *trt-1; pot-2; pot-1::mCherry* | Alleles: *ok410 I; tm1400 II; ypSi2 [Pdaz-1::pot-1::mCherry::tbb-2 3'UTR+Cbr-unc-119(+)] II* | Generated in this study |

| Strain | Genetic background | Source |
|---|---|---|
| *trt-1; pot-2* | Alleles: *ok410 I; tm1400 II* | Generated in this study |

To produce double mutant strains, first, starting with one of the two strains to be crossed, we generated a parental (P0) line with higher amounts of males though heat shock (30°C for 5 hours). We placed together hermaphrodites (e.g. *trt-1*) and males (e.g. *pot-2*) for mating, in a ratio 3:1, overnight at 20°C. Subsequently, we collected hermaphrodites and placed them into a new plate, letting them propagate. Then, 10 of the F1 hermaphrodites were placed singularly into new plates to offspring. When eggs were laid, F1 adult hermaphrodites were genotyped for the paternal gene (e.g. *pot-2*): if the mating occurred, they should be heterozygous. Lastly, about 40 F2 hermaphrodites were grown singularly in new plates and once they each laid eggs, the hermaphrodites were genotyped for both paternal and maternal genes. Those plates where both e.g. *trt-1* and *pot-2* resulted mutated were selected for *trt-1; pot-2* propagation. Genotyping was done using sets of 3 primers (when possible) in order to visualize distinct bands between wild type and mutant genes.

The sequences of primers used for genotyping are listed in the following table:

| Gene | Primer | Sequence (5'-3') |
|---|---|---|
| *ypSi2[Pdaz-1::pot-1::mCherry::tbb-2 3'UTR+Cbr-unc-119(+)]II* | Common forward | CAAGACACCCGGGTTTGTCT |
| | WT reverse | CGTTCATACGGCCGAAATTT |
| | Mutant reverse | CAATTCATCCCGGTTTCTGT |
| *pot-2* | Common forward | AAGTTCATTCGGTTGTCGAA |
| | Common reverse | CAATTGTCCAACTCCATATCCA |

| Gene | Primer | Sequence (5'-3') |
|---|---|---|
| *pot-1* | Common forward | TGCAATACACTTACCAGCACA |
| | WT reverse | CTGACCCTTTCACTGTCTTCA |
| | Mutant reverse | TGAACGGAACACTACCAACC |
| *trt-1* | Common forward | ATGGTTGAAATCGAGTGAGCT |
| | WT reverse | TGTCGTAAAGCCATCAGAGC |
| | Mutant reverse | TCACTCCACACCATTGAAGG |

The *trt-1* strain was outcrossed periodically to maintain the line. All the analyses were performed on homozygous mutant strains. Additional information were published in [103].

## Telomere restriction fragment (TRF) coupled with Southern blot

Genomic DNA (gDNA) was extracted by incubating a pool of worms with 1 ml of lysis buffer (50 mM KCl, 1 mM Tris pH 8, 1.5 mM $MgCl_2$, 0.045% Tween-20, 0.045% NP40) and 10 µL of proteinase K (Invitrogen) at 60°C for 1 hour. Then, 200 µl of STE buffer (100 mM NaCl, 1 mM EDTA, 10 mM Tris-HCl pH 8.0) and 200 µl of NaCl 5M were added to the mix. After vortexing, gDNA was subjected to phenol/chloroform extraction and ethanol precipitation. For the TRF reaction, 3 µg of gDNA were digested with the restriction enzyme HinfI (NEB) and separated by an overnight run in 1% agarose 0.5X TBE gel at 30 V. Prior blotting, the gel was incubated in denaturation buffer (0.5 M NaOH, 1.5 M NaCl) for 30 minutes and subsequently in neutralization buffer (1.5 M Tris, 1.5 M NaCl, pH 7.5) for 30 minutes. Blotting was performed by capillarity on a Hybond-N+ hybridization membrane (Cytiva) using 2x SSC buffer. The DNA was cross-linked to the membrane with 120 mJ/$cm^2$ with UVP CL-1000L Longwave Crosslinker. The membrane was incubated in the hybridization buffer [5X SSC, 0,04% v/v SDS, 0.1% v/v sarcosyl] for 1 hour at 42°C and then in hybridization buffer containing the telomeric probe 5'-$(GCCTAA)_5$-3' at 1 nM final concentration, overnight at 42°C. The probe was labelled with digoxigenin using the DIG Oligonucleotide 3'-End Labeling Kit, 2nd generation (Roche) according to the manufacturer instructions. After the hybridization, the membrane was washed twice in 2x SSC, 0.1% v/v SDS at RT, then twice with 0.2x SSC, 0.1% v/v SDS at RT and then twice with 0.2x SSC, 0.1% v/v SDS at 42°C. The membrane was subsequently rinsed in 2x SSC,

incubated with blocking buffer [maleic buffer pH 7.5 (340 mM NaCl, 100 mM maleic acid, 180 mM NaOH), 1% w/v blocking reagent (Roche)] for 1 hour and then with Anti-Digoxigenin-AP Fab fragments (Merck), diluted 1:10.000 in blocking buffer, for up to 6 hours. The membrane was then washed twice with 0.3% v/v Tween-20 (Sigma-Aldrich) in maleic buffer pH 7.5 at RT and equilibrated with AP buffer (100 mM Tris–HCl pH 9.5, 100 mM NaCl). The membrane was then incubated with CDP-Star chemiluminescent substrate (Merck) diluted 1:100 in AP buffer and developed using a ChemiDoc XRS+ (BioRad) for the detection of the signal.

## Telomere restriction fragment (TRF) coupled with Southern blot with pulse-field gel electrophoresis (PFGE)

The procedure for PFGE was similar to what is described for telomere restriction fragment coupled with Southern blot, with the difference that 8 µg of gDNA were digested with the restriction enzyme HinfI (NEB) and run for 13 hours in 1% agarose 0.5X TBE gel using a CHEF DR III Electrophoresis Cell (Biorad) at 6 V/cm, with an included angle of 120°. The TBE buffer was kept at 14°C during the run through the CHEF cooling module.

## Northern blot

Total RNA extraction was performed using the following procedure: worms were collected by centrifugation in M9 buffer (22 mM $KH_2PO_4$, 42 mM $Na_2HPO_4$, 8.6 mM NaCl, 19 mM $NH_4Cl$ in water) from two 6 cm plates, containing about 500 worms. Worm pellets were frozen in liquid nitrogen and subsequently mechanically homogenized with a pestle. RNA was then extracted using TRIzol (Invitrogen) following the manufacturer instructions. RNA integrity was assessed by run on MOPS gel. 15 µg of the extracted RNA was subjected to DNase I (Invitrogen) treatment. RNase-treated control samples were treated with 2 mg/mL PureLink RNase A (Invitrogen). 15 µg of DNase I-treated RNA were run on a denaturing gel [1.5% agarose, 1x MOPS buffer pH 7 (20 mM MOPS, 2 mM sodium acetate, 1mM EDTA) 0.7% w/w formaldehyde (Fisher Scientific), 1:10.000 Xpert Green (GRiSP)] for 4 hours at 90 V. Blotting on Hybond-N+ hybridization membrane (Cytiva) was performed by capillarity using 10× SSC buffer pH 7 (150 mM (tri)sodium citrate dihydrate, 1.5 M sodium chloride). The RNA was cross-linked to the membrane with 120 mJ/cm$^2$ with UVP CL-1000L Longwave Crosslinker. TERRA probe 5'-$(GCCTAA)_5$-3' was terminally labeled with

32P-γATP or 32P-γCTP (Perkin-Elmer) using a forward phosphorylation reaction by T4 polynucleotide kinase (Thermo Fisher Scientific) and the labeled probe was purified using Illustra Microspin G-50 columns (GE Healthcare). The crosslinked membrane after blotting was pre-hybridized 1 hour at 45°C in Church buffer (1% BSA, 1 mM EDTA, 0.5 M phosphate buffer, 7% SDS). 50 µCi of the labeled probe was added, and the hybridization was carried out overnight at 45°C. The membrane was washed twice with 0.1% SDS/2x SSC, four times with 0.1% SDS/0.2× SSC, exposed for 1-7 days and the signal was acquired on Amersham Typhoon 5 (Cytiva).

## RNA dot blot

Total RNA was extracted as indicated in the Northern blot procedure. 500 ng of the extracted RNA was subjected to DNase I (Invitrogen) treatment and 500 ng were treated with 2 mg/mL PureLink RNase A (Invitrogen) as RNase-treated controls. RNA samples were then diluted with EDTA (final concentration 1 mM), added 1 volume of ice-cold pure formamide (Applichem) and denatured at 65°C for 10 minutes, then immediately chilled on ice. RNA is then spotted on a Hybond-N+ hybridization membrane (Cytiva) using 10x SSC buffer using a 96-well Bio-Dot apparatus (BioRad). The RNA was cross-linked to the membrane with 120 mJ/cm$^2$ with UVP CL-1000L Longwave Crosslinker and subsequent probe annealing, membrane exposure and image acquisition were carried out as described in the section of TRF coupled with Southern blot. Quantification of the spots were done using the software CFX Manager 3.1 (BioRad).

## Reverse transcription quantitative PCR (RT-qPCR)

Total RNA was extracted as indicated in the Northern blot procedure. 4 µg of the extracted RNA was subjected to DNase I (Invitrogen) treatment and 2 µg were reverse transcribed using the Superscript III Reverse Transcriptase enzyme (Invitrogen). Two separate RT reactions were performed, using oligo-dT primer for amplification of the housekeeping genes and with a telomeric repeats primer (5'-(GCCTAA)$_5$-3') for TERRA amplification. MRT controls were included in the experiments. Quantitative real-time PCR reactions were performed using the 2x qPCRBIO SyGreen Mix Separate ROX (PCR Biosystems) on the BioRad CFX96 machine.

The primers used in this study are the following:

| Primer | Sequence (5'-3') |
|---|---|
| TERRA-1L_Fw | AAGCCTAAAAAATTGAGATAAGAAAACAT |
| TERRA-1L_Rv | AGGCAGGCAAAATTAGAGGTAC |
| TERRA-1R_Fw | AAGCCTAAGACCAATACCGCAAC |
| TERRA-1R_Rv | GTTTCGGTTGTTGCATCTCTAC |
| TERRA-3R_Fw | ACTGAGCTTTTCCATCCTCGT |
| TERRA-3R_Rv | AACAAACGCGGTGCGGAG |
| TERRA-4L_Fw | AAGCCTAAGAAGAGACCAAACC– |
| TERRA-4L_Rv | GCGAAAGATGAATGTTCAAAGC |
| TERRA-XR_Fw | GCCTGAAAATTCTCATTATTCGATAG |
| TERRA-XR_Rv | TTGATGTGACCAATTGTACTTTTCC |
| arp-6_Fw | AACCATCTACGACGAATCGCT |
| arp-6_Rv | CATGCATTTCAGCTTTTCAGTGATG |

## RNA FISH in combination with immunofluorescence (IF)

Early adult worms (20 hours post L4 stage) were cut in M9 buffer (22 mM $KH_2PO_4$, 42 mM $Na_2HPO_4$, 8.6 mM NaCl, 19 mM $NH_4Cl$ in water) to expose the gonads. 30 bodies for each sample were collected in one 1.5 mL tube. In the tube, samples were fixed with 4% v/v PFA in PBS-T (0.1% Tween in 1x PBS) and permeabilized overnight in 70% v/v ethanol at 4°C on a rotor. Samples were washed twice with 2x SSC-T [0.1% Tween-20 in 2× SSC (0.3 M NaCl, 30 mM (tri)sodium citrate dihydrate)]. Control RNase A treatment samples were treated with 2 mg/mL PureLink RNase A (Invitrogen) in 2x SSC and incubated for 2 hours at 37°C. Samples not treated with RNase were incubated in 2x SSC for 2 hours at 37°C. Samples were washed with wash buffer (10% v/v formamide, 2x SSC in nuclease free water), and then incubated with the telomeric repeat probe (5'-$(GCCTAA)_5$-3'), conjugated with the 6-FAM fluorophore at the 3' and 5' ends, at the final concentration of 2 µM, in hybridization buffer [1% w/v dextran sulphate, 10 mg/mL of *E. coli* tRNA (Roche), 2 mM vanadyl ribonucleoside complex (VRC) (NEB), 0.2 mg/mL RNase-free BSA (Melford), 10% v/v formamide (Fisher Bioreagents) in nuclease-free water], at 37°C overnight. Samples

were washed twice with wash buffer, the first wash was performed at RT for 5 minutes, the second wash was performed at 37°C for 30 minutes, and then samples were washed three times in 2x SSC-T. Samples were then blocked in 3% BSA (Melford) in 2x SSC-T for at least 30 minutes, up to 2 hours and then incubated at 4°C overnight with the primary antibody diluted in 2x SSC-T. Samples were washed three times in 2x SSC-T and incubated with the secondary antibody diluted in 2x SSC-T, for 2 hours at RT. Then samples were stained with 2 µg/mL DAPI. Coverslips were mounted with Prolong Diamond Antifade Mountant (Invitrogen).

The antibodies used in this study are the following:

| Antibody | Source | Dilution |
|---|---|---|
| Rabbit anti-mCherry | Invitrogen #PA5-34974 | 1:500 |
| Goat anti-Rabbit IgG (H+L) Cross-Adsorbed Secondary Antibody, Alexa Fluor 555 | Invitrogen #A-21428 | 1:1500 |

# Human cells

## Cell culture

Human cervical adenocarcinoma (HeLa) cells and human osteosarcoma (U2OS) cells were cultured in DMEM (Gibco), supplemented with 10% fetal bovine serum and 1% penicillin/streptomycin at 37°C with 5% $CO_2$. Cells were regularly tested for mycoplasma contamination. HeLa long telomeres (LT)[104] were kindly provided by the Karlseder lab and were cultured in the same manner as the other cell lines.

## RNA dot blot

RNA extraction was done using TRIzol reagent (Invitrogen) and following the manufacturer's instructions. The procedure for the RNA dot blot is identical to the one described for *C. elegans* RNA dot blot, blotting 500 ng of total RNA and 500 ng of RNA treated with RNase A as control. The hybridization of the probe for TERRA visualization and housekeeping visualization was done in the same way that is described for *C. elegans* Northern blot, using radioactive 32-P probing.

Sequences of the oligos used for 32-P labeling were the following:

| Oligo | Sequence (5'-3') |
|---|---|
| TERRA | CCCTAACCCTAACCCTAACCCTAACCCTAA |
| Actin | CTGCGCAAGTTAGGTTTTGTCAAGAAAGGG |

## RT-qPCR

Total RNA was extracted using TRIzol reagent (Invitrogen) and 2 µg were treated with DNase-I (Invitrogen) following the manufacturer's instructions. Of those 2 µg, 1 µg was used for the RT reaction and 1 µg was used for MRT control reaction. The RT was carried out using SuperScript III (Invitrogen) similar to what is described for *C. elegans*, with the difference that for human samples we performed the reaction using 1 µM TERRA-RT primer $(CCCTAA)_5$ and 1 µM random hexamers in the same mixture.

The primers used in this study are the following:

| Primer | Sequence (5'-3') |
|---|---|
| TERRA-2q_Fw | AAAGCGGGAAACGAAAAGC |
| TERRA-2q_Rv | GCCTTGCCTTGGGAGAATCT |
| TERRA-9p_Fw | GAGATTCTCCCAAGGCAAGG |
| TERRA-9p_Rv | ACATGAGGAATGTGGGTGTTAT |
| TERRA-15q_Fw | CAGCGAGATTCTCCCAAGCTAAG |
| TERRA-15q_Rv | AACCCTAACCACATGAGCAACG |
| TERRA-17q_Fw | GTCCATGCATTCTCCATTGATAAG |
| TERRA-17q_Rv | AGCTACCTCTCTCAACACCAAGAAG |
| TERRA-17p_Fw | CTTATCCACTTCTGTCCCAAGG |
| TERRA-17p_Rv | CCCAAAGTACACAAAGCAATCC |
| TERRA-XqYq_Fw | GAAAGCAAAAGCCCCTCTGA |
| TERRA-XqYq_Rv | CCCCTTGCCTTGGGAGAA |
| TERRA-XpYp_Fw | AAGAACGAAGCTTCCACAGTAT |
| TERRA-XpYp_Rv | GGTGGGAGCAGATTAGAGAATAAA |
| GAPDH_Fw | ACATCGCTCAGACACCAT |
| GAPDH_Rv | TGTAGTTGAGGTCAATGAAGG |

## ALT-FISH

The ALT-FISH was carried out as described in the paper by Frank and colleagues[105]. Briefly, cells were grown on coverslips and fixed with cold ethanol, prior hybridization with 5nM fluorescently ATTO647N-labeled oligos with sequences $(TTAGGG)_5$ or $(CCCTAA)_5$ (Eurofins genomics) for 20 minutes at 37°C. After washing, cells were stained with 1 µg/mL Hoechst 33342 (Invitrogen) for 15 minutes. Coverslips were finally dehydrated and mounted using Prolong Diamond Antifade Mountant (Invitrogen).

# Zebrafish

## Animal housing and transgenic lines

Zebrafish (*D. rerio*) were bred and kept in the Model Organism Facility (MOF) at the Department of Cellular, Computational, and Integrative Biology (CIBIO) at the University of Trento, following standard protocols[106]. Experimental protocols involving zebrafish were in line to European legislation on Animal Protection.

The transgenic lines used were the following:

| Transgenic line | Abbreviation |
|---|---|
| *Et(zic4:Gal4TA4;UAS:mCherry)hmz5* | zic:Gal4 |
| *Tg(UAS:eGFP-HRASG12V)io006* | UAS:RAS |
| *Et(zic4:Gal4TA4;UAS:mCherry)hmz5; Tg(UAS:eGFP-HRASG12V)io006* | zic:RAS |

zic:RAS results from the crossing of zic:Gal4 together with UAS:RAS. Controls animals mentioned in the results section refer to zic:Gal4 animals, which are not developing the tumor. In the zic:Gal4 transgenic line the zic4 enhancer drives the expression of mCherry in the proliferating domains of the developing central nervous system of the fish[91]. In the UAS:RAS transgenic line the oncogenic human HRAS has a point mutation and is fused with GFP; its expression is driven by UAS, which is inactive without Gal4[93].

## Micro-injection

Zebrafish adults from the selected genotypes were bred and embryos were collected and micro-injected using a FemtoJet 1000 (Eppendorf) up to 2-cells stages. Injection mix were prepared in ultrapure water with 0.05% phenol red (Sigma-Aldrich), 1x CutSmart buffer (NEB), 1 mg/mL Dextran-Rhodamine B 10.000 MW Neutral (Invitrogen) and LNA GapmeR ASOs (Qiagen) at variable concentrations. Embryos were grown at 28°C in E3 medium (5 mM NaCl, 0.17 mM KCl, 0.33 mM $CaCl_2$, 0.33 mM $MgSO_4$, 0.0002% methylene blue, pH 6.5).

ASOs sequences were the following:

| ASO | Sequence (5’-3’) |
|---|---|
| TERRA-ASO | TAACCCTAACCCTAAC |
| SCRB-ASO | AACACGTCTATACGC |

## RNA dot blot

Total RNA extraction was performed using the following procedure: the extraction was performed either with pools of whole larvae when working at 5 dpf or with pools of whole brains dissected from adult fish when working with animals at 1 mpf. Mechanical dissection was done using a motorized pestle in TRIzol reagent (Invitrogen) and following the manufacturer’s instructions. RNA was then treated with DNase-I (Invitrogen) following the manufacturer’s instruction and then reaction mixture clean-up was performed using RNA Spin Columns (Macherey-Nagel) following the manufacturer’s instructions. 500 ng of RNA was used for membrane blotting, using 500 ng for RNase A treatment as described in the RNA dot blot section for *C. elegans*. Blotting on the nylon membrane was carried out as described in the RNA dot blot section for *C. elegans* while the radioactive labeling and detection with 32-P probes was done as described in the Northern blot section for *C. elegans*.

Sequences of the oligos used for 32-P labeling were the following:

| Oligo | Sequence (5’-3’) |
|---|---|
| TERRA | CCCTAACCCTAACCCTAACCCTAACCCTAA |
| rps11 | GTCTCTTCTCAAAACGGTTGTACTTGCGGA |

## Reverse transcription quantitative PCR (RT-qPCR)

Total RNA was extracted as indicated in the Northern blot procedure. 2 µg of the extracted RNA was subjected to DNase I (Invitrogen) treatment and 2 µg were reverse transcribed using the Superscript III Reverse Transcriptase enzyme (Invitrogen). Two separate RT reactions were performed, using random hexamers for amplification of the housekeeping gene and with a telomeric repeats primer (5’-$(CCCTAA)_5$-3’) for TERRA amplification. MRT

controls were included in the experiments. Quantitative real-time PCR reactions were performed using the 2x qPCRBIO SyGreen Mix Separate ROX (PCR Biosystems) on the BioRad CFX96 machine.

The primers used in this study are the following:

| Primer | Sequence (5'-3') |
|---|---|
| TERRA-3S_Fw | GAGGTAATGTTCAACTTAATAATTG |
| TERRA-3S_Rv | GTTTCTTAACCAATCCTAAACTTC |
| TERRA-17S_Fw | TGAAGAGGATTCAAACTGCTGG |
| TERRA-17S_Rv | CCTCTCTCTTCAAACACTAGCC |
| TERRA-17L_Fw | TGTTGTTGTTGGGTTTGCGA |
| TERRA-17L_Rv | AGCACACATTTCGGGGAGTA |
| TERRA-18L_Fw | AACCTTATCTTGGATCGATGTCA |
| TERRA-18L_Rv | AAAGAGGATTCAAAATGCTGGTT |
| TERRA-24S_Fw | CCCTACACTCACCCTAACCC |
| TERRA-24S_Rv | TTATGTGTGCGTGTGTGTGC |
| rps11_Fw | ACAGAAATGCCCCTTCACTG |
| rps11_Rv | GCCTCTTCTCAAAACGGTTG |

## Whole brain immunofluorescence (IF)

Embryos were grown in E3 medium supplemented with 200 µM 1-phenyl 2-thiourea (PTU, Sigma) starting from 24 hpf until 5dpf, when the whole larvae were then fixed in 4% PFA overnight. The next day, larvae were washed three times with 0.1% Triton X-100 in PBS 1x and fixed brains were dissected from the rest of larvae and placed in 0.1% Triton X-100 in PBS 1x for 30 minutes. Then brains were placed into blocking solution (0.5% Triton X-100, 5% Normal Goat Serum, 0.001 sodium azide, PBS 1x), washed three times in it and incubated overnight in blocking solution at 4°C. The next day, brains were incubated with a rabbit antibody anti-PHH3 (Sigma-Aldrich #06-570), 1:1000, in blocking solution overnight at 4°C. The next day, brains were washed three times in blocking solution and incubated with goat anti-rabbit-AF633 (Invitrogen) overnight at 4°C. The next day, brains were washed three times in 0.1% Triton X-100 in PBS 1x and imaged using a confocal

microscope Nikon AX, using air 20x magnification. Endogenous HRAS-GFP was imaged using the laser at 488 nm for excitation. Analysis of the images were done using ImageJ.

## Survival curve

20 larvae were placed starting from 5 dpf in the zebrafish water tank (Tecniplast) and kept in the MOF at CIBIO following the standard protocols. Starting from 7 dpf, the number of living animals were counted each week, for a total of 5 weeks. The experiment was repeated three times per each condition.

## Morphology analysis

To study morphology alterations, larvae were grown to 10 dpf, then anesthetized using 0.2 mg/mL MS-222 (Sigma-Aldrich) and placed sideways in 1% low-melting agarose. Once the agarose solidified, colored images of the animals were taken using a Leica MZ16F stereomicroscope. 25 animals were used per each condition. Analysis of the images were done using ImageJ.

## Statistical analyses

Statistical analyses shown in all results sections were done by using the software GraphPad Prism. In particular, significance among different conditions were measured through unpaired t-test when analyzing two conditions at the time, while ordinary one-way ANOVA was used when comparing three or more conditions simultaneously.

The symbols used in all graphs correspond to the following p-values:

| Symbol | Meaning |
|---|---|
| No symbol | $P > 0.05$ |
| * | $P \leq 0.05$ |
| ** | $P \leq 0.01$ |
| *** | $P \leq 0.001$ |
| **** | $P \leq 0.0001$ |

All histograms in this thesis show the mean and the error bars represent the standard error of the mean (SEM). Instead, violin plots are depicted as truncated violin plots (to avoid having negative values); dotted lines within the plot represent median and quartiles.

# Results

As this thesis comprises work done on several model systems, both of animal and human origins, we decided, for a matter of clarity, to stratify results, discussion and future perspectives based on the model used.

First, we started with *C. elegans*, as the simplest of the three models and the only one where we did not implement TERRA downregulation. In worms we are interested in deepening our understanding on TERRA and its involvement in ALT, as ALT spontaneously arises in animals lacking telomerase. It is important to keep in mind that our analyses in *C. elegans* are done in a non-cancerous background.

Subsequently, we moved our focus on more complex and cancerous backgrounds (namely human cancer cells and the zebrafish) where we decided to manipulate TERRA levels though its downregulation via ASO. In human cancer cells, we employed an ALT-positive line and looked at the effect of TERRA downregulation on ALT, with the idea of analyzing the effect of TERRA depletion in telomerase-positive cells when the telomerase-to-ALT transition is induced.

We then moved to zebrafish, in particular to an *in vivo* model where we can induce the formation of brain cancers that develops to become ALT-positive. The practicality of this model stems in the fact that 1-cell stage zebrafish embryos can be micro-injected with antisense oligonucleotides (such as morpholinos or ASOs) to downregulate genes of interest from the earliest developmental stages through animal growth.

## *C. elegans*

### *pot-1* and *pot-2 C. elegans* mutants present enhanced TERRA transcription

In a work recently done in our lab, we showed that TERRA in *C. elegans* is expressed with differences among different strains. In particular, we took advantage of two mutant lines that are lacking two human orthologues of the shelterin complex protein POT-1, namely pot-1 and pot-2[107]. By performing Northern blot and RT-qPCR using primers for the detection of TERRA transcribed from single telomeres, we showed that both *pot-1* and *pot-2* mutant worms displayed increased levels of TERRA, in a telomere specific-manner (Figure 14). To investigate the expression of TERRA at the level of single telomeres, Manzato and colleagues from our lab developed RT-qPCR primers to detect specific and unique regions found at the 5' ends of TERRA transcripts[103]. More specifically, upon the generation of cDNA through reverse transcription using a common primer annealing to TERRA repetitive hexamers $(GCCTAA)_5$, 5 (out of 12 possible telomeric ends found in the nematode) primers couples were designed and validated to visualize single TERRA transcripts expressed from *C. elegans* telomeres 1L, 1R, 3R, 4L, XR, namely TERRA-1L, TERRA-1R, TERRA-3R, TERRA-4L, and TERRA-XR.

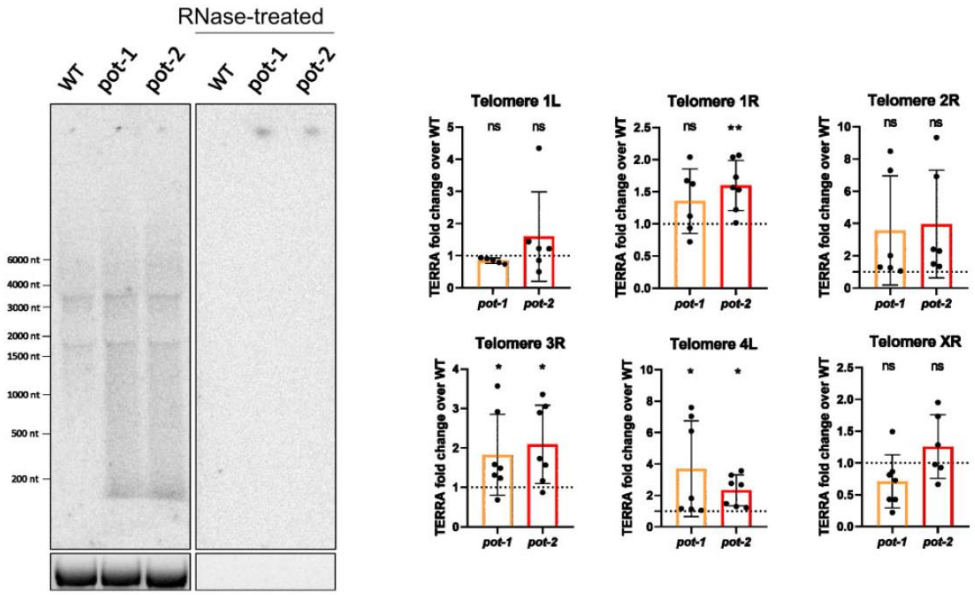


***Figure 14 |*** *pot-1 and pot-2 mutant strains show increased TERRA expression compared to WT animals. Northern blot analysis (**left**) and RT-qPCR analysis (**right**) demonstrate an increased transcription of TERRA in the absence of pot-1 and pot-2, compared to WT animals. Bottom image shows 18S rRNA band upon gel run. RNase-treated samples are shown to ensure specificity of the signal is not directed to DNA. Taken from Manzato 2023 [103].*

Such findings indicated that pot-1 and pot-2 not only were already known to be negative regulators of telomere replication[107], but they also repress TERRA transcription, possibly through the capping of telomeres thus impeding the RNA polymerase to operate transcription.

Interestingly, the absence of either *pot-1* or *pot-2* is not sufficient to trigger the activation of ALT-like mechanisms to elongate telomeres, as this can be done in worms where telomerase is not active[83,84]. For instance, a phenotype that can be observed when telomere homeostasis is not active and telomeres become critically short is sterility. In the case of *pot-1* and *pot-2* mutants no such phenotype is detectable in the animals, regardless of their generation of growth.

Taken together, these data show that *pot-1* and *pot-2* repress TERRA transcription in a telomere-specific manner.

## The *C. elegans trt-1* mutant displays progressive telomere shortening and chromosome aberrations

The expression of TERRA has been shown to change based on the length of telomeres[40,46,108]. To this aim, we decided to exploit the strain *trt-1*, a *C. elegans* strain lacking the catalytic subunit of telomerase and where telomeres were shown to progressively shorten over generations[82]. We performed a telomeric restriction fragment (TRF) analysis coupled with Southern blotting to enable the visualization of telomeric length (Figure 15).

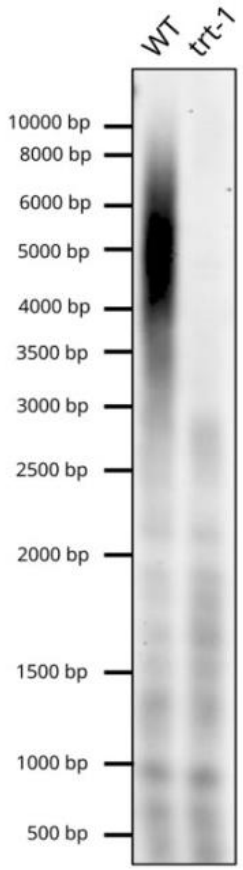


***Figure 15 |*** *trt-1 mutants display shorter telomeres. TRF analysis coupled with Southern blot shows a reduction of telomeres in the trt-1 strain (F14) compared to WT. The pattern visible from 2.5 kb and lower represents internal telomeric regions (ITRs).*

In these experiments we observed a clear reduction in telomere length at generation 14 (F14) in *trt-1* mutants, with bands starting from approximately 2.5 kb and lower representing internal telomeric regions (ITRs). It is worth noting that *trt-1* worms at F14 displayed a sterility phenotype, with a decreased reproduction rate compared to WT. A

greater number of starved worms (>100) were then chunked to new plates in comparison to WT (10-20) to have a higher chance of selecting non-sterile worms and allow the continuity of the line[82].

A phenotype that has been previously correlated with telomere erosion is chromosomes fusions[82]. In particular, by staining condensed chromosomes in maturating oocytes during diakinesis, in WT worms it is possible to visualize the canonical 6 chromosomes that are found in *C. elegans*, while in *trt-1* mutants we can appreciate chromosome fusions, resulting in a lower number of separate chromosomes (typically 2 to 4) which in turn tend to be longer than the WT (Figure 16).

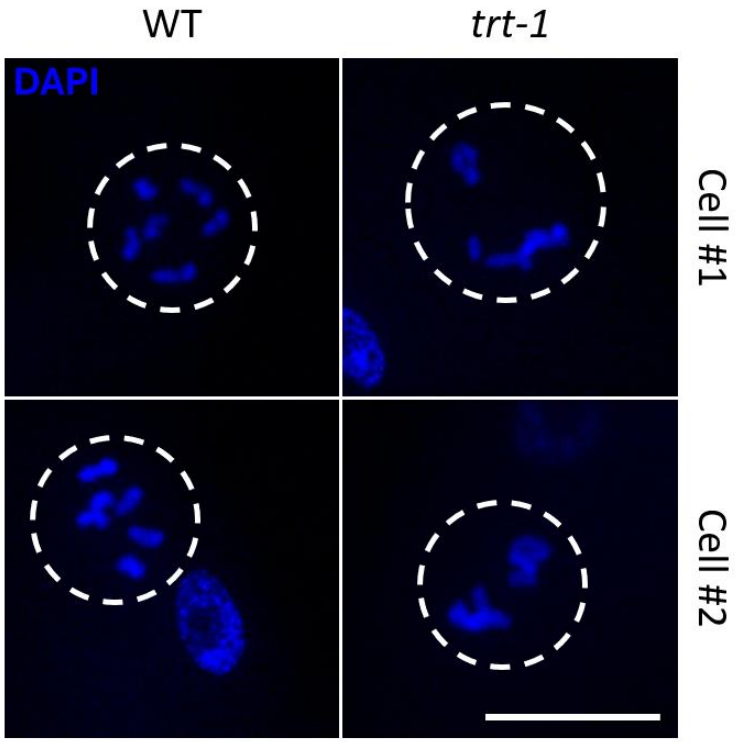


***Figure 16 |*** *During diakinesis, through confocal imaging and DAPI staining maturating oocytes in trt-1 animals show the presence of chromosome fusions, while in WT animals 5-6 separate chromosomes can be detected. Scale bar: 10 µM.*

Taken together, these data confirm that trt-1 mutants display short telomeres and chromosome aberrations, most likely due to the absence of a mechanism to ensure telomere elongation, as previously described in literature.

## TERRA expression in *trt-1* is regulated in a telomere-specific manner upon telomeric shortening

Once telomere shortening was confirmed, we investigated the expression of TERRA. Indeed, TERRA expression has been previously shown to be regulated by telomere length in different organisms, with short telomeres expressing high TERRA levels in yeasts[46], while telomere over elongation associates with decreased signal of TERRA in human cells[40]. Therefore, we asked whether telomere length influences TERRA levels in *C. elegans*. To analyze the bulk population of TERRA, we performed a Northern blot using total RNA from *trt-1* mutants and visualized TERRA through the use of radioactively labeled probe with telomeric sequence $(GCCTAA)_5$ which is able to recognize the repetitive sequences found at the 3' ends of TERRA transcripts in *C. elegans*.

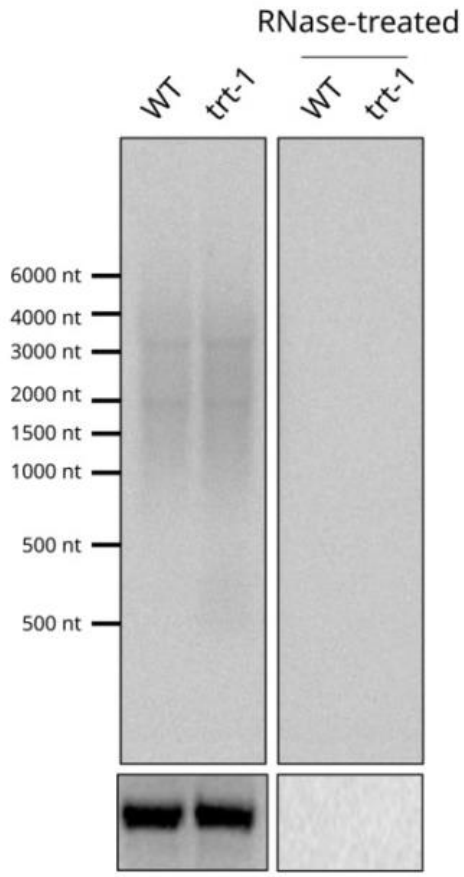


***Figure 17 |*** *Total TERRA levels remain unchanged in in trt-1 worms. Northern blot analysis shows no expression difference in terms of the total population of TERRA in trt-1 animals when compared to WT. Bottom image shows 18S rRNA band upon gel run. RNase-treated samples are shown to ensure specificity of the signal is not directed to DNA. The experiment was repeated 4 times.*

These experiments indicated that total TERRA levels remain unchanged in *trt-1* mutant worms, retaining short telomeres, as compared to a WT strain (Figure 17). Furthermore, TERRA signal in worms appears as a heterogeneous smear (similar to what is found in other organisms) ranging from 0.5 to 6 kb, with a more intense signal from 1.5 to 3 kb. The RNA nature of the signal is confirmed by a complete abolishment of the signal in RNase A treatment.

Interestingly, the RT-qPCR analysis using the same primers mentioned in the previous paragraph shows a finely tuned telomere-specific regulation, displaying a statistically significant reduction of TERRA 1L and 1R in *trt-1* as in comparison to WT, while no difference was detected in TERRA 3R and a slight increase was found in TERRA 4L (Figure 18).

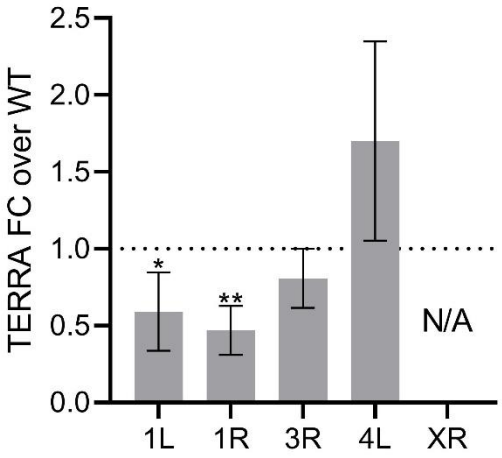


***Figure 18 |*** *A telomere-specific regulation of TERRA expression in trt-1 animals is visible when analyzed at the level of five individual telomeres by RT-qPCR analyses. N/A means Ct values in RT-qPCR were above 40. X axis indicates telomeres. t-test was used to assess significance. * = p≤0.05; ** = p≤0.01. The experiment was repeated 3 times. FC: fold change.*

Notably, TERRA XR was non-detectable in *trt-1* mutants. We do not know the exact reason behind such phenomenon, but we believe it could not be attributed to technical issues as the same pattern (non-detectable TERRA XR signal in *trt-1* animals) was seen in all replicates among different experiments. We speculated that, as chromosome fusions and degradation with consequent loss of telomeric repeat tract are taking place in worms lacking telomerase, the deriving aberrations in *trt-1* might alter preferentially a number of chromosome ends such as telomere XR. The absence of telomeric repeat tract at the

telomere XR would result in TERRA molecules devoid of G-rich 3' end which are not reverse transcribed using the TERRA-RT primer and thus remaining undetectable at RT-qPCR analyses. However, this possibility will need to be further investigated.

Taken together, these data suggest that *trt-1* display a progressive shortening of telomeres due to the lack of an active telomerase, while the expression of TERRA is finely tuned in a telomere-specific manner and might correlate at least in part to telomere length and erosion.

## ALT survivors *trt-1; pot-2* worms display long and heterogeneous telomeres

A number of studies showed how an increase of TERRA levels is found in human and yeast telomerase-negative which utilize ALT as a telomere maintenance mechanism[27,109]. To study the regulation of TERRA in an ALT-positive background, we decided to employ a double mutant *C. elegans* model, *trt-1; pot-2*[83,84]. The lack of telomerase in the nematode, together with a progressive telomere shortening and the need to elongate telomeric ends to overcome cell cycle arrest and sterility, is sufficient to trigger stochastic events, yet unknown, that trigger the activation of an ALT-like mechanism for telomere elongation; however, the number of "ALT survivor" worms that spontaneously form is extremely low, many times leading to full sterility of *trt-1* animals and loss of the mutant line before the formation of an ALT survivor. To overcome such issue, the loss of pot-2, the homolog of human telomere binding protein POT-1, which is capping and protecting *C. elegans* telomeres, is sufficient to increase the chance of generating ALT survivors. The unprotected telomeres in *pot-2* mutants might be more accessible to the HDR machinery that is exploited during ALT.

First, we generated the double mutant *trt-1; pot-2* line by crossing *trt-1* and *pot-2* single mutants and selecting homozygous double mutants through genotyping. The mutant line we generated started showing sterility phenotype, with a decreased replication rate within F14-F16. We grew the *trt-1; pot-2* worms using the favorable conditions described in the previous paragraph[83], until growth rate was restored to those found in WT animals. In this manner, we were able to isolate 3 independent ALT survivors, which we will refer to as clone 10, clone 14, and clone 18 that were propagated for up to F150 under standard growing conditions.

The normal growth rate found In ALT survivors suggest the activation of a telomere maintenance mechanism and to test this hypothesis we performed a TRF coupled with pulse-field gel electrophoresis (PFGE) and Southern blotting to visualize telomere length (Figure 19). Interestingly, telomere length is increased in early generation worms as in comparison to WT. Strikingly, the 3 clones also present longer telomeres than WT and comparable in terms of size to those found in early generations animals (considering

clones were at F90 at the moment of the analysis); however, the band patterns found in the clones not only is different from the parental line, but also differ from one another, possibly due to the heterogeneity nature resulting upon ALT activation.

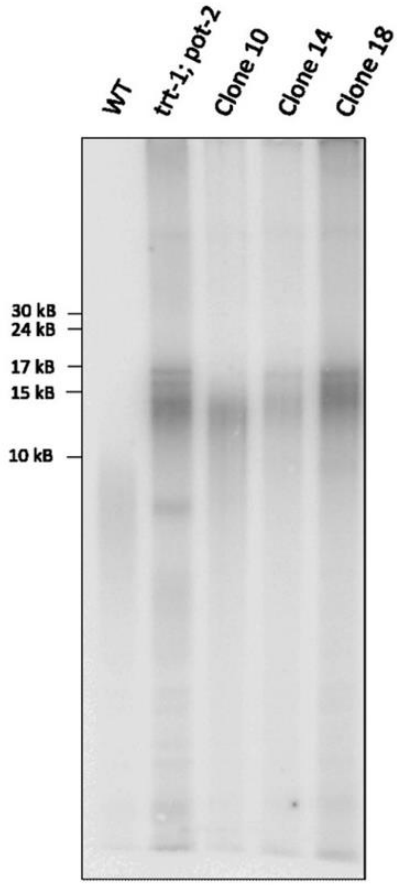


***Figure 19 |*** *ALT survivors present long and heterogeneous telomeres and high levels of TERRA. Telomere restriction fragment (TRF) analysis coupled with pulsed-filed gel electrophoresis (PFGE) and Southern blotting shows how trt-1; pot-2 double mutants elongate telomeres in an ALT-like manner, making them extremely long and heterogeneous. Such phenotype is visible during both early generations (trt-1; pot-2 lane) and in ALT survivor clones. WT average telomeric length can be visualized in the WT lane.*

## TERRA levels increase in the double mutant *trt-1; pot-2 C. elegans* strain prior the insurgence of ALT

To investigate TERRA expression, we performed a Northern blot analysis on early generations animals and the ALT survivors. Interestingly, we found that the bulk population of TERRA was upregulated during early generations in comparison to WT (Figure 20). Surprisingly, the levels of TERRA in the 3 clones where the ALT-like telomere mechanism has been going on for about 90 generations were similar to the parental line, with clone 18 showing a stronger signal compared to clone 10 and clone 14.

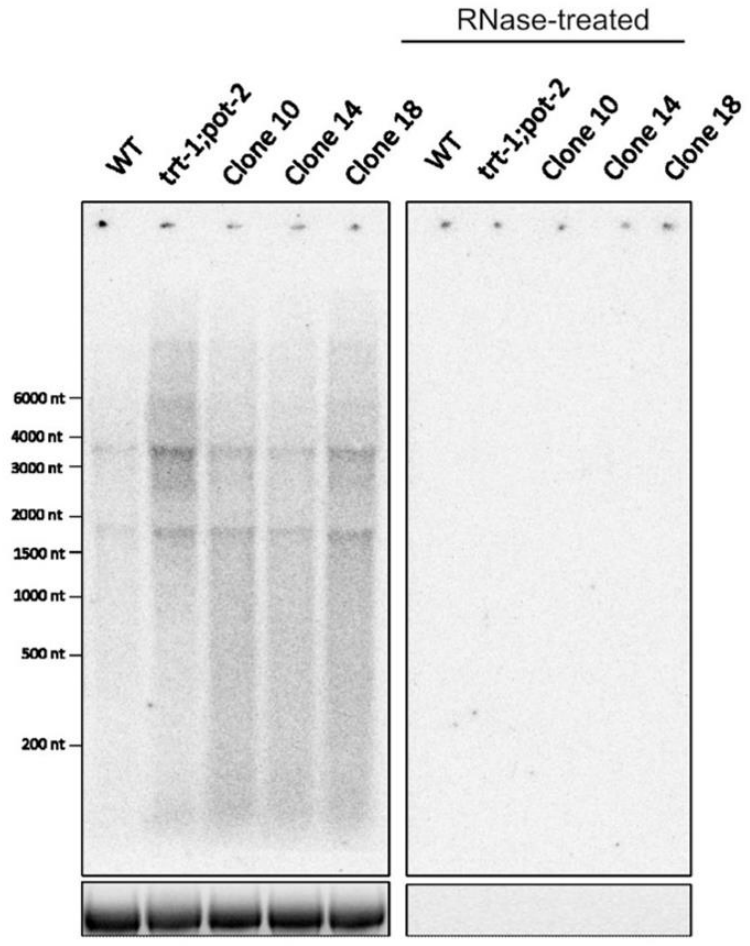


***Figure 20 |*** *Northern blot on total RNA shows an increase of total TERRA levels during early generations trt-1; pot-2 and in ALT survivor clones (clone 10, clone 14, clone 18), as in comparison to WT animals. The experiment was repeated 4 times. RNase-treated samples are shown to ensure specificity of the signal is not directed to DNA. Bottom image shows 18S rRNA band upon gel run.*

We then employed the same RT-qPCR primers as described in the previous paragraph to analyze TERRA expression from single telomeres. In line with the findings described in other *C. elegans* strains, we found telomere-specific differences in TERRA levels between

WT and *trt-1; pot-2* double mutants (Figure 21), while no significant difference between early and late generations animals were detected from most telomeres except for telomeres 1R in clones 10 and clone 18 (Figure 22).

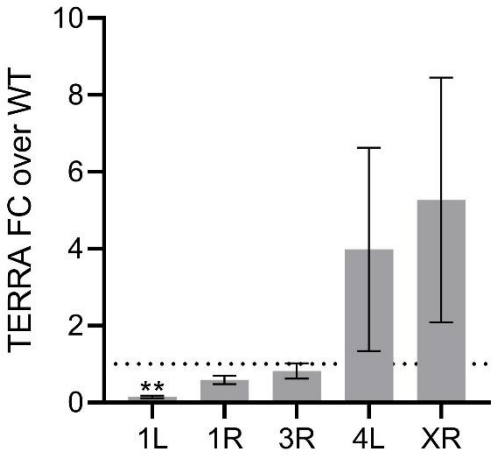


***Figure 21 |*** *RT-qPCR on trt-1; pot-2 early generations shows a telomere-specific regulation of TERRA when compared to WT animals. Results are shown as fold change (FC) over WT animals. t-test was used to assess significance. ** = p≤0.01. The experiment was repeated 4 times.*

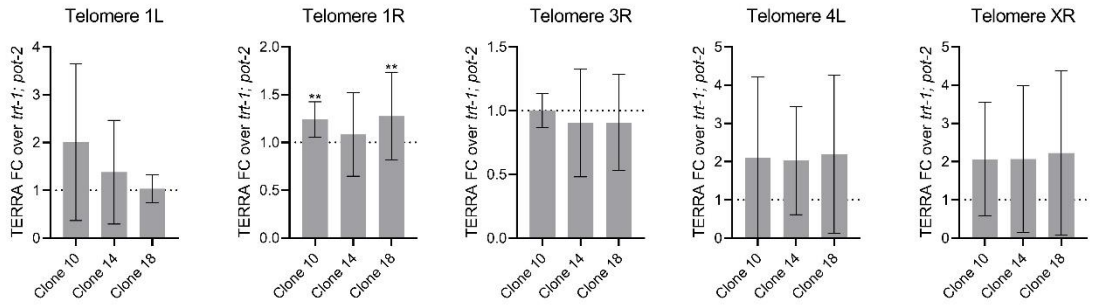


***Figure 22 |*** *RT-qPCR on trt-1; pot-2 early and late clones show no difference in TERRA levels from most telomeres between early and late generations. Results are shown as fold change (FC) over WT animals. . One-way ANOVA was used to assess significance. ** = p≤0.01. The experiment was repeated 4 times.*

Taken together, these data show how prior the ALT onset the *trt-1; pot-2* double mutants display long and heterogeneous telomeres with an increase of TERRA levels. These features are then maintained during later stages once the ALT-like mechanism for telomere maintenance has been active for many generations.

## The triple mutant *trt-1; pot-2; pot-1::mCherry* can be used to analyze the dynamics of TERRA and telomeres

Given that TERRA levels increase prior the activation of the ALT-like mechanism for telomere maintenance, we wondered whether TERRA dynamics change upon the activation of ALT. To do so, we generated a new *C. elegans* strain by crossing the double mutant *trt-1; pot-2* that we already employed in the previous analyses with the *pot-1::mCherry line*[107,110]. This line, which was generated in Dr. Ahmed lab, expresses a fusion protein composed of the full length pot-1 lacking the stop codon and the fluorescent protein mCherry. At microscope analyses, animals with the *pot-1::mCherry* genetic background were shown to generate approximately 12 discrete pot-1:mCherry foci that were demonstrated to colocalize with telomeric ends. The generation of the triple mutant line *trt-1; pot-2; pot-1::mCherry* (which we will refer to as *t;p;p* line from now on) will enable us to study TERRA dynamics with telomeres using imaging techniques in an ALT-positive background. The *t;p;p* line was obtained by selecting homozygous triple mutants through genotyping. Similarly to what has been done for the generation of *trt-1; pot-2*, the *t;p;p* worms started to display the sterility phenotype early on upon their formation, therefore they were maintained in culture using the same favorable conditions as done for the *trt-1; pot-2* until growth rate was restored to the one of WT animals. During this process, we were able to isolate and grow 3 individual ALT survivors that we will refer to as clone 1, clone 6 and clone 20.

In order to further confirm the ALT-like nature of this animals, we performed a TRF analysis coupled with Southern blot (Figure 23). From this experiment we can appreciate how an ALT-like mechanism has been used by the cells to elongate the telomeres, considering the absence of *trt-1*. In line with what was previously seen with *trt-1; pot-2* double mutants, *t;p;p* worms display telomeres that present higher molecular weights, compared to WT, both in early and late generations. Strikingly, the band patterns found among early generations and the 3 separate clones are highly heterogeneous, not only among them, but they also differ from those found in *trt-1; pot-2* animals (Figure 19), underlying the extremely heterogenous nature of telomeres when maintained through ALT.

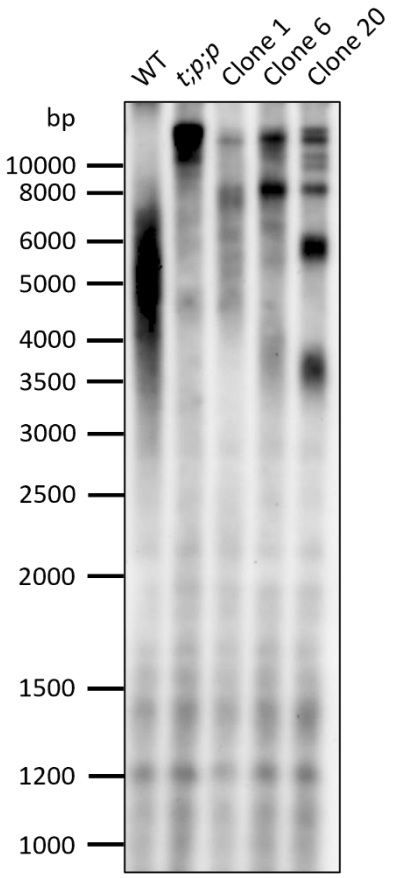


***Figure 23 |*** *The C. elegans triple mutant trt-1; pot-2; pot-1::mCherry (t;p;p) displays ALT-like features similar to the double mutant trt-1; pot-2. TRF analysis coupled with Southern blot shows longer and heterogeneous telomeres in t;p;p early and late generation clones compared to WT animals. The pattern visible from 2.5 kb and lower represents internal telomeric regions (ITRs).*

We then analyzed the expression of TERRA in *t;p;p*. Regarding TERRA from single telomeres, we employed RT-qPCR using the previously mentioned primers and found out that early generations *t;p;p* presented significantly higher levels of TERRA from telomere 4L (Figure 24); while, there is a clear trend of TERRA expression being upregulated in at least 4 out of 5 telomeres that we analyzed, which is in line with the evidences found via RNA dot blot, this difference did not reach significance in these experiments.

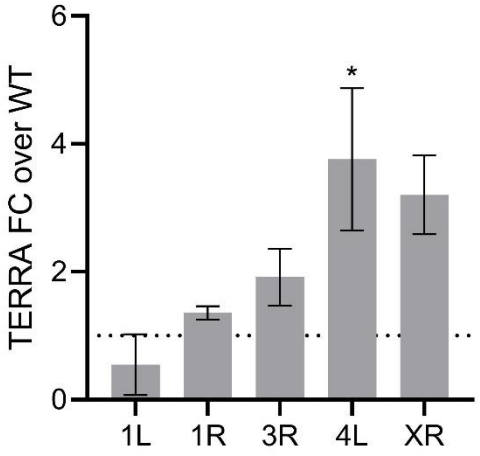


***Figure 24 |*** *RT-qPCR analysis shows a telomeric-specific regulation of TERRA in trt-1; pot-2; pot-1::mCherry (t;p;p) early compare to WT animals. Data shown as fold change (FC) of TERRA expressed from telomere 1L, 1R, 3R, 4L and XR over WT. t-test was used to assess significance. * = p≤0.05. The experiment was repeated 3 times.*

Moving then to analysis of individual TERRA molecules in the ALT survivors, we can appreciate by RT-qPCR how there are no significant changes between early and late generations *t;p;p* and the same applies among the 3 clones (Figure 25). Also for these experiments, it is interesting to see a clonal effect on ALT survivors which is then propagated through generations, looking for instance at differences between *trt-1; pot-2* and *t;p;p* when comparing patterns in telomere length and expression of individual TERRA molecules, that are, however, maintained from early to late generations.

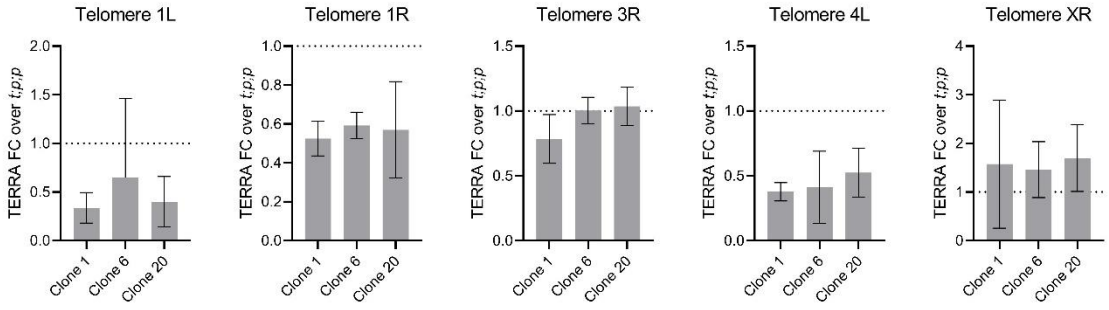


***Figure 25 |*** *RT-qPCR analysis shows no difference at the level of single TERRA molecules between trt-1; pot-2; pot-1::mCherry (t;p;p) animals grown at early and late generations and among the individual clones. Data are shown as fold change (FC) over t;p;p animals. The experiment was repeated 3 times.*

For what concern the bulk population of TERRA, we performed a RNA dot blot on *t;p;p* early and clones 1, 6 and 20 which, unfortunately, encountered technical issues. We still visualized some signal in all samples treated with RNase, meaning the RNase treatment

was not strong enough to elicit a complete degradation of RNA or an incomplete DNase treatment of the samples led to the visualization of leftover gDNA signal. As for other RNA dot blots samples were treated in the same way with RNase and the signal was abolished, we reasoned that the contamination found in this RNA dot blot was most likely due to gDNA. Even though no solid conclusions can be drawn from this experiment, we still tried to quantify TERRA expression by subtracting the dots treated with RNase to those non-treated with RNase, thus removing the portion of signal generated by leftover gDNA in each sample. In these experiments, *t;p;p* at early generations presented an increase in TERRA expression compared to WT. Notably, in clone 1 and clone 6 we did not see a change in TERRA expression, or even a decrease in bulk TERRA levels, compared to WT, while clone 20 displayed increased TERRA signal even as compared to the parental line. These findings, which need to be repeated addressing the technical issues first, are in line with RT-qPCR results and emphasize the heterogeneity among individual ALT clones.

Taken together, these data suggest that *t;p;p* worms can be used to generate and isolate ALT survivors with features similar to those described in *trt-1; pot-2* background animals. The presence of *pot-1::mCherry* did not alter the generation of ALT clones and so it can be employed to further investigate the dynamics of TERRA and telomeres by imaging analyses.

## Only a fraction of TERRA localizes at telomeres during pachytene in *C. elegans* gonads

Haploid gametes are generated within the germline, where meiosis halves the number of chromosomes and rearranges the genome. Throughout the extended prophase of meiosis I, DNA double-strand breaks occur and are repaired through HR, leading to the creation of connections between the parental homologous chromosomes. The gonad of the *C. elegans* hermaphrodite comprises cells undergoing mitotic division, which subsequently transitions into different meiotic events during oogenesis in the germ line: leptotene, zygotene, pachytene, diplotene and diakinesis. Oocytes within diakinesis become cellularized and undergo fertilization upon being pushed through the spermatheca, triggering then both meiotic divisions.

To investigate the expression of TERRA and analyze its dynamics related to telomeres, we performed an RNA-FISH analysis coupled with immunofluorescence (IF) on dissected gonads, divided into seven zones corresponding roughly to the different meiotic events taking place during oogenesis in the *C. elegans* germ line. These zones include the mitotic zone located at the distal tip of the gonad, housing actively proliferating cells (z1 and z2), the transition zone where homologous chromosome pairing occurs (z3), early, mid, and late-pachytene stages (z4, z5, and z6, respectively), characterized by crossing-over events and the diplotene stage where chromatin condensation forms bivalent structures (z7) (Figure 26). In particular we employed *t;p;p* gonads taken from early generations worms and gonads taken from ALT clone 1 and clone 20.

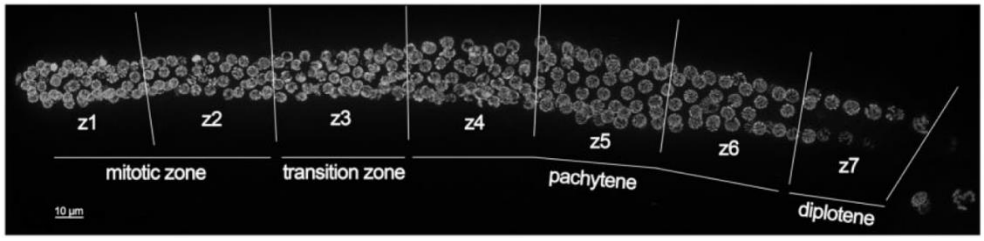


***Figure 26 |*** *Low magnification confocal image of a C. elegans gonad stained with DAPI and divided into the seven zones found in mitotic and meiotic events during oogenesis in the germ line. Scale bar: 10 µm. Image adapted from Manzato 2023* [103].

The analysis was carried out by utilizing a fluorescently labelled probe that would recognize the 3' end repetitive sequences of TERRA molecules $(UUAGGC)_n$, while the

detection of telomeres was achieved through the use of an antibody that would recognize the mCherry tag of the fusion protein pot-1::mCherry, which localizes at telomeres. As the instrument used for imaging was a Nikon Eclipse Ti2 equipped with a spinning disc, the spinning disc module was necessary to remove the high background generated upon hybridization of the TERRA-FISH probe, but it also reduced the detected signal, which may lead to underestimating the number of TERRA foci in the analysis.

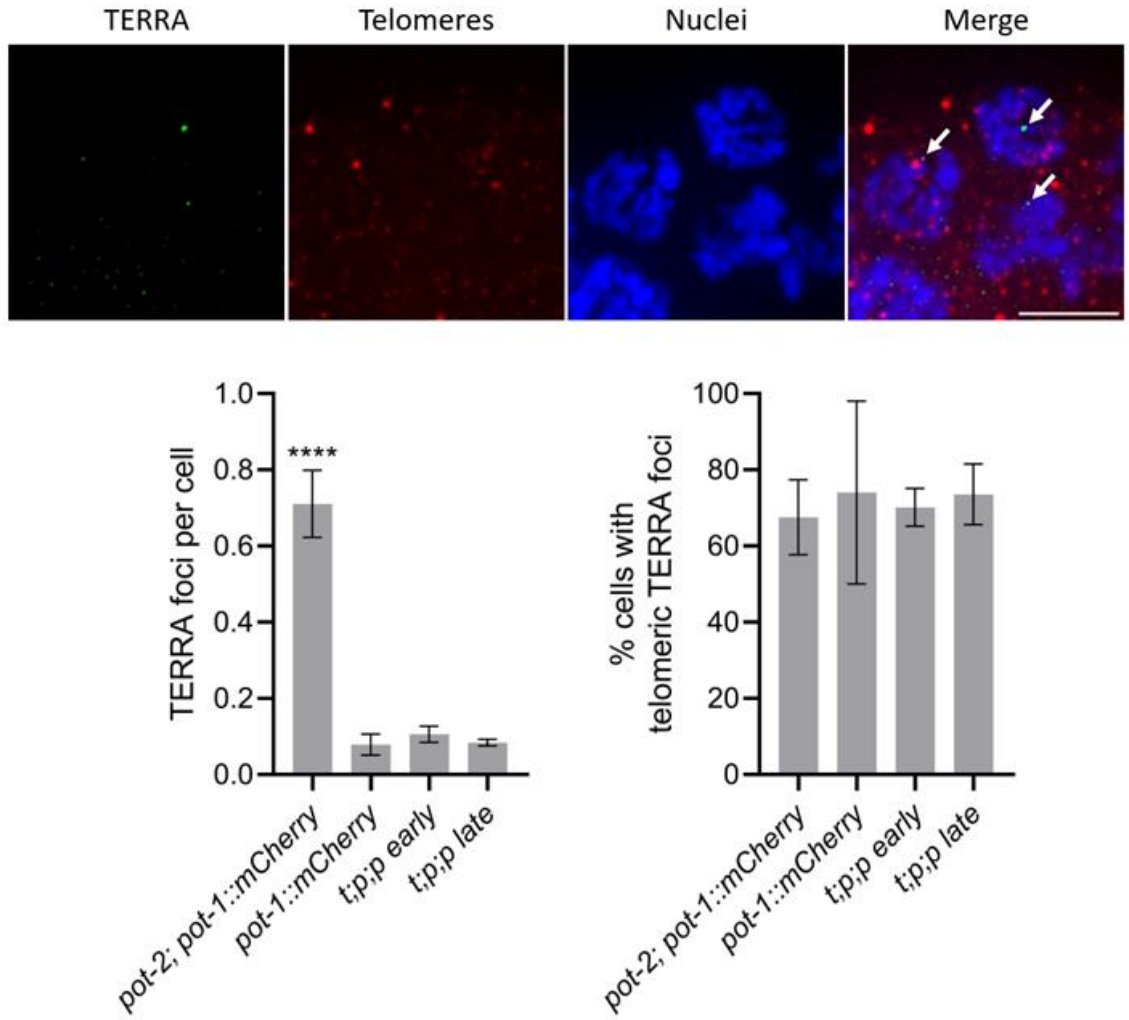


***Figure 27 |*** *TERRA only partially colocalizes with telomeres in C. elegans gonads. Panel showing gonad cells imaged for TERRA, mCherry (telomeres) and nuclei. Arrows show TERRA foci in the merge. Scale bar: 5 µm (**top**). Number of TERRA foci per cell found in the z4-z6 regions (trt-1; pot-2; pot-1::mCherry grown at late generations (t;p;p late) comprises clone 1 and clone 20, **bottom, left**). One-way ANOVA was used to assess significance. **** = p≤0.0001. Percentage of TERRA positive cells presenting at least one TERRA focus colocalizing with telomere signal in the z4-z6 regions (t;p;p late comprises clone 1 and clone 20, **bottom, right**). The experiment was done on 4 gonads.*

For this reason, we decided to focus our analysis on the pachytene regions of the gonads (z4, z5 and z6), where TERRA is mostly expressed and where crossing-over events are occurring, possibly being of interest for the ALT mechanism.

First, we counted the number of TERRA foci per cell in the pachytene (Figure 27). All cells presented at least one spot positive for POT1::mCherry. From our analysis, despite the technical difficulties already mentioned in this paragraph, we were able to identify several TERRA foci forming in pachytene cells. For this analysis, we also included *pot-1::mCherry* worms as a control expressing the fusion protein and *pot-2; pot-1::mCherry*, a line in which the absence of pot-2 was characterized to induce the expression of TERRA[103]. As expected, by averaging the number of TERRA foci per number of cells found in the pachytene in each gonad, we can see a significant increase in the number of TERRA spots in *pot-2; pot-1::mCherry* as in comparison to *pot-1::mCherry*. Strikingly, we did not find a difference in terms of TERRA expression between *t;p;p* and the control line. In addition, we did not find any changes in between early and late generations in *t;p;p*.

We then exploited the mCherry tagging for telomere visualization and stratified the number of TERRA foci whether they colocalized with telomeres or not (Figure 27). In this case, all genotypes analyzed displayed approximately three fourths of TERRA foci colocalizing with telomeres, while the remaining one fourth did not.

Taken together, these RNA-FISH data indicate a similar number of TERRA foci detected in WT and *t;p;p* strains even upon ALT induction in clones. Given the technical challenges incurred for TERRA and pot-1:mCherry detection, in these experiments we may be underestimating TERRA foci, detecting only the brightest ones. RT-qPCR and Northern blot experiments should be performed in order to confirm these results.; Despite these challenges, we have selected ALT-like strain in the *pot-1::mCherry* background which, upon optimization of signal detection, may be used as a tool to study telomere dynamics and TERRA localization not at telomeres in an ALT multicellular organisms.

Given the interesting results obtained so far using a non-cancerous background model for the study of TERRA and ALT such as *C. elegans*, we decided to move our focus onto a cancerous background field of study. To do so, we employed human cancer cell lines.

## Human cells

### TERRA levels are reduced in the ALT-positive human cell line U2OS upon TERRA-ASO transfection

To study the impact of TERRA downregulation in ALT in human cells, we first needed to transfect TERRA-ASO and measure its effect on the cells. To do so, we employed U2OS, a widely used ALT-positive osteosarcoma cancer cell line, which has been transfected with 200 nM TERRA-ASO for 48 hours before analyses. As a control, we performed the transfection of a scramble ASO (SCRB-ASO) at the same concentration and duration of transfection.

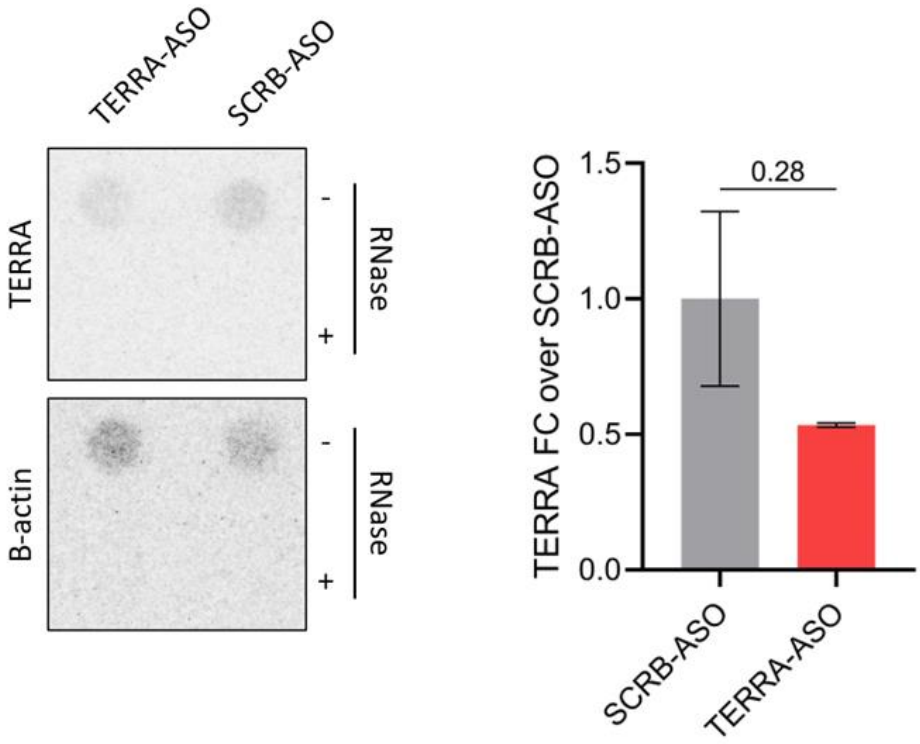


***Figure 28 |*** *TERRA-ASO reduces TERRA levels in U2OS cells. RNA dot blot analysis (**left**) and its relative quantification (**right**) on U2OS transfected with TERRA-ASO (TERRA) or scramble-ASO(SCRB). Data are shown as fold change (FC) over SCRB-ASO. The value on top of histograms is the p-value. t-test was used to assess significance. The experiment was performed 2 times.*

Upon harvesting of cells, we measured whether TERRA-ASO effectively reduced TERRA levels; in particular, we analyzed both the bulk population of TERRA through RNA dot blot (Figure 28), while we analyzed TERRA from single telomeres through RT-qPCR (Figure 29).

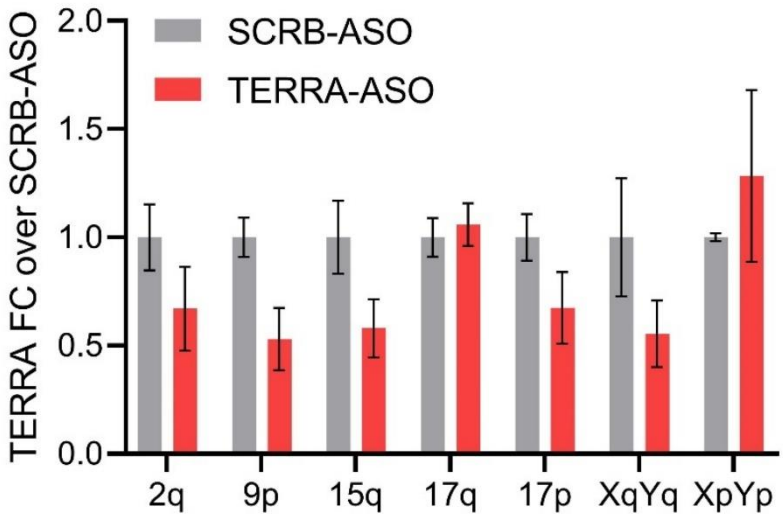


***Figure 29 |*** *RT-qPCR analysis of U2OS cells transfected with TERRA-ASO (TERRA) or scramble-ASO (SCRB) shows a telomeric specific downregulation upon TERRA-ASO transfection. Data are shown as fold change (FC) over SCRB-ASO. The experiment was performed 2 times.*

With this approach, we used primers to detect TERRA from multiple telomeres: TERRA-2q, TERRA-9p, TERRA-15q, TERRA-17q, TERRA-17p, TERRA-XqYq, and TERRA-XpYp[111].

For both the RNA dot blot and the RT-qPCR analyses, we can appreciate a reduction of TERRA, which accounts for about 30-50%, depending on whether we are analyzing the total population of TERRA or TERRA molecules transcribed from single telomeres. Interestingly, not all TERRA transcripts behave the same upon TERRA-ASO treatment. Indeed, TERRA-17q and TERRA-XpYp are not affected by the ASO, which may be due to differences in their telomeric-repeat tract, which is targeted by ASO, or accessibility of these particular transcripts to ASO binding, given to binding with protein complexes. Notably, previous analyses done in our lab showed that those same TERRA molecules are part of the poly(A) fraction of TERRA transcripts and are more stable in cells knocked-out for the RNA binding protein RALY[111]. Therefore, intrinsic features of these transcripts may render them more impervious to ASO depletion.

Taken together, these data suggest that TERRA-ASO transfection is effective in reducing total TERRA levels of about 30-50% in U2OS cells, with differences in TERRA depletion extent from distinct telomeres.

## ALT-FISH as an imaging technique to evaluate changes in the ALT phenotype

The ALT-FISH imaging technique was developed by Frank and colleagues as reliable tool to detect ALT phenotype [105]. This methodology relies on the uses of telomeric probes, consisting of repetitions of hexamers found in both strands of telomeres (such as TTAGGG and CCCTAA), that are fluorescently labeled. ALT-FISH allows to hybridize probes under non-denaturing conditions single stranded RNA and DNA consisting of telomeric sequences. ALT-positive cells are characterized by i) increased levels of TERRA (detectable with a C-rich probe), ii) the presence of C-rich and G-rich single stranded telomeric overhangs resulting from telomeric elongation through HDR (detectable with both probe types) and iii) C- and G-circles (detectable with both probe types). All these ALT features are detectable by ALT-FISH. Therefore, by counting the number of ALT-FISH spots per cell it is possible to assess the ALT status of cells (Figure 30).

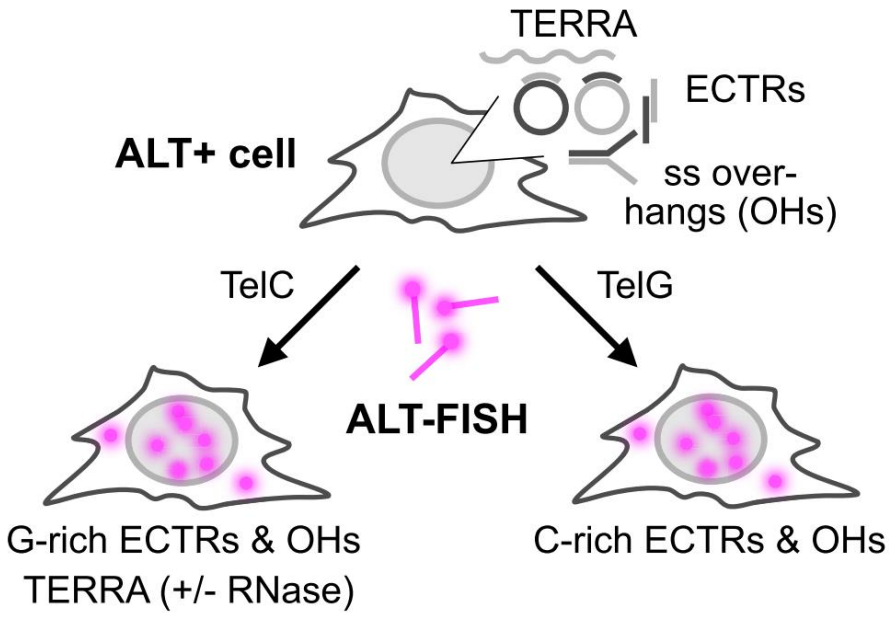


***Figure 30 |*** *Schematic representation of the ALT-FISH workflow. ALT-FISH comprises the use of fluorescently labeled probes (in this image called "TelC" and "TelG", depending on the sequence) to detect ssDNA and ssRNA elements that were found to be enriched in ALT-positive cells. Taken from Frank 2022 [105].*

First, we performed the ALT-FISH on HeLa and U2OS cells, which are used as controls to set up the thresholds for the stratification of ALT-negative and ALT-positive cells. The hybridization of cells was done using both C-rich and G-rich probes. With this analysis, we were able to obtain similar results as shown in the work by Frank and colleagues (Figure 31). We acquired the images using a Nikon AX confocal microscope and by using a ImageJ

macro script that was developed by the Advanced Imaging Facility at CIBIO we were able to successfully visualize discrete foci forming within nuclei. We measured the number of foci per each nucleus, defining an "ALT-positive focus" as a spot that is at least 7-fold higher in intensity than the average background of the nucleus. In this manner, we were able to detect a significant difference between HeLa and U2OS, the latter having a greater number of ALT-FISH spots per cell. In line with what was reported by Frank and colleagues, we detected a greater number of foci when using a C-rich probe than a G-rich probe, as TERRA molecules account as one of the highest sources of ALT-FISH detectable foci and TERRA transcripts can only be visualized through a C-rich probe binding their UUAGGG repeats.

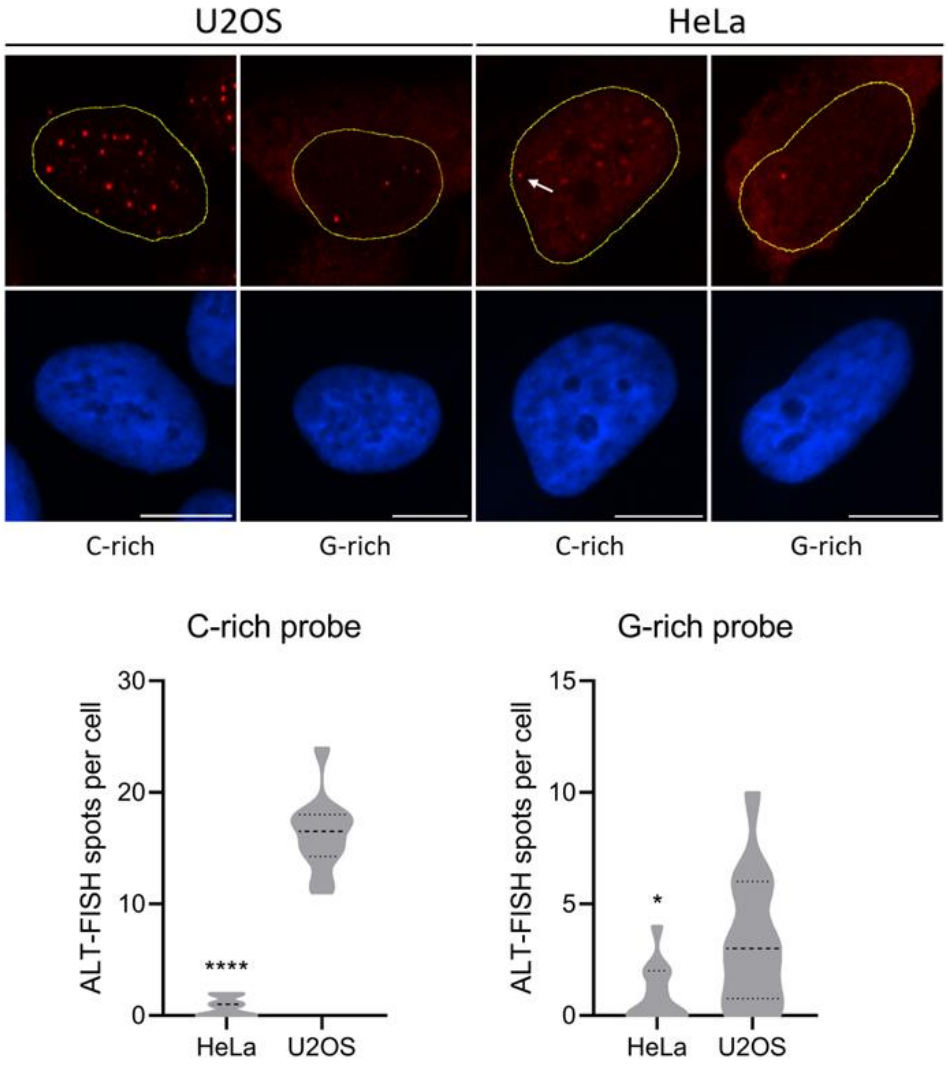


***Figure 31 |*** *ALT-FISH imaging technique enables to measure the status of ALT at a single cell level. Panel showing HeLa and U2OS cells hybridized with C-rich and G-rich probes. The white arrow indicates a positive spot among the non-specific signals found in HeLa C-rich cells. Scale bar: 10 µm (**top**). Number of ALT-FISH positive foci per cell found in C-rich (**bottom, left**) and G-rich (**bottom, right**) HeLa and U2OS cells. t-test was used to assess significance. * = p≤0.05; **** = p≤0.0001. At least 30 cells were analyzed in each condition.*

Upon the validation of ALT-FISH with our settings, we employed this technique to measure changes in the ALT status of U2OS cells upon the transfection of TERRA-ASO. In this case, we decided to use the C-rich probe for a number of reasons. Firstly, according to Frank and colleagues, both probes can be used interchangeably to measure the ALT phenotype, as both C-rich and G-rich elements are enriched in ALT-positive cells. Secondly, the number of C-rich detectable spots is higher than G-rich spots, therefore we reasoned it would be easier to see changes in ALT when looking at a higher number of foci. Thirdly, we actually tried to quantify the number of ALT-FISH spots using U2OS cells transfected with TERRA-ASO using a G-rich probe; however, the number of foci was found increased upon TERRA-ASO transfection, possibly due to the binding of the G-rich probe to the TERRA-ASO, as they are complementary to one another (data not shown).

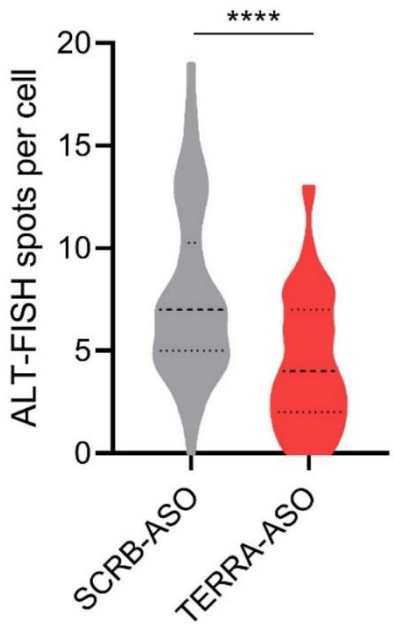


***Figure 32 |*** *TERRA-ASO transfection (TERRA) reduces the number of ALT-FISH spots as compared to scramble ASO transfection (SCRB) in U2OS cells. t-test was used to assess significance. **** = p≤0.0001. At least 30 cells were analyzed in each condition.*

In these experiments, we were able to see a reduction of ALT-FISH spots upon TERRA-ASO transfection, which was not detected with the transfection of the SCRB-ASO (Figure 32). To further assess the contribution of TERRA signal detection in the quantification of ALT-FISH spots we performed a RNase A treatment on cells prior the hybridization of the probe. Upon RNase A treatment, we detected an increased number of ALT-FISH foci, possibly due to an overall reduction of the nuclear background signal, which resulted in a higher

number of spots that are exceeding the 7-fold threshold limit for the detection (data not shown).

Taken together, these data suggest that ALT-FISH is a powerful tool to measure and assess tumors on their ALT background at a cellular levels; however, due to the use of oligo probes that are complementary to either the TERRA-ASO or to the direct targets of the TERRA-ASO, in may be difficult to use ALT-FISH to assess ALT phenotypes in TERRA ASO transfected cells. Further experiments will need to be performed to confirm these observations.

To further deepen our understanding on TERRA and ALT still in the field of cancer, we finally moved to a more complex *in vivo* tumor model which has already been proven to be a valid tool for the study of both TERRA and ALT: the zebrafish.

# Zebrafish

## TERRA-ASO is not toxic in zebrafish during early development if used within a wide range of concentrations

As mentioned during the introduction, one of the many advantages of the zebrafish as model organism is the possibility to micro-inject molecules in embryos at the stage of 1-2 cells and have them delivered throughout the tissues of the animal as it develops. For this study, we aim to downregulate TERRA molecules in our ALT-positive zic:RAS model by employing a LNA Gapmer ASO that is targeting the bulk population of TERRA (TERRA-ASO) in the zebrafish and promoting its degradation through the activity of RNase H[51]. As a control, we utilized a scramble ASO which sequence is not binding any known transcript (SCRB-ASO). The same ASOs are currently being used for TERRA downregulation with cell cultures and have been shown to work efficiently.

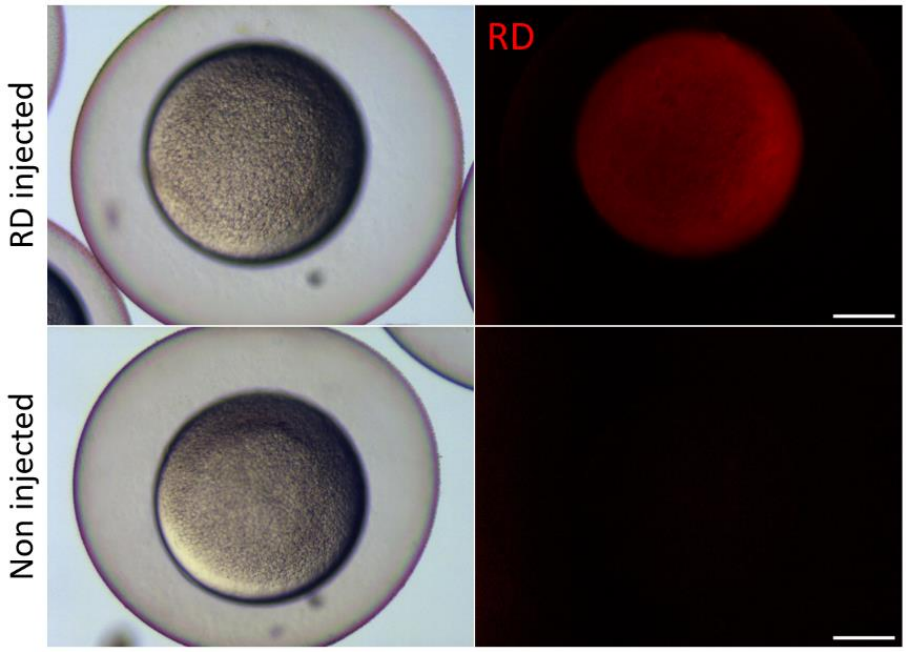


***Figure 33 |*** *Representative fluorescent images showing zebrafish embryos at 4 hours post fertilization (hpf) which has been injected with RD (**top row**) and a control where no injection was done (**bottom row**). Scale bar: 0.2 mm.*

First, we needed to assess whether the ASOs were toxic once delivered into the embryos or could impair the correct development of the larvae. To do so, we micro-injected increasing concentrations of TERRA-ASO (and SCRB-ASO): 0.1 µM, 0.5 µM, 1 µM, 5 µM and 10 µM. As control, we also injected water (RD). As the micro-injection of the mix is done

within the yolk and then the molecules contained in the injection mix are absorbed by the embryo, together with the ASO we included rhodamine dextran (Figure 33), a fluorescent dye that is commonly used for lineage tracing in zebrafish and enables us to know whether the mix has been uptaken[112–114]. The injection of the ASO mix was performed in embryos no later than at the 2-cells stage. We let the animals grow and develop until 5 dpf, at the end of which we counted the number of animals that developed normally, the number of morphologically altered animals and the number of deaths.

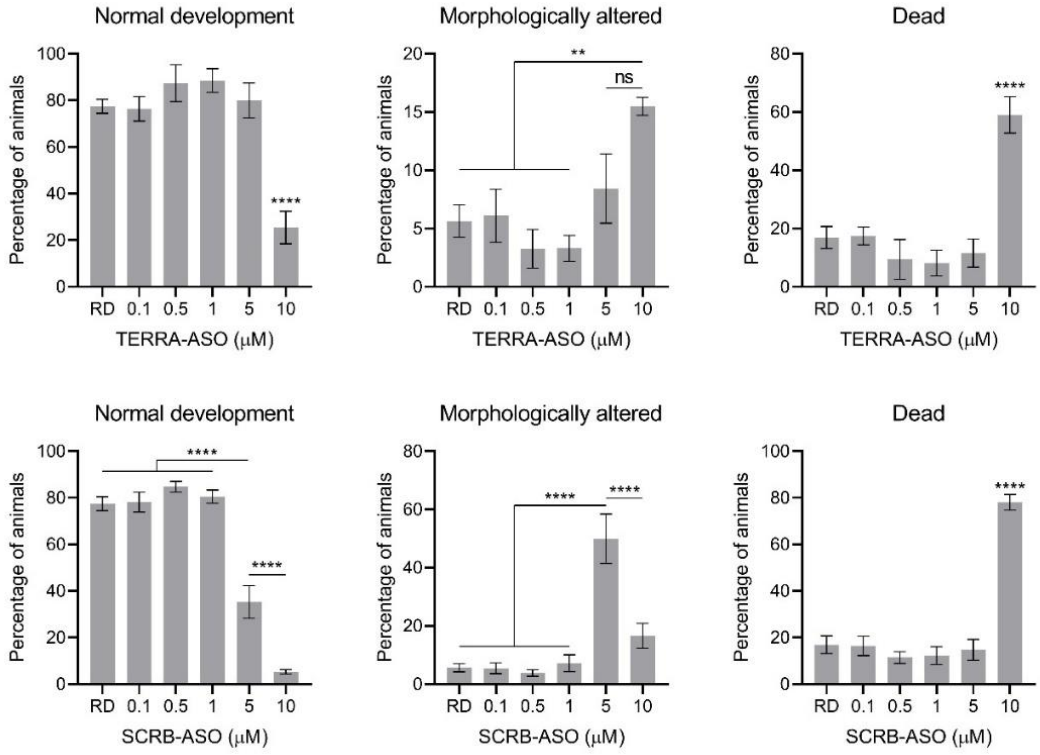


***Figure 34 |*** *Percentage of animals alive, morphologically altered and dead upon micro-injection of increasing concentrations of TERRA-ASO (**top row**) and SCRB-ASO (**bottom row**). RD (rhodamine) is the control where only rhodamine dextran was included in the mix. One-way ANOVA was used to assess significance. ** = p≤0.01; *** = p≤0.001; *** = p≤0.0001; ns = non-significant. Each ASO concentration was injected and quantified 4 times.*

Interestingly, TERRA-ASO micro-injected at 10 µM showed the highest toxicity effect, producing a significant increase in terms of dead and morphologically altered animals within 5 dpf (Figure 34). No significant differences were found between RD-injected embryos and those injected with concentrations of TERRA-ASO ranging from 0.1 µM to 5 µM. Strikingly, SCRB-ASO scored differently in terms of toxicity, as no difference was seen until the concentration of 5 µM was reached, where an increase in morphological

alterations was observed, concluding then with a massive death of animals injected with the highest concentration of 10 µM. Similarly to TERRA-ASO, no differences were noticed between RD-injected animals and those injected with the lower concentrations.

These data indicated the concentrations of ASO that are toxic to the animals and revealed which are the recommendable ASO working concentrations to use for further analysis in zebrafish until 5 dpf.

## TERRA-ASO is not capable of reducing TERRA levels at 5 dpf in the zic:RAS model

Now that we identified range of concentrations at which the ASOs are not toxic to the larvae, we performed new rounds of micro-injections to test an effective reduction of TERRA molecules in the animals. In particular, we decided to use the following concentrations of TERRA-ASO and SCRB-ASO: 0.02 µM, 0.1 µM and 0.5 µM as what could be addressed as small, intermediate and high amounts of ASO delivered to the embryo. We also included animals injected with RD alone as controls.

To investigate TERRA reduction upon micro-injection of TERRA-ASO, we extracted the RNA from pools of zic:RAS larvae that were grown until 5 dpf and performed a RNA dot blot (Figure 35). We measured the intensity of the spots for both the total population of TERRA and *rps11*, an housekeeping gene coding for the ribosomal protein subunit 11 in zebrafish, and normalized TERRA values over the *rps11* values. Results show how there is no difference among all samples, regardless of whether the larvae were non-injected, mock-injected or injected with TERRA-ASO or SCRB-ASO. There appears to be a trend where a slight increase in bulk TERRA happens upon the injection of SCRB-ASO, comparing it to TERRA-ASO, though not significant.

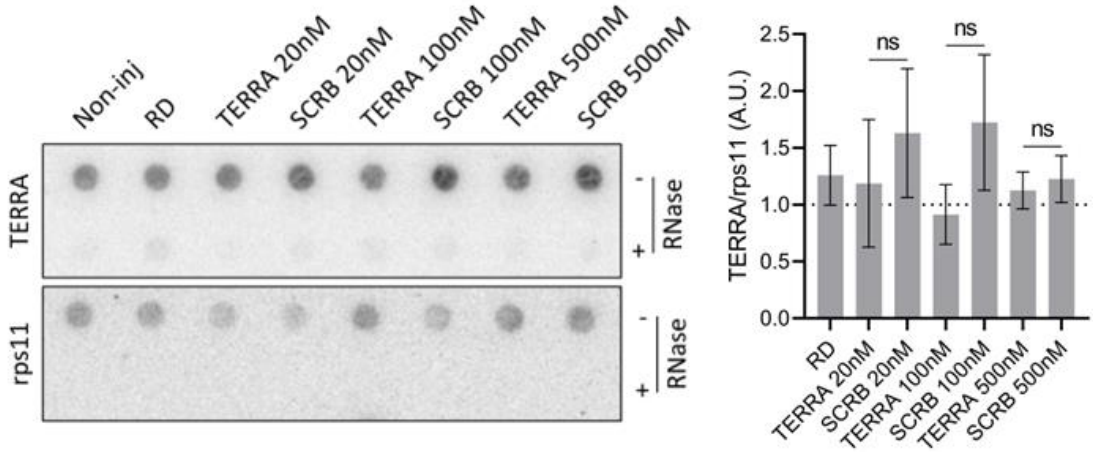


***Figure 35 |*** *TERRA-ASO does not produce a detectable reduction of TERRA at 5 days post fertilization (dpf)in zebrafish larvae. RNA dot blot using 32-P labeled TERRA-specific and rps11 gene probes on 5 dpf whole larvae (**left**) and its quantification (**right**) show no reduction of TERRA in 5 dpf zic:RAS larvae injected with variable concentrations of TERRA-ASO (TERRA) (20 nM, 100 nM and 500 nM) as compared to SCRB-ASO (SCRB) injected animals at the same concentrations. Samples on the bottom lane of each membrane were treated with RNase A to assess RNA specificity. t-test was used to assess specificity. ns on top of histograms indicates p-values > 0.05. The experiment was performed 3 times.*

Similar to the experiments performed in human and *C. elegans*, we decided to analyze the expression of TERRA from single telomere to understand whether an effect of TERRA-ASO could elicit a telomere-specific effect, which is clearly not detectable when investigating the total population of TERRA. To do so, as nothing was known about the expression of single telomere TERRA in zebrafish, we decided to design specific RT-qPCR primers for the detection of single TERRA molecules. As the generation and validation of such primers are part of an additional work currently going on in the lab and as it is not the final aim of this thesis work, it will be described briefly. We took advantage of a long-read Nanopore sequencing zebrafish genome assembly (fDanRer4.1)[115], which constitutes an implementation over the default zebrafish genome assembly currently in use (GRCz11), as with long-read sequencing it was possible to fill in many gaps on the zebrafish genome, mainly at telomeres and repetitive sequences in general. Of note is the fact that before the publication of fDanRer4.1 we tried to design RT-qPCR primers with the same purpose but it was not possible to find more than a couple of telomeric ends within the genome, according to a simple $(TTAGGG)_n$ search. Starting from fDanRer4.1, we looked for telomeric ends (where at least 1 kb of TTAGGG hexameric repeats were found) and analyzed the upstream sequences. Interestingly, of the 50 possible chromosome ends (*D. rerio* has 25 chromosomes), 27 contained the TTAGGG repeats and most of them also presented what we termed "degenerated subtelomeres", where repetitions of 16 nucleotides that are telomeric like (e.g. TAGAGCGAACTAGGGG) were present at different length (from 600 bp to 12 kb). These degenerated subtelomeric regions were not all identical, although very similar to one another and many chromosome ends presented the same repeats. Having this in mind and not knowing where the transcription start site (TSS) for each TERRA transcript is, we designed primer couples that would specifically anneal within the unique subtelomeric region of each chromosome end, being within the first 500 nt from telomeric or degenerated subtelomeric regions. Another important point was the length of the degenerated subtelomeric region: as TERRA RT is done by using a RT primer that binds all telomeric regions $(CCCTTA)_5$, we selected chromosome ends where there were no degenerated subtelomeres or degenerated telomeres that were no longer than 1 kb, because there is a limit to the cDNA length that can be produced by the RT enzyme (Figure 36). By following these parameters, we were able to design 5 subtelomeric-specific TERRA primers: 3S, 17S, 17L, 18L and 24S (nomenclature wise, S and

L stand for *short* and *long chromosome arm* and are the zebrafish equivalent of the Q and P chromosome arms in human, respectively).

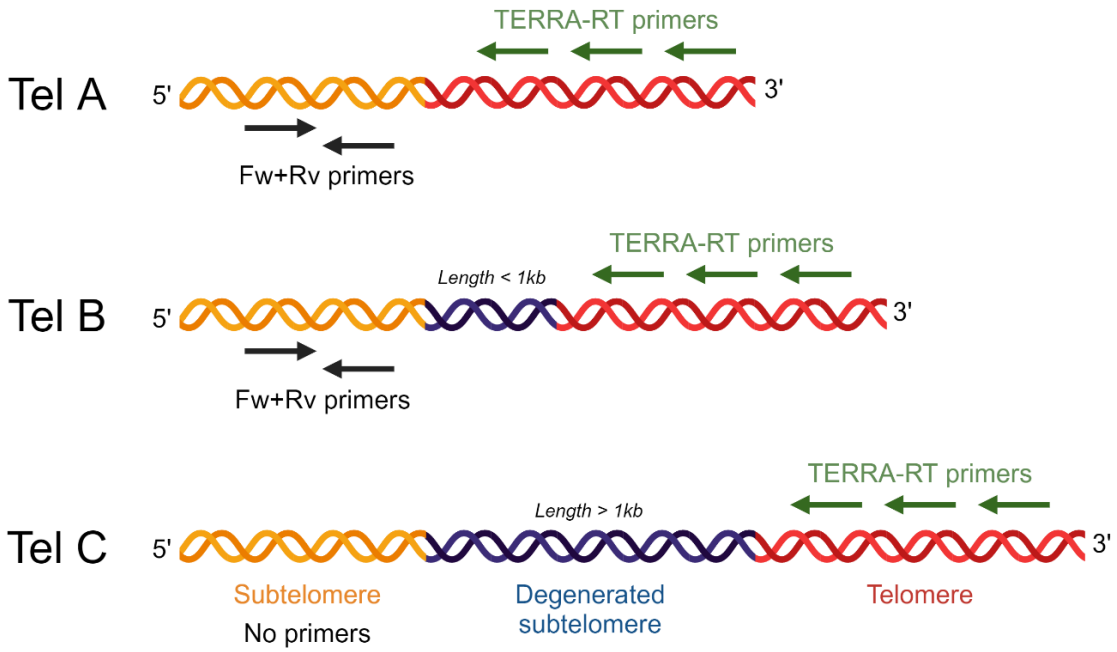


***Figure 36 |*** *Schematic representation on how RT-qPCR primers were designed for the analysis of TERRA expressed from single telomeres in zebrafish. Briefly, TERRA-RT primers bind to telomeric repeats found in all TERRA transcripts and are used to produce cDNA, while primers designed specifically for subtelomeric sequences, which differ among TERRA molecules, are used in qPCR for telomere-specific TERRA quantification. Due to low yields of cDNA, telomeres where the distance between telomeric tracts and telomere-specific qPCR primers is higher than 1 kb are not suitable for this application.*

The greatest difference (although not significant) in terms of TERRA reduction between TERRA-ASO and SCRB-ASO injected animals was found in those injected at 0.1 µM, therefore we decided to analyze the difference of single telomere TERRA in those conditions. As a result, did not detect a difference between TERRA-ASO and SCRB-ASO samples in terms of expression of TERRA from 5 telomeres (Figure 37).

These data suggest that there is not a clear effect of TERRA-ASO in reducing TERRA when analyzed in whole zebrafish larvae at 5 dpf.

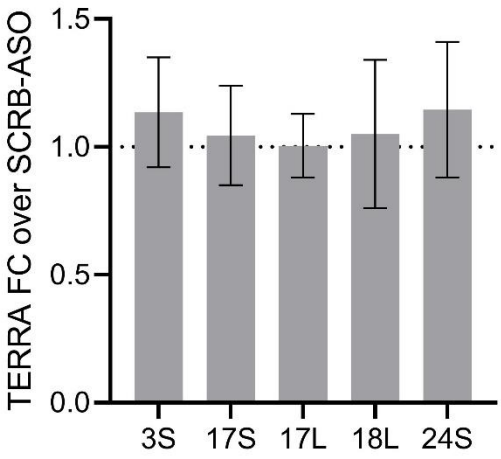


***Figure 37 |*** *RT-qPCR analysis showing the fold change (FC) of TERRA from telomeres 3S, 17S, 17L, 18L and 24S in 100 nM TERRA-ASO injected 5 dpf zic:RAS larvae compared to 100 nM scramble-ASO (SCRB-ASO) injected 5 dpf zic:RAS larvae. Data are shown as fold change (FC) over SCRB-ASO. The experiment was repeated 2 times.*

## TERRA-ASO does not alter the morphology nor the survival of zic:RAS animals

Given the fact that TERRA-ASO does not seem to downregulate TERRA, we wondered whether there could still be an impact of TERRA-ASO on the injected animals on a more macroscopical level. For this reason, we investigated the effect of TERRA-ASO on brain size and cell proliferation in zic:RAS larvae, as they have been reported to increase compared to control (zic:Gal4) larvae[94]. To do so, we fixed whole brains of 5 dpf zic:RAS larvae that were injected with 0.5 µM TERRA-ASO and we performed an IF using an antibody against the phosphorylated form of the histone H3 (PHH3), which can be used as a marker for mitotically active cells[116].

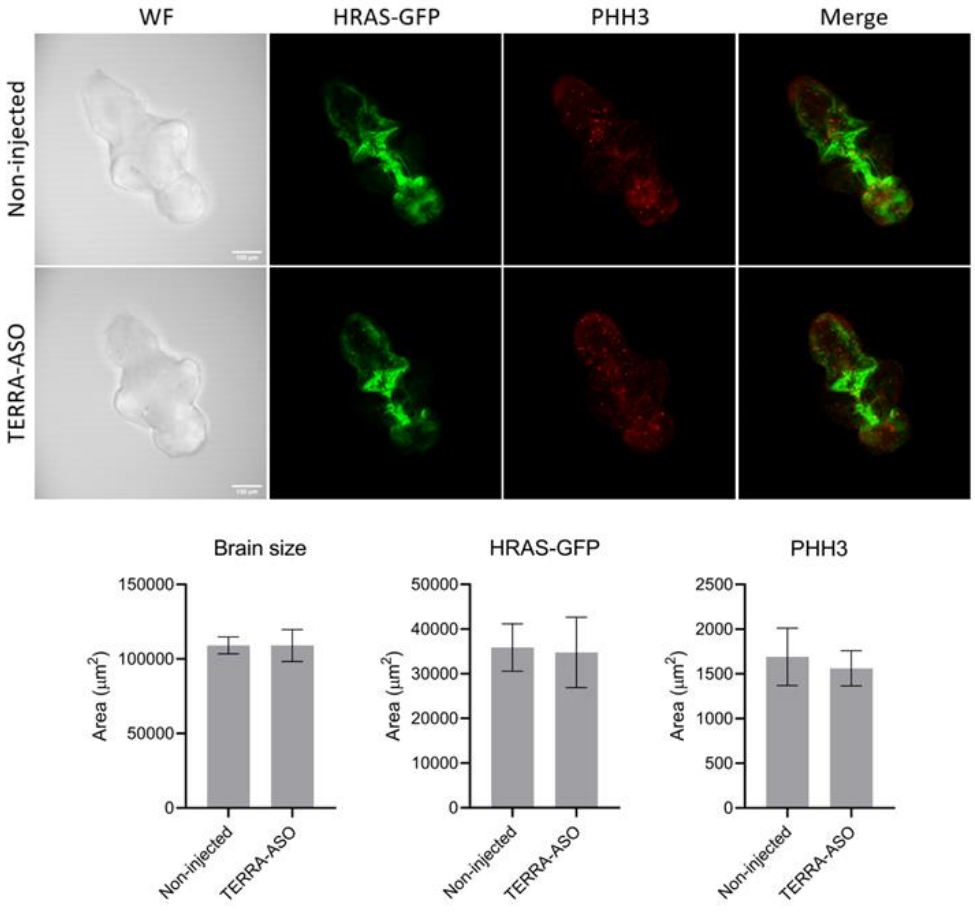


***Figure 38 |*** *TERRA-ASO does not alter brain size at a macroscopical level. Immunofluorescence (IF) on whole brains extracted from 5 days post fertilization (dpf) zic:RAS larvae using an antibody anti-phospho histone 3 (PHH3) for proliferating cells and the imaging of endogenous HRAS-GFP (**top row**). No changes upon the injection of 500 nM TERRA-ASO were measured in brain size, HRAS-GFP-positive area and PHH3-positive area (**bottom row**). Scale bar: 100 µm. 6 whole brains were used for this analysis.*

For this analysis and future functional characterizations of TERRA-ASO, we decided to employ 0.5 µM TERRA-ASO for micro-injections, as it is the highest concentrations at which we do not see a toxic effect (also in the use of SCRB-ASO), and we reasoned that using the highest concentration would provide us with a higher chance of a long-lasting effect. Together with the IF, we also imaged and quantified the amount of HRAS-GFP expressed in the brain, as a read-out on the brain size (Figure 38).

We did not observe a difference in terms of the overall size of the brains between non-injected and TERRA-ASO injected larvae; also, we did not found a difference in the signal-positive area for both HRAS-GFP and PHH3, indicating there is no alteration in brain size and in the number of actively proliferating cells in zic:RAS larvae at 5 dpf injected with TERRA-ASO.

Next, we wanted to verify whether the activity of the TERRA-ASO may alter the survival of the zic:RAS fish. Due to high severity of the tumor forming mainly in the telencephalon, IV ventricle and diencephalon within the first month of development of zic:RAS animals, the overall survival was shown to be highly impacted in those animals developing the tumor, compared to controls[95]. We injected 0.5 µM TERRA-ASO in zic:RAS embryos and let them grow for up to 5 weeks, monitoring the number of living organisms weekly, starting from day 5, when the animals were placed into the animal facility. In this analyses, we observed similar results to those that were previously reported, with a survival rate of about 40-50% in zic:RAS non-injected (Figure 39).

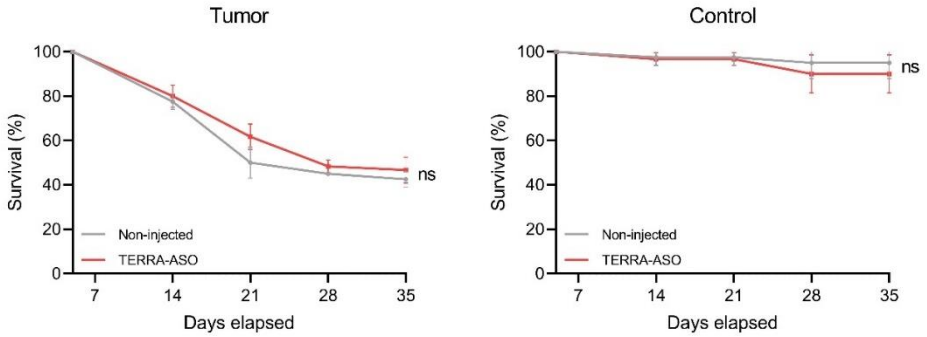


***Figure 39 |*** *Survival curve showing the percentage of animals alive at different time points up to 35 days post fertilization (dpf) in zic:RAS and control animals injected with 500 nM TERRA-ASO. t-test was used to assess specificity. ns indicates p-values > 0.05. This experiment was performed 3 times, with 20 animals growing per experiment.*

Similar results were obtained in zic:RAS animals injected with 0.5 µM TERRA-ASO, with no significant differences in terms of overall survival. Interestingly, we micro-injected 0.5 µM TERRA-ASO in control animals and we found that also the survival of control animals (95-100%) was not altered upon the injection of TERRA-ASO, suggesting the ASO might not ameliorate the survival in the zic:RAS model but at least is not toxic either.

During development of zic:RAS larvae, morphological alterations of the animals become visible starting from 7-8 dpf, most likely due to cachexia and more in the general to the aggressiveness of a tumor that is impacting such an important organ in the animal as it the brain. Among those alterations, the bending of the spinal cord occurs in such a way that the larvae become shaped like a comma, a condition that is not found in control animals, where the axis that goes from head to tail is a straight line. These morphological alterations impede the development in most larvae, in fact starting from 11-12 dpf survival of zic.RAS dramatically drops and those that survive are probably those in which the morphological alterations are not too strong to impede the animals to swim and feed. While we observed that TERRA-ASO in not altering the survival of zic:RAS, we wondered whether it could at least partially alter the morphological alteration during early development.

To test this hypothesis, we injected 0.5 µM TERRA-ASO in zic:RAS and let them grow until 10 dpf, a time point where morphological alterations are well visible and before the beginning of the massive death due to the aggressiveness of the tumor, which, as mentioned, start from 11-12 dpf. Larvae were placed sideways in low-melting agarose and imaged with a brightfield microscope. We then drew two axes that pass through the two extremities of “comma-shaped” larvae: one going through the mouth and being tangent to the swim bladder; one going on top of the spinal cord. Lastly, we measured the obtuse angle that generates from the intersection of the two lines (Figure 40). The smaller the angle, the more bended the spinal cord of the larvae; the closer the angle gets to 180, the more similar to a straight line it gets, thus resembling the control condition. The results of this analysis did not show a significant change of the morphology of zic:RAS larvae injected with 0.5 µM TERRA-ASO, but it displayed the previously known high heterogeneity in terms of morphological alterations in zic:RAS during development.

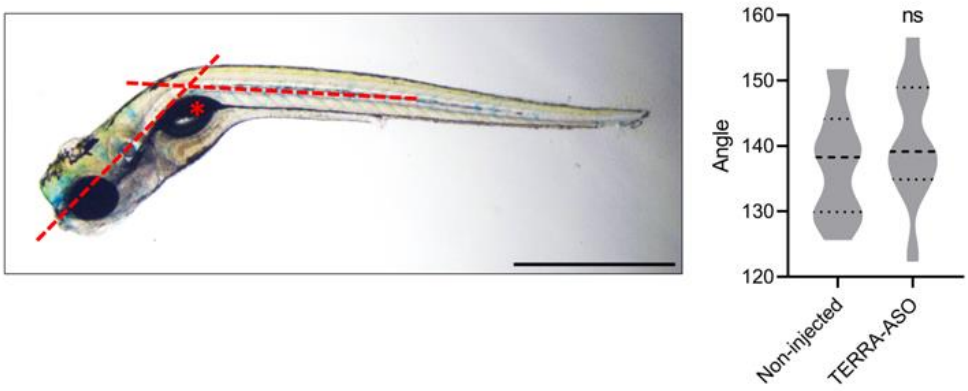


***Figure 40 |*** *Quantification of the distortedness of 500 nM TERRA-ASO injected 10 days post fertilization (dpf) zic:RAS larvae, by measuring the angle that the tilted spinal cord form during development, shown by the red * (**left**). No significant difference in the angle was found in animals injected with TERRA-ASO, when compared to non-injected zic:RAS larvae (**right**). t-test was used to assess specificity. ns (not significant) on top of violin plot indicates p-values > 0.05. Scale bar: 1 mm. At least 25 animals were imaged and for this analysis.*

Taken together, these data suggest that TERRA-ASO is not altering at a macroscopic level the morphology of the brain or the whole larvae, nor it does it on the overall survival of zic:RAS larvae up to 5 weeks of age.

## TERRA-ASO is not capable of reducing TERRA levels at 1 mpf in the zic:RAS model

In the previous paragraph we saw that the morphology and survival of zic:RAS animals injected with TERRA-ASO were not altered, at least until 1 mpf which was the longest time point in the analysis. We decided to measure total TERRA levels in zic:RAS animals at 1 mpf which were injected with both 0.5 µM TERRA-ASO, as well as 0.5 µM SCRB-ASO through RNA dot blot (Figure 41).

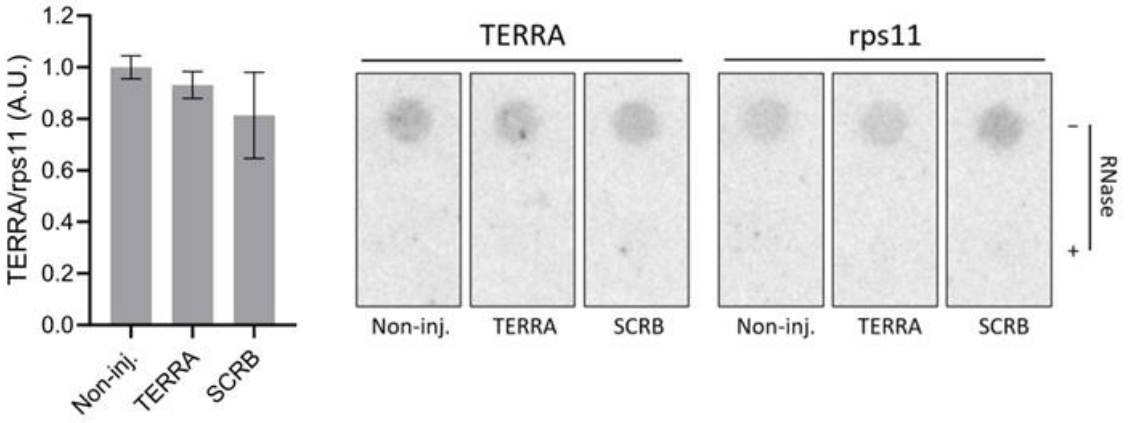


***Figure 41 |*** *TERRA-ASO does not produce a detectable reduction of TERRA in 1 mpf in zebrafish animals. RNA dot blot using 32-P labeled TERRA-specific and rps11 probes on 1 mpf whole fries (**right**) and its quantification expressed as TERRA fold change over rps11 (**left**) show no reduction of TERRA in animals injected with 500 nM TERRA-ASO (TERRA) as compared to 500 nM SCRB-ASO (SCRB) injected animals. Samples on the bottom lane of each membrane were treated with RNase to assess RNA specificity. The experiment was performed 3 times.*

Similarly to what has been done with 5 dpf larvae, we measured the intensity of each spot that corresponds to a single zic:RAS animals and normalized the values over the housekeeping *rps11*. Once again, no significant difference was found between animals injected with TERRA-ASO when compared to SCRB-ASO or the non-injected controls.

Taken together, these data suggest that an effect of TERRA-ASO is not visible at 1 mpf. The fact that TERRA is not being affected by the activity of TERRA-ASO is in line with not seeing any morphological or developmental changes during the growth of the animals up to 1 month of age.

## TERRA-ASO might have an effect on fully developed tumors at later developmental stages

It was observed upon the generation of the zic:RAS model that, when using the germline approach, there is a full penetrance of the tumor, with essentially all animals developing a severe tumor that significantly impact the survival of the animals[94]. Those animals that are able to survive the first 12 days, moment at which the majority die, display morphological alterations to some degrees that are most likely relatable to the brain tumor.

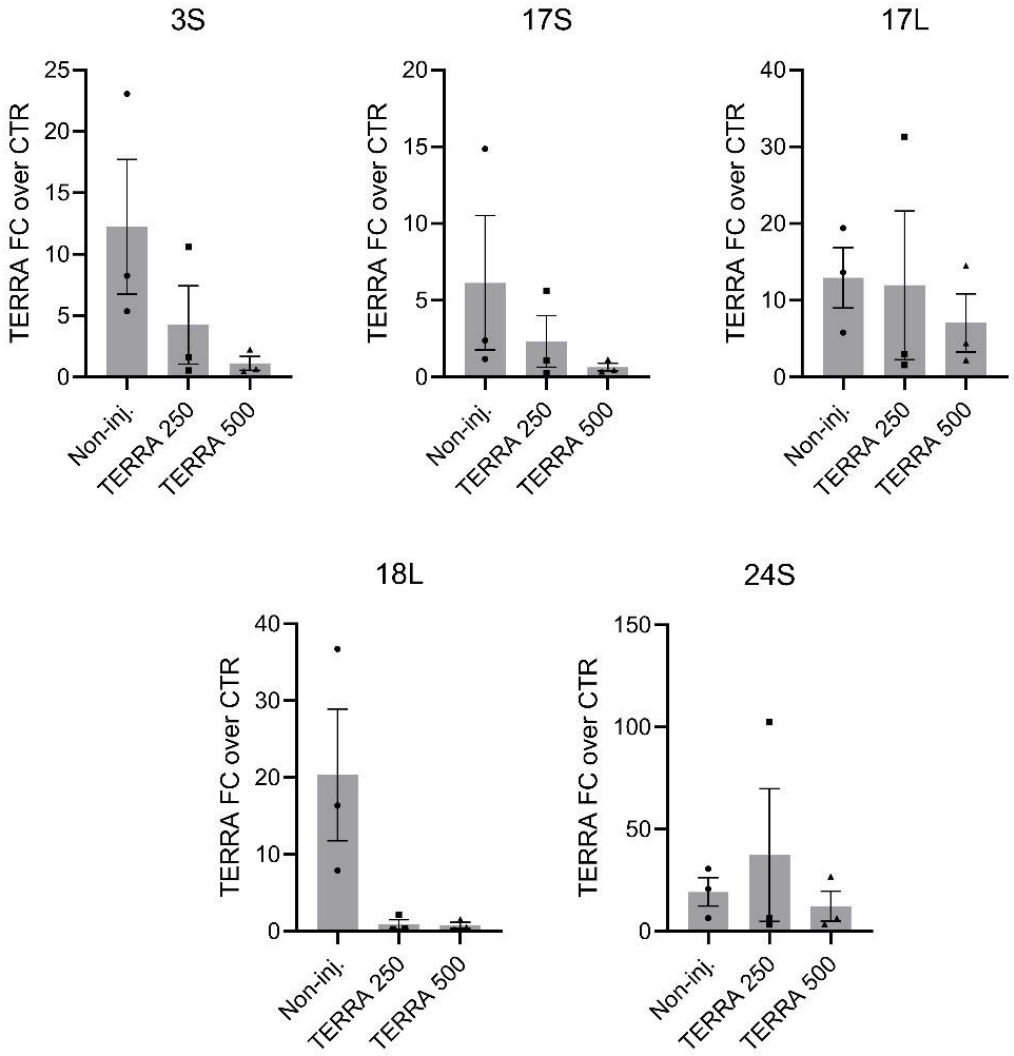


***Figure 42 |*** *RT-qPCR analysis for telomere-specific TERRA expression on 1 year old zic:RAS adult brains injected with TERRA-ASO at 250 nM (TERRA 250) and 500 nM (TERRA 500). TERRA expressed from the indicated telomeres was analyzed: telomere 3S, 17S, 17L, 18L, and 24S. Data are shown as fold change (FC) over non-injected zic:RAS control brains. The experiment was done using 3 adult brains per each condition.*

Strikingly, by looking at TERRA-ASO injected animals that were left from previous experiments and reached about 1 year of age, we saw that a number of them were not displaying any morphological deformities, or at least presented some that were not as strong as those found in all zic:RAS animals that were not injected (data not shown). We wondered whether such phenomenon could be attributed to the injection of TERRA-ASO, so we extracted the brains from those few 1 year old animals that we had in our animal facility that presented “ameliorated phenotypes” and quantified single TERRA molecules using the previously described RT-qPCR assay. These analyses revealed a reduction of TERRA levels from different telomeres in brains obtained from TERRA-ASO injected zic:RAS animals, as compared to non-injected brains (Figure 42).

These data indicate that TERRA-ASO could have an impact in TERRA expression and, potentially, to the tumor itself during late developmental stages. These analyses are preliminary and will need to be confirmed.

# Discussion

A key aspect of this thesis work is our use of three different model organisms to explore the role of TERRA in ALT and during the telomerase-to-ALT transition. Each model has its own advantages and disadvantages, and the specific reasons for choosing these organisms will be discussed in detail in the following paragraphs.

Using *C. elegans*, we gained insights into the dynamics of TERRA before and after the onset of ALT. We employed established *in vivo* models where an ALT-like mechanism for telomere maintenance is triggered in a non-cancerous background upon the loss of telomerase, counteracting progressive telomere shortening. Our group was the first to characterize TERRA expression in *C. elegans*, both in bulk and from single telomeres. These tools allowed us to visualize and investigate TERRA transcripts in terms of expression (using RNA dot blot and RT-qPCR) and their dynamics with telomeres, through the generation of the strain *trt-1; pot-1; pot-1::mCherry* and RNA-FISH coupled with IF.

Working with human cells and zebrafish provided insights into TERRA's role in cancer. Despite the simplicity of human cancer cell models, they are powerful tools for manipulating TERRA. They are easy to work with and useful for characterizing ALT features upon TERRA downregulation, which is a part of the future perspectives of this project. We have both ALT-positive and ALT-negative cancer cell lines, and importantly, ALT-negative cells in which the telomerase-to-ALT transition can be induced. This allows us to determine whether TERRA is crucial during the transition.

Finally, zebrafish offers a valuable compromise between a TERRA and telomere study system relevant to humans and the added complexity of an *in vivo* model. We have an ALT-positive brain tumor model in zebrafish where we can downregulate genes like TERRA and track their development over time as the ALT mechanism activates. We possess the tools to study TERRA and ALT dynamics in zebrafish. The next step, part of the future perspectives of this work, is to determine the optimal time frame for these studies.

## *C. elegans*

The nematode *C. elegans* revealed to be a powerful tool to study the dynamics of TERRA and ALT in a non-cancerous background. First, *C. elegans* is a relatively inexpensive and easy model to work with, as it is small, requires little attention and its life cycle is short (less than 4 days), enabling the possibility to grow it over a huge number of generations within a relatively short timeframe (such as a PhD project). In addition, the large number of characterized mutants available from wormbase.org and the ease in crossing and maintaining a homozygous genotype made it particularly interesting for this project, as we were able to successfully generate double and triple mutant lines (*trt-1; pot-2* and *trt-1; pot-1; pot-1::mCherry*) which were then kept in culture for over a hundred generations.

The use *C. elegans* for the study of TERRA and ALT, has proven to be very advantageous for several reasons. Previous studies have already shown that the nematode is the only multicellular organism able to survive without a functional telomerase, possibly because of the holocentric nature of its chromosomes, enabling them to segregate during mitosis even if telomere shortening and fusion events took place[117]. When combined with *pot-2* deficiency, telomerase-deficient organisms were discovered to activate an ALT-like mechanism, during which telomeres become long and heterogenous, similarly to those found in ALT-positive tumors. The expression of TERRA in *C. elegans* was still an open question, as no previous studies investigated such topic but at the same time telomeres were shown to be transcribed in a myriad of organisms, from invertebrates to vertebrates.

In this work, we were able to successfully characterize telomeric shortening in the telomerase-deficient *trt-1* line through TRF coupled with Southern blotting. Taking advantage of the information about TERRA expression and visualization in *C. elegans* from Manzato et al. (some of the experiments shown in this PhD thesis were also part of this work), we were able to show that the overall TERRA expression is not altered in *trt-1*. Interestingly, the analysis of TERRA from single telomeres through RT-qPCR showed a telomere-specific fine tuning of TERRA, with TERRA-XR being undetectable in *trt-1*, possibly as a result of chromosome aberrations as mentioned in the result section.

Moving to the analysis on the dynamics of TERRA in ALT, we were able to generate and maintain in homozygosity the double mutant *trt-1; pot-2* strain, which showed the

expected sterility phenotype during early generations and then eventually overcame it through elongation of telomeres through ALT-mechanisms, as shown through TRF coupled with Southern blotting. Notably, TERRA dynamics as seen by Northern blotting and RT-qPCR appeared to be different from other organisms: an increase of the bulk TERRA population was detected during early generations, which ranged differently depending on the telomere of origin (or at least within the 5 telomeres we were able to analyze with the available primers). Besides the selection of the *trt-1; pot-2* double mutant, we were able to isolate and grow 3 independent ALT survivors (namely clone 10, clone 14, and clone 18) which maintained long and heterogeneous telomeres, but with slight differences from the parental line, as shown by the Southern blot analysis. Interestingly, TERRA levels remained higher in ALT clones as compared to WT worms, but did not change between early and late generations, even if more than 70 generations passed. One possible explanation could stem in the necessity of *trt-1* cells to increase the amount of TERRA required for the ALT-like mechanism to elongate telomeres, as it happens in human cancer cells for instance. The *pot-2* background on the other hand, presenting uncapped telomeres, may help in having an increased expression of TERRA[103] and is also known to increase the chance of give rise to ALT survivors in the absence of a functional telomerase[107], possibly making telomeres more accessible to factors promoting the ALT-like elongation, which to date remain still unknown. Interestingly, not only pot-2 but also pot-1 was shown to act as a repressor of ALT[107]. In Manzato et al., we observed that both *pot-1* and *pot-2* single mutants express higher levels of TERRA than the WT strain. Therefore, increased TERRA expression may represent one of the mechanisms predisposing these strains to ALT activation.

Regarding TERRA localization, we employed the *pot-1::mCherry*, which has been characterized as a validated tool to image telomeres by targeting pot-1, as it localizes exclusively to telomeres[107,110]. To this regard, we successfully generated an additional line which is the *trt-1; pot-2; pot-1::mCherry* (abbreviated *t;p;p*), which presented similar features to the *trt-1; pot-2*, namely displayed the sterility phenotype during early generations which is then reverted as ALT survivors arise. Telomeres are elongated and become long and heterogeneous in comparison to WT telomeres, with TERRA being enriched during early generations and maintained in such way in the ALT survivors.

Remarkably, band patterns found in the TRF analyses coupled with Southern blotting from *trt-1; pot-2* and *t;p;p* show differences between the two strains, highlighting the broad heterogeneity found in *C. elegans* telomeres elongated through ALT, an event that was previously seen in other studies[83,107,110]. Even though Northern blot analysis in *trt-1; pot-2* and RNA dot blot in *t;p;p* are not comparable, we can infer to some extent that TERRA levels are closely correlated to telomere length, in the sense that there is an increase of TERRA during early generations and then its levels mildly differ from clone to clone. Furthermore, differences between clones are expected due to the intrinsic heterogeneity of these clones in terms of telomere length and potential chromosome end fusions.

Through the use of RNA-FISH, we were able to validate TERRA expression in the nematode at single cell resolution, corroborating the hypothesis that TERRA is indeed transcribed and present in *C. elegans*. Unfortunately, for the imaging of TERRA, the settings we had in house were not ideal; for instance, part of the images that are present in the article published by Manzato and colleagues were taken by our collaborators using a different microscope (Deltavision Ultra), which presented a higher resolution and enabled the visualization of more TERRA foci when compared to images acquired through a Nikon Eclipse Ti2 (with a 4 to 5-fold increase number of foci detected), making hard, for example, to visualize any TERRA focus in a WT background. That said, taking into consideration the fact that we are underestimating the number of effective TERRA foci, we were still able to analyze the dynamics of TERRA at telomeres, in particular we saw that only a fraction of TERRA molecules (around 75%) localizes at telomeres, a phenomenon observed in all genotypes studied. These data suggest that TERRA acts at telomeres only transiently and independently from ALT, meaning that in *C. elegans* TERRA may act in trans to other genomic loci similarly to what has been shown to happen in vertebrates.

## Human cells

The use of a human cancer cell line poses some advantages over the use of the animal models used in this study. Besides the fact that working with human cells, even if done *in vitro*, enables us to understand the dynamics of what is happening in human, the practicality of employing cell lines stands also in the possibility to perform TERRA downregulation with a higher success rate than what we were expecting in the animal model. By performing the ASO micro-injection in zebrafish (as it will be discussed in more detail in the next discussion paragraph) was challenging, as ASOs are not so commonly used for micro-injections, while transfection of ASO in human cells for gene manipulation is a common practice, with no exception for the TERRA-ASO, specifically[51]. In fact, transfection of TERRA-ASO resulted in a reduction of TERRA to approximately 40-50% under the conditions we adopted, depending on whether we are quantifying the bulk TERRA population as we observed with RNA dot blot or single-telomere TERRA molecules through RT-qPCR.

Unfortunately, we were not able to fully analyze changes in the ALT phenotype as we experienced issues with the C-circle assay (CCA). To balance the difficulties in measuring changes in C-circles as the golden standard for ALT, we were able to implement ALT-FISH as an alternative methodology to evaluate multiple ALT-related changes upon the activity of TERRA-ASO. In that case, we were able to detect a reduction in terms of G-rich elements in cells treated with TERRA-ASO (imaged through the use of C-rich probes, as reported in the results section); however, it is hard to state whether such reduction can be attributed to an effective reduction in ALT or it is merely an effect of TERRA-ASO downregulating TERRA foci. Even though it appeared to be not ideal for the analysis of TERRA downregulation, ALT-FISH still stands as a valid tool to study ALT where no use of oligos that mimic the sequences of the probes is involved, for example in the induction of ALT through downregulation of ASF1 with siRNA [118] in telomerase-positive HeLa Long Telomeres (LT). Nonetheless, it is of fundamental importance to implement the CCA for ALT evaluation in our lab, together possibly with other approaches.

## Zebrafish

For this PhD work, the zebrafish model served as a powerful tool to study the dynamics of TERRA and telomere and most importantly, to try to modulate TERRA transcripts through downregulation. Telomeres in zebrafish are similar in length to those of human and progressively shorten as the fish age, differently to other models such as the mouse[102,119,120]. Also, previous studies showed that TERRA is expressed in the fish[121].

Perhaps the most interesting aspect in the use of zebrafish is the possibility to micro-inject compounds at the beginning of embryonic development to use them as a gene manipulation tool, as it has been for the enormous use of morpholinos (MOs) in past decades and, to lower extent, antisense oligonucleotides (ASOs). Especially before the advent of the now widely used CRISPR/Cas9 genome editing tool, which is used also in the zebrafish to generate knock-out models, MOs constituted one of the best tools for gene manipulation during early development of the zebrafish, enabling to achieve good levels of gene downregulation in a short period of time. For this specific PhD project, however, MOs could not be used and instead ASOs were preferred for a number of reasons.

MOs are designed in such a way that they either block AUG sites within mRNAs, inhibiting translation, or block splice sites, generating non-functional proteins. The problem when working with TERRA in *D. rerio*, is that TERRA transcription start sites have not been mapped. On top of that, MOs bind and block their targets but, as the number of targets increases over time (e.g. cells dividing and multiplying), their effect is progressively lost and that is reason why MOs can be excellent genetic tools but with a short working time frame (namely 2-3 days post injection). On the other hand, ASOs are less used in gene expression manipulation in zebrafish, but they have an advantage over the MOs: they bind an antisense RNA sequence and they promote their degradation though RNases activity found in the cells, enabling the ASO to be freed in the system and to bind other targets, promote their degradation and continue in their activity. For this reason, TERRA-ASOs are currently being used as leading means for downregulating TERRA in human cell cultures.

We had the possibility to work with a pediatric-like glioblastoma model in zebrafish (zic:RAS), which was characterized to be ALT-positive, thus expressing high levels of TERRA. The model was easy to work with as by crossing two distinct zebrafish lines we could obtain

a large number of tumor-forming animals (more than 200 eggs per lay) with full penetrance. The use of the Gal4-UAS system, designed in a way so that proteins would be fluorescently labeled and visible in transparent embryos starting from about 24 hpf, enabled us to monitor in live the expression and development of the tumor. We could then micro-inject the TERRA-ASO at 1-2 cells stage and have them grow to the desired time points.

We were able to test a range of concentrations for both TERRA-ASO and SCRB-ASO and found that, as we were expecting, there are concentrations above which (namely 5 µM for TERRA-ASO and 1 µM for SCRB-ASO) the ASO becomes toxic to the embryo and leads to death. Besides the acute toxicity of high concentrations, we know the delivery of the ASO into cells was properly done as we co-injected RD together with the ASO and we were able to see the fluorescent RD signal during early embryogenesis, about 4-6 hours post injection.

Unfortunately, at the earliest time point we worked with, which is 5 dpf, moment at which a hyperproliferation of cells in the brain can be detected, or the latest time point, which was 1 mpf, we did not detect a reduction in TERRA levels, compared to neither non-injected nor SCRB-ASO injected animals. A possible explanation is that the LNA Gapmer ASO we used requires RNase H1 activity to degrade the target RNA, but RNase H1 levels in zebrafish embryos may not be strong enough to elicit a measurable effect. Another hypothesis could stem in the fact that amount of TERRA-ASO injected is not enough to significantly downregulate TERRA; if that was the case, as higher amounts of ASOs would be toxic to the animal, it may be needed to revise the type and chemistry of ASO to elicit a stronger effect. What is interesting, however, is that at concentrations of 0.02 µM and 0.1 µM SCRB-ASO, we could detect a mild, yet non-significant, increase in the overall TERRA expression. The reasons behind such phenomenon still remain unclear.

In order to test whether a finely tuned TERRA downregulation could be telomere specific, we designed the RT-qPCR primers to visualize single telomere TERRA transcripts. In all TERRA molecules analyzed (TERRA-3S, TERRA-17S, TERRA-17L, TERRA-18L, TERRA-24S) we could not find a change in TERRA expression when compared to SCRB-ASO injected animals at the same concentration. The array of single telomere TERRA analyzed is quite small, considering zebrafish has 25 chromosomes and thus a theoretical number of 50

different TERRA transcription loci, therefore we cannot exclude that a reduction in TERRA could be present, but non-detectable with the primers we used. Still, we now have in our hands a promising tool for the detection of single TERRA molecules in zebrafish (tool that is currently being further characterized and validated as part of another piece of work carried out in the lab).

Last, some preliminary yet interesting results were observed when looking at fully grown fish and their altered morphology upon injection of TERRA-ASO. Even though solid conclusions cannot yet be drawn due to the limited number of animals analyzed and the lack of all controls included in the analysis (e.g. zic:RAS injected with an equivalent amount of SCRB-ASO), we observed interesting effects on the animals, both at a macroscopic level, having some TERRA-ASO injected fish presenting no or at least less severe morphological deformities, and at molecular levels, as the RT-qPCR read out on individual TERRA transcripts showed a trend on having less amount of TERRA, possibly relatable to the activity of the ASO. It will be interesting to verify whether RNase H1 expression increases at this stage of growth of the animals, as compared to early stages of development, which may in part explain the functionality of TERRA-ASO in fully grown fishes and not at earlier time points.

Results concerning the zebrafish part of the project are shown by first presenting experiments done on animals during early developmental stages, where it is demonstrated that TERRA-ASO is not eliciting an effect in downregulating TERRA, and only subsequently reporting preliminary results on adult brains indicating an important (however to be confirmed) effect on reducing TERRA when analyzed through RT-qPCR. For these experiments, TERRA-ASO micro-injections were performed at roughly the same time and results obtained in 1 year old adults were observed much later then the findings obtained during early developmental stages. As previously mentioned in the results section, what caught our attention was that zebrafish tanks in which animals were injected with TERRA-ASOwere housing a small number of fish that showed ameliorated phenotypes thannot injected fishe, for which a full penetrance of the tumor leads to severe phenotypes in all organisms that survive past 11 days, time at which most fish die due to the aggressiveness of the brain tumor.[3,94]. A few of the animals with ameliorated phenotypes were used for the RT-qPCR analysis and led to the preliminary data we are

currently discussing. We could not have anticipated such a result and unfortunately it turned out only at the end of PhD project, and therefore I had no sufficient time to repeat this experiment. From these observations, though, it is tempting to speculate that the delivery of TERRA-ASO through micro-injection into the whole zebrafish system and its maintenance through time might not be as effective as we reasoned, as only a small fraction of adult tumor-positive animals have present a visible and clear phenotype, enabling us to direct our research on those animals where the ASO seems to have elicited an effect. Perhaps, working with younger larvae and fries excludes the possibility to selectively pick animals where the ASO has been successfully delivered and thus leads to an “apparent non-functional activity of TERRA-ASO at early stages”.

On a final analysis, the zic:RAS brain cancer model resulted to be very interesting and powerful genetic tool to investigate the roles of TERRA in ALT and during ALT induction. We were able to set-up the micro-injection protocol and visualize TERRA in the fish. We observed there are no tangible effects on the tumor until 1 mpf; however, there is room for improvement as it appears there is an effect of TERRA downregulation that is visible on adult fish, meaning we now know “how” and “when” to focus our attention for future analyses.

# Future perspectives

## *C. elegans*

Even though a part of the results obtained in this PhD work using worms as part of a bigger project that focused on investigating the expression of TERRA in *C. elegans* led to a publication, there are still several points that have not be addressed yet.

It could be of interest to generate an additional worm line, namely *trt-1; pot-1::mCherry*, to study TERRA dynamics both in terms of expression and localization, possibly cultivating worms until we are be able to identify ALT survivors, in the absence of *pot-2* background. This would enable us to see whether the pot-2 protein, meaning the capping of telomeres, would somehow change TERRA behavior and possibly the mechanism of ALT.

Another point that is missing is the quantification of ALT. We could think of implementing the CCA or additional assays to assess ALT markers possibly using ALT-FISH on the worms' gonads to assess ALT and its heterogeneity.

As already mentioned in the results paragraph, we have been underestimating the TERRA foci visualized through RNA-FISH due to microscopy settings we have at CIBIO. It would be interesting to use instruments with higher resolutions to have a more complete view on TERRA localization dynamics and, especially, make sure that the TERRA foci we are not viewing, possibly individual TERRA foci that are not clusters, are behaving differently from the brighter ones we are imaging.

Last, to be able to translate as much as possible our findings from nematodes to higher organisms, it would be important to understand the molecular mechanisms behind TERRA induction prior the insurgence of ALT. An example would be to understand which other players are involved in this process, for instance performing a RNA-FISH coupled with IF using an antibody for Rad51, an important player in HDR in ALT or testing the presence of R-loop structure at telomeres using the S9.6 antibody.

## Human cells

The results obtained with ALT-positive U2OS cells were obtained using experimental conditions that enabled a partial reduction of TERRA. In future experiments it will be important to implement transfection strategies, or different antisense oligonucleotide chemistries to increase the magnitude of TERRA reduction, as possibly even a small fraction of TERRA in cells could be sufficient to maintain the ALT mechanism.

For U2OS, we have been working on cells where the ALT mechanism has been firmly established for a multitude of generations. However, to mimic what has been done in *C. elegans* and zebrafish and to better understand the mechanisms mediating the telomerase-to-ALT switch in tumors that are not coming from cell cultures, it would be essential for us to implement a model where a telomerase-to-ALT transition can be initiated on cue. In another project in our lab, we are currently trying to induce telomerase-to-ALT transition using HeLa cells containing long telomeres upon downregulation of the histone chaperone ASF1 through siRNA[118]. In the future, we plan to couple siRNA transfection together with ASO transfection to reduce TERRA during ALT induction, studying whether reduced TERRA levels could impair the telomerase-to-ALT transition.

## Zebrafish

The main analyses done on TERRA-ASO affecting TERRA downregulation in the zic:RAS model were performed in a time frame that spans from 5 dpf, when most of the experiments shown in this PhD thesis were performed, up to 1 mpf. In the process of troubleshooting the variety of techniques used in the zebrafish part of the project, we obtained preliminary results on TERRA expression and on the status of ALT at different developmental stages of the animals: 8 dpf, 10 dpf, 12 dpf, even 45 dpf, but in all cases they led to the same result, which is that TERRA-ASO micro-injection did not result in TERRA downregulation, or at least not in our experimental settings.

Interestingly, RT-qPCR experiments performed on fully grown fish that were about 1 year old, revealed a reduction of all TERRA molecules analyzed. These reduction also correlated with animals displaying less severe morphology alterations to the non-injected zic:RAS. In light of this evidence, it would be fundamental to test whether the data can be replicated. As these findings were obtained during the end of the PhD project, they could not be replicated yet given the long time it takes to repeat the experiment.

Based on this result, there is number of questions that should be addressed: is there a consistent and replicable difference in terms of fish showing less morphological abnormalities between zic:RAS injected with TERRA-ASO and the non-injected? If so, what is the percentage of recovered animals? Does this happen also in zic:RAS injected with SCRB-ASO? Is this amelioration of the phenotype visible also prior the 1 year? If so, when?

In case those results could be replicated, there would be a variety of tests that could be done in order to check alterations in the ALT phenotype, as described by Idilli and colleagues from Mione lab[3]: alterations in TERRA expression, in C-circles production, in telomere length, in T-SCE, in expression of telomerase (through RT-qPCR analysis of *tert* and *terc* and by q-TRAP), in survival and in cellular proliferation. It would be interesting to understand whether a reduction of TERRA could alter the faith of the tumor in a way that an inefficient ALT mechanism (due to the lack of TERRA) could lead to cell death as a result of telomeric stress and/or a switch back from ALT to telomerase could take place.

# Acknowledgments

First and foremost, I express my deepest gratitude to the heads of the laboratories at CIBIO where I dedicated the past three and a half years of my PhD project: Prof. Emilio Cusanelli and Prof. Maria Caterina Mione. They served as exceptional mentors and colleagues, believing in my abilities from the outset and fostering both my scientific and personal growth. I extend my thanks to all past and present members of both labs for the camaraderie shared both professionally and socially. While it's impractical to list everyone by name, I trust they know my appreciation extends to each of them.

I am also indebted to the Advanced Imaging Facility at CIBIO for their invaluable assistance with imaging and microscopy, as well as to the vibrant zebrafish community at CIBIO, including group leaders and fellow lab members, for their insightful guidance and enjoyable interactions.

A special acknowledgment goes to the additional "third" lab that provided support beyond scientific endeavors. Your companionship will be dearly missed.

Lastly, I am deeply grateful to the “true mentors and referees” over the past years – my closest friends and, most importantly, my family. They have been my rock through the highs and lows of this remarkable journey. It may sound cliché, but I genuinely could not have accomplished this without their unwavering support.

# Bibliography


1. Blackburn, E. H. Telomeres and telomerase: their mechanisms of action and the effects of altering their functions. *FEBS Lett.* **579**, 859–862 (2005).
2. Shay, J. W. & Wright, W. E. Telomeres and telomerase: three decades of progress. *Nat. Rev. Genet.* **20**, 299–309 (2019).
3. Idilli, A. I. *et al.* Expression of tert Prevents ALT in Zebrafish Brain Tumors. *Front. Cell Dev. Biol.* **8**, 65 (2020).
4. Raices, M. *et al.* C. elegans Telomeres Contain G-Strand and C-Strand Overhangs that Are Bound by Distinct Proteins. *Cell* **132**, 745–757 (2008).
5. Jain, D. & Cooper, J. P. Telomeric Strategies: Means to an End. *Annu. Rev. Genet.* **44**, 243–269 (2010).
6. Griffith, J. D. *et al.* Mammalian Telomeres End in a Large Duplex Loop. *Cell* **97**, 503–514 (1999).
7. De Lange, T. Shelterin-Mediated Telomere Protection. *Annu. Rev. Genet.* **52**, 223–247 (2018).
8. De Lange, T. Shelterin: the protein complex that shapes and safeguards human telomeres. *Genes Dev.* **19**, 2100–2110 (2005).
9. Karlseder, J. *et al.* The Telomeric Protein TRF2 Binds the ATM Kinase and Can Inhibit the ATM-Dependent DNA Damage Response. *PLoS Biol.* **2**, e240 (2004).
10. Denchi, E. L. & De Lange, T. Protection of telomeres through independent control of ATM and ATR by TRF2 and POT1. *Nature* **448**, 1068–1071 (2007).
11. Sfeir, A. *et al.* Mammalian Telomeres Resemble Fragile Sites and Require TRF1 for Efficient Replication. *Cell* **138**, 90–103 (2009).
12. Sarek, G., Vannier, J.-B., Panier, S., Petrini, J. H. J. & Boulton, S. J. TRF2 Recruits RTEL1 to Telomeres in S Phase to Promote T-Loop Unwinding. *Mol. Cell* **57**, 622–635 (2015).
13. Olovnikov, A. M. A theory of marginotomy. *J. Theor. Biol.* **41**, 181–190 (1973).
14. Chow, T. T., Zhao, Y., Mak, S. S., Shay, J. W. & Wright, W. E. Early and late steps in telomere overhang processing in normal human cells: the position of the final RNA primer drives telomere shortening. *Genes Dev.* **26**, 1167–1178 (2012).
15. Shay, J. W., Pereira-Smith, O. M. & Wright, W. A Role for Both RB and p53 in the Regulation of Human Cellular Senescence.
16. Greider, C. W. & Blackburn, E. H. Identification of a specific telomere terminal transferase activity in tetrahymena extracts. *Cell* **43**, 405–413 (1985).
17. Blackburn, E. H. & Collins, K. Telomerase: An RNP Enzyme Synthesizes DNA. *Cold Spring Harb. Perspect. Biol.* **3**, a003558–a003558 (2011).
18. Schmidt, J. C. & Cech, T. R. Human telomerase: biogenesis, trafficking, recruitment, and activation. *Genes Dev.* **29**, 1095–1105 (2015).
19. Calado, R. T. Telomere Diseases. *N. Engl. J. Med.* (2009).
20. Allsopp, R. C. *et al.* Telomere length predicts replicative capacity of human fibroblasts. *Proc. Natl. Acad. Sci.* **89**, 10114–10118 (1992).

21. Heidenreich, B. & Kumar, R. TERT promoter mutations in telomere biology. *Mutat. Res. Mutat. Res.* **771**, 15–31 (2017).
22. Kim, N. W. *et al.* Specific Association of Human Telomerase Activity with Immortal Cells and Cancer. *Science* **266**, 2011–2015 (1994).
23. Pickett, H. A. & Reddel, R. R. Molecular mechanisms of activity and derepression of alternative lengthening of telomeres. *Nat. Struct. Mol. Biol.* **22**, 875–880 (2015).
24. Tardat, M. & Déjardin, J. Telomere chromatin establishment and its maintenance during mammalian development. *Chromosoma* **127**, 3–18 (2018).
25. Benetti, R. *et al.* Suv4-20h deficiency results in telomere elongation and derepression of telomere recombination. *J. Cell Biol.* **178**, 925–936 (2007).
26. García-Cao, M., O'Sullivan, R., Peters, A. H. F. M., Jenuwein, T. & Blasco, M. A. Epigenetic regulation of telomere length in mammalian cells by the Suv39h1 and Suv39h2 histone methyltransferases. *Nat. Genet.* **36**, 94–99 (2004).
27. Episkopou, H. *et al.* Alternative Lengthening of Telomeres is characterized by reduced compaction of telomeric chromatin. *Nucleic Acids Res.* **42**, 4391–4405 (2014).
28. Baur, J. A., Zou, Y., Shay, J. W. & Wright, W. E. Telomere Position Effect in Human Cells. *Science* **292**, 2075–2077 (2001).
29. Azzalin, C. M., Reichenbach, P., Khoriauli, L., Giulotto, E. & Lingner, J. Telomeric Repeat–Containing RNA and RNA Surveillance Factors at Mammalian Chromosome Ends. *Science* **318**, 798–801 (2007).
30. Schoeftner, S. & Blasco, M. A. Developmentally regulated transcription of mammalian telomeres by DNA-dependent RNA polymerase II. *Nat. Cell Biol.* **10**, 228–236 (2008).
31. Azzalin, C. M. & Lingner, J. Telomere functions grounding on TERRA firma. *Trends Cell Biol.* **25**, 29–36 (2015).
32. Schoeftner, S. & Blasco, M. A. Chromatin regulation and non-coding RNAs at mammalian telomeres. *Semin. Cell Dev. Biol.* **21**, 186–193 (2010).
33. Porro, A., Feuerhahn, S., Reichenbach, P. & Lingner, J. Molecular Dissection of Telomeric Repeat-Containing RNA Biogenesis Unveils the Presence of Distinct and Multiple Regulatory Pathways. *Mol. Cell. Biol.* **30**, 4808–4817 (2010).
34. Nergadze, S. G. *et al.* CpG-island promoters drive transcription of human telomeres. *RNA* **15**, 2186–2194 (2009).
35. Porro, A. *et al.* Functional characterization of the TERRA transcriptome at damaged telomeres. *Nat. Commun.* **5**, 5379 (2014).
36. Deng, Z. *et al.* A role for CTCF and cohesin in subtelomere chromatin organization, TERRA transcription, and telomere end protection: Chromatin organization of human subtelomeres. *EMBO J.* **31**, 4165–4178 (2012).
37. Feretzaki, M. & Lingner, J. A practical qPCR approach to detect TERRA, the elusive telomeric repeat-containing RNA. *Methods* **114**, 39–45 (2017).
38. Farnung, B. O., Brun, C. M., Arora, R., Lorenzi, L. E. & Azzalin, C. M. Telomerase Efficiently Elongates Highly Transcribing Telomeres in Human Cancer Cells. *PLoS ONE* **7**, e35714 (2012).

39. Diman, A. & Decottignies, A. Genomic origin and nuclear localization of TERRA telomeric repeat-containing RNA: from Darkness to Dawn. *FEBS J.* **285**, 1389–1398 (2018).
40. Arnoult, N., Van Beneden, A. & Decottignies, A. Telomere length regulates TERRA levels through increased trimethylation of telomeric H3K9 and HP1α. *Nat. Struct. Mol. Biol.* **19**, 948–956 (2012).
41. Azzalin, C. M. & Lingner, J. Telomeres: The silence is broken. *Cell Cycle* **7**, 1161–1165 (2008).
42. Deng, Z., Norseen, J., Wiedmer, A., Riethman, H. & Lieberman, P. M. TERRA RNA binding to TRF2 facilitates heterochromatin formation and ORC recruitment at telomeres. *Mol. Cell* **35**, 403–413 (2009).
43. Balk, B. *et al.* Telomeric RNA-DNA hybrids affect telomere-length dynamics and senescence. *Nat. Struct. Mol. Biol.* **20**, 1199–1205 (2013).
44. Pfeiffer, V., Crittin, J., Grolimund, L. & Lingner, J. The THO complex component Thp2 counteracts telomeric R-loops and telomere shortening. *EMBO J.* **32**, 2861–2871 (2013).
45. Arora, R. *et al.* RNaseH1 regulates TERRA-telomeric DNA hybrids and telomere maintenance in ALT tumour cells. *Nat. Commun.* **5**, 5220 (2014).
46. Cusanelli, E., Romero, C. A. P. & Chartrand, P. Telomeric noncoding RNA TERRA is induced by telomere shortening to nucleate telomerase molecules at short telomeres. *Mol. Cell* **51**, 780–791 (2013).
47. Avogaro, L. *et al.* Live-cell imaging reveals the dynamics and function of single-telomere TERRA molecules in cancer cells. *RNA Biol.* **15**, 787–796 (2018).
48. Perez-Romero, C. A., Lalonde, M., Chartrand, P. & Cusanelli, E. Induction and relocalization of telomeric repeat-containing RNAs during diauxic shift in budding yeast. *Curr. Genet.* **64**, 1117–1127 (2018).
49. Cusanelli, E. & Chartrand, P. Telomeric noncoding RNA: telomeric repeat-containing RNA in telomere biology. *Wiley Interdiscip. Rev. RNA* **5**, 407–419 (2014).
50. Scheibe, M. *et al.* Quantitative interaction screen of telomeric repeat-containing RNA reveals novel TERRA regulators. *Genome Res.* **23**, 2149–2157 (2013).
51. Chu, H.-P. *et al.* TERRA RNA Antagonizes ATRX and Protects Telomeres. *Cell* **170**, 86-101.e16 (2017).
52. Barthel, F. P. *et al.* Systematic analysis of telomere length and somatic alterations in 31 cancer types. *Nat. Genet.* **49**, 349–357 (2017).
53. Cerone, M. A. Telomere maintenance by telomerase and by recombination can coexist in human cells. *Hum. Mol. Genet.* **10**, 1945–1952 (2001).
54. Perrem, K., Colgin, L. M., Neumann, A. A., Yeager, T. R. & Reddel, R. R. Coexistence of Alternative Lengthening of Telomeres and Telomerase in hTERT-Transfected GM847 Cells. *Mol. Cell. Biol.* **21**, 3862–3875 (2001).

55. Grobelny, J. V. Effects of reconstitution of telomerase activity on telomere maintenance by the alternative lengthening of telomeres (ALT) pathway. *Hum. Mol. Genet.* **10**, 1953–1961 (2001).
56. De Vitis, M., Berardinelli, F. & Sgura, A. Telomere Length Maintenance in Cancer: At the Crossroad between Telomerase and Alternative Lengthening of Telomeres (ALT). *Int. J. Mol. Sci.* **19**, 606 (2018).
57. Bojovic, B., Booth, R. E., Jin, Y., Zhou, X. & Crowe, D. L. Alternative lengthening of telomeres in cancer stem cells in vivo. *Oncogene* **34**, 611–620 (2015).
58. Sobinoff, A. P. & Pickett, H. A. Alternative Lengthening of Telomeres: DNA Repair Pathways Converge. *Trends Genet.* **33**, 921–932 (2017).
59. Lovejoy, C. A., Takai, K., Huh, M. S., Picketts, D. J. & De Lange, T. ATRX affects the repair of telomeric DSBs by promoting cohesion and a DAXX-dependent activity. *PLOS Biol.* **18**, e3000594 (2020).
60. Gauchier, M. *et al.* SETDB1-dependent heterochromatin stimulates alternative lengthening of telomeres. *Sci. Adv.* **5**, eaav3673 (2019).
61. Chung, I., Leonhardt, H. & Rippe, K. De novo assembly of a PML nuclear subcompartment occurs through multiple pathways and induces telomere elongation. *J. Cell Sci.* **124**, 3603–3618 (2011).
62. Fonin, A. V. *et al.* The Role of Non-Specific Interactions in Canonical and ALT-Associated PML-Bodies Formation and Dynamics. *Int. J. Mol. Sci.* **22**, 5821 (2021).
63. Zhang, H. *et al.* Nuclear body phase separation drives telomere clustering in ALT cancer cells. *Mol. Biol. Cell* **31**, 2048–2056 (2020).
64. Zhang, J.-M., Genois, M.-M., Ouyang, J., Lan, L. & Zou, L. Alternative lengthening of telomeres is a self-perpetuating process in ALT-associated PML bodies. *Mol. Cell* **81**, 1027-1042.e4 (2021).
65. Loe, T. K. *et al.* Telomere length heterogeneity in ALT cells is maintained by PML-dependent localization of the BTR complex to telomeres. *Genes Dev.* **34**, 650–662 (2020).
66. Zhang, T. *et al.* Strand break-induced replication fork collapse leads to C-circles, C-overhangs and telomeric recombination. *PLOS Genet.* **15**, e1007925 (2019).
67. Henson, J. D. *et al.* DNA C-circles are specific and quantifiable markers of alternative-lengthening-of-telomeres activity. *Nat. Biotechnol.* **27**, 1181–1185 (2009).
68. Huang, C., Jia, P., Chastain, M., Shiva, O. & Chai, W. The human CTC1/STN1/TEN1 complex regulates telomere maintenance in ALT cancer cells. *Exp. Cell Res.* **355**, 95–104 (2017).
69. Cox, K. E., Maréchal, A. & Flynn, R. L. SMARCAL1 Resolves Replication Stress at ALT Telomeres. *Cell Rep.* **14**, 1032–1040 (2016).
70. Tomaska, L., Nosek, J., Kramara, J. & Griffith, J. D. Telomeric circles: universal players in telomere maintenance? *Nat. Struct. Mol. Biol.* **16**, 1010–1015 (2009).

71. Compton, S. A., Choi, J.-H., Cesare, A. J., Özgür, S. & Griffith, J. D. Xrcc3 and Nbs1 Are Required for the Production of Extrachromosomal Telomeric Circles in Human Alternative Lengthening of Telomere Cells. *Cancer Res.* **67**, 1513–1519 (2007).
72. Wang, R. C., Smogorzewska, A. & de Lange, T. Homologous Recombination Generates T-Loop-Sized Deletions at Human Telomeres. *Cell* **119**, 355–368 (2004).
73. Root, H. *et al.* FANCD2 limits BLM-dependent telomere instability in the alternative lengthening of telomeres pathway. *Hum. Mol. Genet.* **25**, 3255–3268 (2016).
74. Stavropoulos, D. J. *et al.* The Bloom syndrome helicase BLM interacts with TRF2 in ALT cells and promotes telomeric DNA synthesis. *Hum. Mol. Genet.* **11**, 3135–3144 (2002).
75. Mazzucco, G. *et al.* Telomere damage induces internal loops that generate telomeric circles. *Nat. Commun.* **11**, 5297 (2020).
76. Apfeld, J. & Alper, S. What Can We Learn About Human Disease from the Nematode C. elegans? in *Disease Gene Identification* (ed. DiStefano, J. K.) vol. 1706 53–75 (Springer New York, New York, NY, 2018).
77. Corsi, A. K., Wightman, B. & Chalfie, M. A Transparent Window into Biology: A Primer on *Caenorhabditis elegans*. *Genetics* **200**, 387–407 (2015).
78. Hodgkin, J., Horvitz, H. R. & Brenner, S. NONDISJUNCTION MUTANTS OF THE NEMATODE *CAENORHABDITIS ELEGANS*. *Genetics* **91**, 67–94 (1979).
79. C. elegans Sequencing Consortium. Genome sequence of the nematode C. elegans: a platform for investigating biology. *Science* **282**, 2012–2018 (1998).
80. Bailly, A. & Gartner, A. Germ Cell Apoptosis and DNA Damage Responses. in *Germ Cell Development in C. elegans* (ed. Schedl, T.) vol. 757 249–276 (Springer New York, New York, NY, 2013).
81. Brenner, S. The genetics of Caenorhabditis elegans. *Genetics* **77**, 71–94 (1974).
82. Meier, B. *et al.* trt-1 is the Caenorhabditis elegans catalytic subunit of telomerase. *PLoS Genet.* **2**, e18 (2006).
83. Cheng, C., Shtessel, L., Brady, M. M. & Ahmed, S. Caenorhabditis elegans POT-2 telomere protein represses a mode of alternative lengthening of telomeres with normal telomere lengths. *Proc. Natl. Acad. Sci. U. S. A.* **109**, 7805–7810 (2012).
84. Lackner, D. H., Raices, M., Maruyama, H., Haggblom, C. & Karlseder, J. Organismal propagation in the absence of a functional telomerase pathway in Caenorhabditis elegans. *EMBO J.* **31**, 2024–2033 (2012).
85. Kinth, P., Mahesh, G. & Panwar, Y. Mapping of Zebrafish Research: A Global Outlook. *Zebrafish* **10**, 510–517 (2013).
86. White, R., Rose, K. & Zon, L. Zebrafish cancer: the state of the art and the path forward. *Nat. Rev. Cancer* **13**, 624–636 (2013).
87. Dooley, K. Zebrafish: a model system for the study of human disease. *Curr. Opin. Genet. Dev.* **10**, 252–256 (2000).
88. Hason & Bartůněk. Zebrafish Models of Cancer—New Insights on Modeling Human Cancer in a Non-Mammalian Vertebrate. *Genes* **10**, 935 (2019).

89. Idilli, A., Precazzini, F., Mione, M. & Anelli, V. Zebrafish in Translational Cancer Research: Insight into Leukemia, Melanoma, Glioma and Endocrine Tumor Biology. *Genes* **8**, 236 (2017).
90. Asakawa, K. & Kawakami, K. Targeted gene expression by the Gal4-UAS system in zebrafish. *Dev. Growth Differ.* **50**, 391–399 (2008).
91. Distel, M., Wullimann, M. F. & Köster, R. W. Optimized Gal4 genetics for permanent gene expression mapping in zebrafish. *Proc. Natl. Acad. Sci.* **106**, 13365–13370 (2009).
92. Elsen, G. E., Choi, L. Y., Millen, K. J., Grinblat, Y. & Prince, V. E. Zic1 and Zic4 regulate zebrafish roof plate specification and hindbrain ventricle morphogenesis. *Dev. Biol.* **314**, 376–392 (2008).
93. Santoriello, C. *et al.* Kita Driven Expression of Oncogenic HRAS Leads to Early Onset and Highly Penetrant Melanoma in Zebrafish. *PLoS ONE* **5**, e15170 (2010).
94. Mayrhofer, M. *et al.* A novel brain tumour model in zebrafish reveals the role of YAP activation in MAPK/PI3K induced malignant growth. *Dis. Model. Mech.* dmm.026500 (2016) doi:10.1242/dmm.026500.
95. Idilli, A. I. *et al.* Changes in the Expression of Pre-Replicative Complex Genes in hTERT and ALT Pediatric Brain Tumors. *Cancers* **12**, 1028 (2020).
96. Heaphy, C. M. *et al.* Prevalence of the Alternative Lengthening of Telomeres Telomere Maintenance Mechanism in Human Cancer Subtypes. *Am. J. Pathol.* **179**, 1608–1615 (2011).
97. Pompili, L., Leonetti, C., Biroccio, A. & Salvati, E. Diagnosis and treatment of ALT tumors: is Trabectedin a new therapeutic option? *J. Exp. Clin. Cancer Res.* **36**, 189 (2017).
98. Goytisolo, F. A. & Blasco, M. A. Many ways to telomere dysfunction: in vivo studies using mouse models. *Oncogene* **21**, 584–591 (2002).
99. Calado, R. T. & Dumitriu, B. Telomere Dynamics in Mice and Humans. *Semin. Hematol.* **50**, 165–174 (2013).
100. Xie, M. *et al.* Structure and Function of the Smallest Vertebrate Telomerase RNA from Teleost Fish. *J. Biol. Chem.* **283**, 2049–2059 (2008).
101. Anchelin, M., Murcia, L., Alcaraz-Pérez, F., García-Navarro, E. M. & Cayuela, M. L. Behaviour of Telomere and Telomerase during Aging and Regeneration in Zebrafish. *PLoS ONE* **6**, e16955 (2011).
102. Anchelin, M. *et al.* Premature aging in telomerase-deficient zebrafish. *Dis. Model. Mech.* dmm.011635 (2013) doi:10.1242/dmm.011635.
103. Manzato, C. *et al.* TERRA expression is regulated by the telomere-binding proteins POT-1 and POT-2 in Caenorhabditis elegans. *Nucleic Acids Res.* **51**, 10681–10699 (2023).
104. Jones, C. Y. *et al.* Hyperextended telomeres promote formation of C-circle DNA in telomerase positive human cells. *J. Biol. Chem.* **299**, 104665 (2023).

105. Frank, L. *et al.* ALT-FISH quantifies alternative lengthening of telomeres activity by imaging of single-stranded repeats. *Nucleic Acids Res.* **50**, e61 (2022).
106. Kimmel, C. B., Ballard, W. W., Kimmel, S. R., Ullmann, B. & Schilling, T. F. Stages of embryonic development of the zebrafish. *Dev. Dyn. Off. Publ. Am. Assoc. Anat.* **203**, 253–310 (1995).
107. Shtessel, L. *et al.* Caenorhabditis elegans POT-1 and POT-2 repress telomere maintenance pathways. *G3 Bethesda Md* **3**, 305–313 (2013).
108. Moravec, M. *et al.* TERRA promotes telomerase-mediated telomere elongation in Schizosaccharomyces pombe. *EMBO Rep.* **17**, 999–1012 (2016).
109. Misino, S., Bonetti, D., Luke-Glaser, S. & Luke, B. Increased TERRA levels and RNase H sensitivity are conserved hallmarks of post-senescent survivors in budding yeast. *Differ. Res. Biol. Divers.* **100**, 37–45 (2018).
110. Lister-Shimauchi, E. H., Dinh, M., Maddox, P. & Ahmed, S. Gametes deficient for Pot1 telomere binding proteins alter levels of telomeric foci for multiple generations. *Commun. Biol.* **4**, 158 (2021).
111. Savoca, V. *et al.* TERRA stability is regulated by RALY and polyadenylation in a telomere-specific manner. *Cell Rep.* **42**, 112406 (2023).
112. Wetts, R. & Fraser, S. E. Multipotent precursors can give rise to all major cell types of the frog retina. *Science* **239**, 1142–1145 (1988).
113. Wetts, R. & Fraser, S. E. Microinjection of fluorescent tracers to study neural cell lineages. *Dev. Camb. Engl. Suppl.* **Suppl 2**, 1–8 (1991).
114. Woo, K. & Fraser, S. E. Order and coherence in the fate map of the zebrafish nervous system. *Dev. Camb. Engl.* **121**, 2595–2609 (1995).
115. Chernyavskaya, Y., Zhang, X., Liu, J. & Blackburn, J. Long-read sequencing of the zebrafish genome reorganizes genomic architecture. *BMC Genomics* **23**, 116 (2022).
116. Lee, L. H., Yang, H. & Bigras, G. Current breast cancer proliferative markers correlate variably based on decoupled duration of cell cycle phases. *Sci. Rep.* **4**, 5122 (2014).
117. Senaratne, A. P., Cortes-Silva, N. & Drinnenberg, I. A. Evolution of holocentric chromosomes: Drivers, diversity, and deterrents. *Semin. Cell Dev. Biol.* **127**, 90–99 (2022).
118. O'Sullivan, R. J. *et al.* Rapid induction of alternative lengthening of telomeres by depletion of the histone chaperone ASF1. *Nat. Struct. Mol. Biol.* **21**, 167–174 (2014).
119. Henriques, C. M., Carneiro, M. C., Tenente, I. M., Jacinto, A. & Ferreira, M. G. Telomerase is required for zebrafish lifespan. *PLoS Genet.* **9**, (2013).
120. Carneiro, M. C. *et al.* Short Telomeres in Key Tissues Initiate Local and Systemic Aging in Zebrafish. *PLOS Genet.* **12**, e1005798 (2016).
121. Rivosecchi, J., Jurikova, K. & Cusanelli, E. Telomere-specific regulation of TERRA and its impact on telomere stability. *Semin. Cell Dev. Biol.* **157**, 3–23 (2024).